METABOTROPIC GLUTAMATE RECEPTOR 1 IN HUMAN MALIGNANCIES

By

JESSICA LI FONG TEH

A dissertation submitted to the

Graduate School - New Brunswick

Rutgers, The State University of New Jersey

and

The Graduate School of Biomedical Sciences

University of Medicine and Dentistry of New Jersey

in partial fulfillment of the requirements

for the degree of

Doctor of Philosophy

Graduate Program in Cell and Developmental Biology

written under the direction of

Dr. Suzie Chen

and approved by

_____

_____

_____

_____

_____

New Brunswick, New Jersey

October 2013

ABSTRACT OF THE DISSERTATION

METABOTROPIC GLUTAMATE RECEPTOR 1 IN HUMAN MALIGNANCIES

By

JESSICA LI FONG TEH

Dissertation Director: Dr. Suzie Chen

The role of the glutamatergic system in cancer cell homeostasis has expanded exponentially over the last decade. Once thought to participate only in synaptic transmission and neuronal excitability, the presence of functional glutamate receptors has since been demonstrated in peripheral tissues. Most notable is the implication of glutamatergic signaling in the pathophysiology of various human malignancies presenting intriguing possibilities to make glutamate receptors putative novel targets for human cancers. Our group previously described the oncogenic properties of metabotropic glutamate receptor 1 (mGluR1/Grm1), a GPCR, in melanoma development *in vivo*. TG-3, a transgenic mouse line, developed spontaneous melanoma with 100% penetrance in the absence of any known stimuli. Stable Grm1-mouse melanocytic clones display transformed phenotypes *in vitro* and were aggressively tumorigenic *in vivo*.

This thesis has two key aims. The first is to elucidate key downstream effectors of mGluR1 in melanocyte transformation. MAPK and PI3K/AKT signaling were previously identified as downstream targets of mGluR1. Here, we demonstrate a novel pathway for mGluR1-mediated tumorigenesis involving the transactivation of IGF-1R. Disrupted IGF-1R signaling in stable Grm1-melanocytic cells led to the abolishment of mGluR1-induced AKT activation and the suppression of tumor growth. We propose that IGF-1R activation represents a previously overlooked key pathway involved in the mechanisms by which mGluR1 exerts its transformative properties.

In my second aim, as most human cancers are of epithelial origin, we utilized immortalized mouse mammary epithelial cells (iMMECs) as a model system to study the transformative properties of Grm1. Phenotypic alterations in acinar architecture were assessed using 3D morphogenesis assays. We found that mGluR1-expressing iMMECs exhibited delayed lumen formation in association with decreased central acinar cell death, disrupted cell polarity and a dramatic increase in the activation of the MAPK pathway. Orthotopic implantation of mGluR1-expressing iMMEC clones into mammary fat pads of athymic mice resulted in tumor formation. Persistent mGluR1 expression was required for the maintenance of the tumorigenic phenotypes as demonstrated by an inducible Grm1-silencing RNA. Moreover, relevance to human breast cancer may be suggested by the observed expression of mGluR1 in human breast tumor biopsies and cell lines, and the consequences of mGluR1 modulation on tumorigenicity therein. Our findings demonstrate that mGluR1 may be oncogenic in mammary epithelial cells and may play a role in the pathophysiology of breast cancer.

ACKNOWLEDGEMENTS

I would like to express my deepest gratitude to my thesis advisor, Dr. Suzie Chen not only for taking a chance on me early in my graduate school career but also for providing me with tireless guidance, valuable opportunities and an ideal setting where I was allowed to grow and flourish to become an independent thinker and scientist.

I would like to sincerely thank Dr. Vassiliki Karantza for invaluable guidance throughout graduate school. The second aim of my thesis would have never been completed if not for her insightful suggestions and expertise. Thank you Dr. Karantza for welcoming me into your lab and for all the support you have shown.

I would like to sincerely thank Dr. Kim Hirshfield for being exceptionally supportive and encouraging during meetings and always providing helpful discussions.

I would like to sincerely thank committee members, Dr. Shridar Ganesan and Dr. James Goydos not only for sharing their knowledge but also for their significant contributions in their respective fields. I have learned so much from our interactions during meetings.

I would like to also thank undergraduate, Raj Shah for his diligence and efforts in assisting with lab experiments during the last 12 months.

Finally, I am extremely grateful to the friendships formed along the way that have guided me through both research and life. For those who have helped me throughout the years- I thank you.

DEDICATION

This thesis is dedicated to my family in Penang especially my parents whose love and support has carried me this far.

TABLE OF CONTENTS

LIST OF TABLES

LIST OF FIGURES

LIST OF SUPPLEMENTAL FIGURES

CHAPTER 1

AN INTRODUCTION TO METABOTROPIC GLUTAMATE RECEPTOR 1 AND CANCERS

1.1. Metabotropic glutamate receptors in the central nervous system

The role of the glutamatergic pathway has been well documented since the discovery that acidic amino acid, L-glutamate, can serve as an excitatory neurotransmitter throughout the central nervous system (CNS) [1, 2]. L-Glutamate exerts its signaling properties on glutamate receptors, which are key counterparts in synaptic transmission. Glutamate receptors are divided into two major classes on the basis of the mechanism by which they relay signal. The first components of the glutamatergic system discovered belong to ionotropic glutamate receptors (iGluRs), which are ligand-gated ion channels that mediate fast synaptic transmission by allowing the flow of cations through the plasma membrane, leading to depolarization or influx of calcium. IGluRs are further subdivided into N-methyl-D-aspartate (NMDA), a-amino-3-hydroxy-5-methyl-4-isoxazolepropionic acid (AMPA) and kainite (KA) subfamilies. The second, metabotropic glutamate receptors (gene:Grm for mouse and GRM for human, protein:mGluR) are members of the class C G-protein coupled receptor (GPCR) superfamily characterized by their seven-transmembrane domain structure and the ability to modulate downstream cellular signaling. To date, eight subtypes of Grms have been identified and classified into three groups according to their sequence homologies, pharmacological responses and intracellular second messengers. Group I Grms consist of Grm1 and Grm5. Upon activation, Group I mGluRs stimulate phospholipase C via $G_{q/11}$, leading to the formation of two second messengers, inositol 1,4,5-triphosphate (IP3) and diacylglycerol (DAG). In contrast, Group II and Group III mGluRs are negatively coupled via $G_{i/o}$ to adenyl cyclase, leading to 3'–5'-cyclic adenosine monophosphate (cAMP) formation.

1.2. Metabotropic glutamate receptors beyond the brain

Evidence that glutamate signaling can play dual roles in synaptic transmission and in the physiology of non-neuronal cells, came in the form of the widespread functional expression of glutamate receptors in peripheral cells, some of which are not derived from the neural crest. For instance, in the mid-1990s, poly-glutamate peptides were found to be capable of stimulating bone resorption [3]. This finding spurred a host of subsequent functional studies, which implicated NMDA subunit 1 receptor as the predominant receptor involved in bone cells [4, 5]. In bone tissue, osteoblasts and osteoclasts represent two types of cells involved in bone formation and remodeling. Using osteoclasts isolated from rabbit long bones, Chenu et al. reported that NMDA receptor antagonists MK-801 and DAP5 were capable of inhibiting bone resorption [4]. A follow-up study by a different group also uncovered cross-talk between mGluR1 and NMDA receptors in rat osteoblastic cells [6]. They showed that mGluR1 could negatively modulate NMDA receptors, suggesting that complex glutamatergic signaling also exists in bone cells, similar to the CNS. Recently, it was discovered that glutamate might also act as a negative molecular switch for osteoblastogenesis via the cystine/Glu antiporter (xCT) in mesenchymal stem cells [7]. Results from these studies suggest that glutamate encompasses cytokine-like properties in regulating bone physiology.

In a developing dorsal neural tube, the neural crest is composed of a dynamic group of progenitor cells that migrate throughout the embryo to give rise to a diverse host of cells such as smooth muscle cells, endocrine cells and melanocytes. Frati et al. were the first to describe the presence of a glutamatergic system in melanocytes [8]. They identified functional expression of mGluR5 in cultured human melanocytes, which upon stimulation by a Group I agonist, L-Quisqualate (Q), resulted in the modulation of cell proliferation in subconfluent cultures. In confluent cultures, induction of melanocytes with

1 mM L-glutamate reduced cell viability by 75%, suggesting glutamate toxicity similar to that observed in neuronal cells.

Other components of the glutamatergic system have also been found in melanocytes, including AMPA and NMDA receptors as well as glutamate transporters [9]. In the presence of AMPA and NMDA inhibitors, altered cell morphologies with a loss of melanocytic dendricity were observed. In addition, this modulation was accompanied by a down-regulation of microphthalmia-associated transcription factor (MiTF) expression in AMPA inhibitor-treated melanocytes within 24 h. MiTF, a basic helix-loop-helix leucine zipper, dimeric transcription factor, is known to be involved in the regulation of melanocytic differentiation and pigmentation. MiTF-null mice exhibit small eyes (microphthalmia) and an albino coat due to the lack of melanocytes [10]. Hornyak et al. showed that melanoblasts from MiTF-mutated embryos (MiTFmi/MiTFmi) lose the ability to enter the dorsolateral pathway during neural cell migration [11]. The notion that glutamate receptors may modulate MiTF expression presents an intriguing implication of glutamate signaling participation in maintaining melanocyte development and differentiation.

In the skin, keratinocytes make up the outermost layer of the epidermis. The first evidence of glutamate signaling in keratinocytes was shown by NMDAR1 mRNA expression [12], which was later confirmed by Genever et al. who described the functional expression of both iGluRs and mGluRs and glutamate transporter, EACC1, in the basal layer of keratinocytes [13]. Only NMDA receptors were implicated in maintaining cutaneous barrier homeostasis and re-epithelialization of keratinocytes after wounding [13-15]. Calcium serves as a crucial factor in keratinocyte differentiation and keratinization. NMDA has the ability to modulate intracellular calcium levels in keratinocytes that was attenuated by NMDA-antagonist MK-801 [16]. Whereas melanocytes normally do not release glutamate extracellularly, a potential source of

ligand (glutamate) for glutamatergic signaling in melanocytes is via adjacent keratinocytes [9]. Human keratinocytes were found to release extracellular glutamate as a function of cell density, which suggests formation of paracrine or autocrine loops for glutamate receptor activation in the epidermis [16].

In the studies highlighted previously, we discussed the role of glutamate signaling in fully matured peripheral cell types. In early CNS development, mGluRs can direct both maintenance and differentiation of neural stem (NS) cells, a source of neurons in neurological disorders. Neural progenitors derived from the subventricular zone (SVZ) respond to glutamate by increasing cell proliferation and are resistant to apoptosis in contrast to the excitatoxic effects in neurons [17]. The pharmacological blockade of mGluR5 with its antagonist, 2-methyl-6-(phenylethynyl)pyridine hydrochloride (MPEP) led to the apoptosis of NS cells, suggesting the benefit of utilizing mGluR5 agonist in maintaining an NS cell niche in the SVZ. In addition, mGluR3 is known to negatively regulate SVZ-derived NS cells toward astrocyte differentiation.

Similar to NS cells, embryonic stem (ES) cells have self-renewal properties but with a capacity to differentiate into virtually all cell types in the body. To maintain mouse ES cells as undifferentiated colonies in culture, inclusion of leukemia inhibitory factor [18], a member of the interleukin-6 family of cytokines, is a required supplement. mGluR5 is expressed in ES cells and supports their self-renewal ability [19]. However, unlike NS cells, pharmacological blockade of mGluR5 with MPEP was able to override LIF and drive the cells toward differentiation *in vitro* [20]. Moreover, these investigators were the first to describe the synergistic relationship of mGluR5 and LIF in the up-regulation of c-Myc, an essential factor in self-renewal. These findings demonstrate the functional expression of glutamate receptors in a wide range of peripheral tissues from immature to fully differentiated cell types.

1.3. Oncogenic properties of metabotropic glutamate receptors

1.3.1. GPCRs as oncoproteins

The G-protein coupled receptor (GPCR) superfamily comprises over 800 members and currently makes up the majority of drug discovery targets. Their 'druggable' properties stem from several factors including their cell membrane localization, widespread expression and modulation of signaling cascades. The rat MAS was the first GPCR discovered to have oncogenic properties [21]. However, it was surprising that MAS lacked activating mutation(s) in contrast to most oncogenes identified at the time. Subsequent studies uncovered the ability of GPCRs to mediate support for tumor growth by either aberrant expression or the excessive local production of ligands by tumor cells themselves (autocrine) or stromal counterparts (paracrine). Both are well known characteristics of GPCRs with oncogenic activities [22, 23]. Growth factor receptors such as receptor tyrosine kinases (RTKs) are key constituents that help sustain GPCR signaling. One such example is the functional cross-talk between GPCRs and EGFRs, known to induce tumor progression in various malignancies [24]. Similarly, Group I mGluRs activate the MAPK pathway via the recruitment of platelet-derived growth factor receptor (PDGFR) and epidermal growth factor receptor (EGFR) [25, 26]. On the flipside, cultured astrocytes exposed to growth factors such as epidermal growth factor (EGF), fibroblast growth factor (FGF) and transforming growth factor a (TGF-a) were capable of inducing mGluR3 expression [27]. Furthermore, it has been established that Group I mGluRs and NMDA could modulate each other's receptor signaling [28-30]. Further studies will determine whether these transactivations also occur in peripheral cells and whether they are involved in the transmission of proliferative signals in transformed cells.

Immediate downstream effectors of stimulated GPCRs consist of guanosine triphosphate (GTP)-binding heterotrimeric proteins, alpha, beta and gamma subunits. When inactive, the alpha subunit is bound to guanosine diphosphate (GDP). Upon activation, GDP is released and exchanged for GTP, which dissociates the alpha subunit from the beta and gamma subunits preceding a host of signaling events. However, a gain of function mutation in G proteins may lead to constitutive activation that is independent of GPCR activity. This is often a consequence of specific amino acid substitutions in the region where alpha subunit binds to GTP, which results in defective GTPase activity that locks the G protein in an active mode.

Hypermorphic mutant G proteins were initially identified to produce a dark skin phenotype in mice [31]. The cause of increased dermal pigmentation was pinpointed to missense mutations in two functionally related G protein subunits; GNAQ and GNA11 (encodes $G\alpha_q$ and $G\alpha_{11}$, respectively). For constitutive activation, this group also demonstrated a requirement for coupling of these mutant G protein subunits to endothelin receptor B (Ednrb). Recent breakthrough studies identified both GNAQ and GNA11 as hotspot somatic mutations (80%) in uveal melanoma and the potential novel targets for therapeutic intervention [32, 33]. Uveal melanomas represent a subset of melanocytic tumors that do not display the common activating B-RAF and N-RAS mutations found in cutaneous melanoma [34]. A hotspot mutation in position 209 (Q209) in GNAQ and GNA11 was detected in blue nevi (benign intradermal melanocytic proliferations), primary and metastatic ocular melanocytic tumors. Both GNA11 and GNAQ share 90% sequence homology [35] and their variants can induce the transformation of immortalized C57BL/6-derived mouse melanocytes (melan-a) but not primary or genetically modified human melanocytes (hTERT/CDK^{R24C}/$p53^{DD}$), suggesting that other factors are required for the initiation of uveal melanoma. Although GNAQ mutations have not been detected in cutaneous melanoma, some authors have repeated

their frequent occurrence in primary melanocytic lesions originating from the CNS [36]. In addition, mutations in several other novel heterotrimeric G proteins such as GNG10 and GNAZ have also been identified in a screening of malignant melanoma tumors [37]. However, additional studies are warranted to determine possible involvement of one or more of these mutations in melanoma pathogenesis.

1.3.2. Glutamate signaling in melanoma

1.3.2.A. An introduction to melanoma

Skin cancer is the most common cancer in the United States with more than a million cases diagnosed each year. There are three forms of skin cancer; the two that occur most frequently are squamous cell carcinoma (SCC) and basal cell carcinoma (BCC). Both SCC and BCC are slow growing, rarely metastasizing cancers and generally non-life-threatening [38]. Melanoma is the least common but also the most aggressive form of skin cancer. In 2013, it is estimated that 76,690 new cases of melanoma will be diagnosed, with the disease occurring more often in men than in women [39]. With early detection, melanoma patients have a higher chance for survival when treated by surgical resection of the primary tumor. However, advanced melanoma is a fatal disease with poor prognosis and chemoresistance to most current therapeutic modalities.

SCC and BCC both arise from epidermal keratinocytes whereas cutaneous melanomas originate in epidermal melanocytes. During embryogenesis, melanocytes, originally derived from the neural crest [40], migrate to the epidermis and reside in the basal layer in contact with keratinocytes. Melanocytes function as the producer of the pigment melanin that is largely responsible for skin color providing effective

photoprotection, by way of pigmentation in the skin. This is suggested by the fact that light, poorly melanized skin is more vulnerable to acute and chronic injury by ultraviolet (UV) damage [41].

The recent substantial rise in the number of people diagnosed with skin cancer (melanocytic or non-melanocytic) has been attributed to increased exposure to UV radiation from the sun and indoor tanning devices. UVB radiations at short wavelengths (290–320 nm) induce damage in the form of cyclobutane pyrimidine dimers and pyrimidine (6-4) pyrimidone photoproducts [42]. UVA wavelengths (320–400 nm) causes single-stranded breaks, DNA-protein crosslinking and generates free radicals that cause oxidative damage [43]. Cells respond to this damage through the activation of various DNA repair pathways protecting them from mutations that lead to cancer. As with other cancers, deficits in DNA repair capacities may influence the likelihood for the development of melanoma [44, 45]. In addition to their contribution to skin pigmentation, melanocytes also collectively form melanocytic nevi. Epidemiological studies have suggested that high numbers of acquired and dysplastic nevi correspond with an increased risk of developing melanoma [46, 47].

Based on their clinical and histopathological features, melanoma progression is suggested to be categorized into five distinct steps: 1) common acquired and congenital nevi with structurally normal melanocytes; 2) dysplastic nevi with structural and architectural atypia; 3) radial growth phase (RGP), non-tumorigenic primary melanomas without metastatic competence; 4) vertical growth phase (VGP), tumorigenic primary melanomas with competence for metastasis; and 5) metastatic melanoma [48]. During RGP, transformed melanocytes proliferate horizontally staying within the upper layer of the epidermis whereas melanomas in the VGP invade into deeper layers such as the dermis and subcutaneous tissue increasing the risk for spread to vital organs. Hence,

the transition from the radial growth phase to the vertical growth phase is thought to be a critical step in melanoma progression and survival [49].

Early traditional linkage mapping studies pointed to a susceptibility gene that underlies familial melanoma, CDKN2A. Products of the CDKN2A locus through alternative splicing, $p16^{INK4A}$ and ARF, are two potent tumor suppressors of melanomagenesis and their loss predisposes the development of the disease [50, 51]. Nearly 60% of melanoma tumor cell lines have homozygous deletions in 9p21, a finding that strongly suggests the presence of a tumor suppressor gene in this locus. CDKN2A has been mapped to the 9p21 region [50]. However, familial melanomas account for only 8-12% of diagnosed melanomas, pointing to the presence of additional genes that are implicated in disease pathogenesis [52].

Polymorphic variants of the pigmentation-associated GPCR, melanocortin-1 receptor (MC1R), have also been found to be associated with the genetic predisposition to melanoma, particularly those variants encoding red hair, freckling, fair skin and sun sensitivity. Minimal receptor activity, as in polymorphisms that result in the phenotype of red hair/fair skin, produces the red/yellow pheomelanin pigment, whereas increasing MC1R activity stimulates the production of black/brown eumelanin. MC1R variants have been associated with substantial increase in the penetrance of CDKN2A mutations [53, 54]. A recent study also suggest the pheomelanin pathway to be carcinogenic in a manner that is independent of UV radiation, giving rise to melanomas when the inactivated form of MC1R was introduced in mice with inducible, melanocyte-specific expression of oncogenic B-RAFV600E [55].

The understanding of how genetic aberrations contribute to melanomagenesis and progression allows new insights to tumor biology and the development of successful therapeutic regimes. Early studies in melanoma genetics focused on candidate gene sequencing approach focusing on aberrations in a wide range of cancers. The RAS–

RAF–MEK–ERK–MAP kinase pathway mediates cellular responses to growth signals. A search for mutations in a component of the mitogen-activated protein (MAP) kinase pathway in a large panel of common cancers revealed that 40 to 60% of melanomas, and 7 to 8% of all cancers, carry an activating mutation in the gene encoding the serine–threonine protein kinase B-RAF (B-RAF) [56]. Over 80% of these somatic missense mutations consist of a single acidic substitution of glutamic acid for valine at amino acid 600 (V600E mutation) inducing constitutive BRAF activation and downstream signal transduction in the MAP kinase pathway. Further studies identified similar mutations in 82% of benign nevi suggesting a role for B-RAF mutations in the initiation step of the disease [57]. Most importantly, the identification of mutant BRAF has offered opportunities to test targeted therapy for this disease. FDA-approved for late-stage melanoma, Vemurafenib/Zelboraf (PLX4720/PLX4032) is a highly selective small molecule inhibitor against cells with mutated BRAF and has shown remarkable clinical activity in patients harboring mutant B-RAFV600E [58, 59].

In contrast to other tumor types, the RAS family of proto-oncogenes; H-RAS, N-RAS, and K-RAS are not as frequently mutated in human melanoma compared to other malignancies. Of the three isoforms, N-RAS is the most commonly mutated however occurring only in a fraction of melanomas (10%–15%), with a higher frequency noted in amelanotic nodular melanoma subtypes. Both B-RAF and N-RAS require another stimulus, such as loss of PTEN for B-RAF and inactivating mutations in INK4A for RAS to yield transformed melanoma cells [60, 61].

Currently, a few encouraging cancer therapies targeting tyrosine kinases that have positively impacted patient survival include antibody, trastuzumab (Herceptin®) for ERBB2/HER2-positive breast cancer and small molecule kinase inhibitors targeting EGFR in non–small cell lung carcinoma [62]. Recent mutational analysis of the protein tyrosine kinome identified ERBB4/HER4 mutations in 19% of melanoma patients

including two other kinases, FLT1 and PTK2B in 10% of the individuals with melanomas [63]. ERBB4 mutations were distributed throughout the gene unlike oncogenes with mutational hotspots such as mutated B-RAF, N-RAS and PI3KCA. ERBB4 mutants also resulted in increased kinase activity and transformative properties in mouse fibroblast NIH3T3 cells and melanoma cells, SK-Mel-2. These mutants were also sensitive to pharmacological inhibition by broad spectrum ERBB inhibitor, lapatinib as compared to cells bearing wild-type ERBB4.

A separate report also identified putative receptor tyrosine kinases (RTKs) as therapeutic targets in melanoma. Tworkoski and colleagues conducted a phosphoproteomic screen of 58 RTKs in a panel of 25 melanoma cell lines [64]. Among those they found to be commonly activated in melanoma were the insulin receptor family (IGF-1R, IR), MET family (MET, MST1R), EGFR family (EGFR, HER3, HER4), and TAM family (TYRO3, AXL, MERTK). Furthermore, suppression of IGF-1R, AXL and HER3 activity was effective in decreasing cell proliferation and migration in a manner that is independent of B-RAF or N-RAS mutation status suggest the value of combining RTK and BRAF/MEK inhibition.

Most recently, whole-exome and whole-genome sequencing has uncovered previously unknown genes with function in melanomagenesis, thus identifying novel therapeutic targets in addition to contributing to the development of personalized therapies for melanoma. Elevated point mutation rates were observed in melanomas derived from those with chronic sun exposure with enrichment of dipyrimidines at C→T transitions [65]. Acral melanomas, observed on the palms, soles, under the nails and in the oral mucosa, showed similar C→T substitutions indicating that they were just as susceptible to UV-induced DNA damage. The same analysis uncovered significant chromosomal rearrangements in PREX2 (phosphatidylinositol-3,4,5-trisphosphate-dependent Rac exchange factor 2)—a PTEN-interacting protein and known negative

regulator of PTEN. In addition to the nine somatic rearrangements in PREX2 (six interchromosomal translocations, five with intronic breakpoints), PREX2 was highly amplified suggesting multiple mechanisms of PREX2 dysregulation in melanoma. Functional studies utilizing N-RAS(G12D)-TERT-immortalized human melanocytes engineered to express three truncated variants as well as a point mutant (G844D) of PREX2 significantly accelerated *in vivo* tumorigenesis when compared to GFP control.

Although sun exposure has been shown to be a leading risk factor for melanoma [66], it has been puzzling that the most prevalent UVB-induced genetic change, the transition of a cytosine to a thymidine, has not been shown to be the molecular basis for known oncogenic mutations in melanoma, including B-RAFV600E and N-RASQ61L/R. The identification of new driver mutations, RAC1, STK19, and PPP6C resulting from C>T transitions offers missing genomic evidence linking UVB mutagenesis mechanistically to this malignancy [18, 67]. The discussion on whole exome sequencing is continued in Section 1.3.2.C. Glutamate receptors in melanoma.

1.3.2.B. mGluR1 in melanoma

Our lab was the first to suggest the role of aberrant mGluR1 expression in melanomagenesis. In the CNS, mGluR1 participates primarily in post-synaptic transmission and, in its absence, results in severe deficits in learning and memory, as shown in mGluR1-knockout mice [68, 69].

TG-3, a transgenic mouse line, was constructed using a 2-kb genomic fragment, clone B, previously shown to commit fibroblasts to differentiate to adipocytes in vitro [70, 71]. Instead of the expected obese phenotype, one of five founder mice, TG-3, spontaneously developed heavily pigmented lesions at 8 months of age [71]. Lesions were also detected in distant organs including the eyes, lymph nodes, brain, bone, lung

and muscle. The other four founder mice exhibited normal phenotypes past the age of 2 yr. By histological analysis, we determined the pigmented lesions to be melanoma. Physical mapping identified a single tandem copy of clone B in mouse chromosome 10 region A2 orthologous to human chromosome 6q23-24. Molecular mapping identified a concurrent insertion of clone B and a 70-kb deletion of the host sequences in intron 3 of the gene (Grm1) encoding for mGluR1. An assessment of mGluR1 expression at both protein and mRNA levels between normal and tumor pinnae revealed that mGluR1 expression was only detected in tumor specimens.

To distinguish between cause or consequence in mGluR1 expression in melanocytes, a second transgenic line [TG(Grm1)EPv] was constructed targeting the expression of Grm1 to melanocytes under dopachrome tautomerase (Dct) promoter [72]. TG(Grm1)EPv line displayed very similar onset and progression of melanoma as TG-3, thus we concluded that, *in vivo*, ectopic expression of Grm1 in melanocytes was sufficient to induce melanocytic neoplasia. Our findings were validated by Ohtani et al. in an inducible mGluR1 expression transgenic line; furthermore, they demonstrated that continuous mGluR1 expression is required for the maintenance of melanocytic tumorigenesis *in vivo* [73].

As earlier studies by others have shown mGluR5 (the mGluR most similar to mGluR1) expression in normal human melanocytes [8], we were interested to know whether mGluR5 contributed to the melanoma pathogenesis in our system *in vivo*. We crossed Grm5-null mice with TG-3 and the resulting progenies exhibited melanoma-prone phenotype indistinguishable from the original TG-3 [74]. Taken together, these results suggest that, independent of mGluR5, aberrant mGluR1 signaling alone is sufficient to drive spontaneous melanoma formation with 100% penetrance in the absence of other tumor types.

Our aforementioned findings prompted us to study the mechanisms underlying mGluR1-mediated melanocyte transformation. mGluR1 confers oncogenic activities *in vitro* and is sufficient for malignant transformation of melan-a cells *in vivo* [75]. Despite modest alterations in growth properties *in vitro*, stable mGluR1-mouse melanocytic clones, termed MASS clones, were aggressively tumorigenic, with a short latency of 5–7 days when allografted into both immunodeficient nude mice and syngeneic C57BL⁄6 mice. Moreover, these allografted tumors displayed angiogenic activities and were very invasive in both lung and muscle. We further examined the downstream targets that are commonly dysregulated in cutaneous melanoma in our model system. Functionality assays revealed that the MAP Kinase pathway is specifically activated by mGluR Group I agonist and suppressed by Bay 36-7620, a specific antagonist of mGluR1 or siRNA to Grm1. Furthermore, we also observed activated protein kinase B⁄AKT in these MASS tumors *in vivo*.

In addition, we identified AKT2 isoform in particular as the key player in mGluR1 mediated transformation as well as in human melanoma biopsy tissues [76]. When these cells were situated in the *in vivo* environment they exhibited very aggressive tumorigenic phenotypes in comparison with *in vitro* cultured conditions, perhaps by the paracrine supply of its natural ligand, glutamate, which leads to constitutive activation of the receptor, mGluR1. Dysregulation of the members of the PI3K⁄AKT signaling cascade has major implications for the initiation and progression of melanoma. Tumor suppressor, phosphatase and tensin homolog deleted on chromosome 10 (PTEN), is a key negative regulator of the PI3K signaling pathway by degradation of the substrate, phosphatidyl inositol 3,4,5-triphosphate (PIP3) [77]. PTEN is inactivated due to deletion or mutations in about 29–43% melanoma cell lines or biopsies and is one of the classic mechanisms contributing to aberrant activation of AKT. As alluded to in the previous section, although mutated BRAFV600E is detected in 60–70% of nevi and melanoma and is believed to be

the major inducer of activated MAPK in melanoma, B-RAFV600E by itself is not sufficient to induce melanoma *in vivo*. Recently, Dankort et al. described a metastatic melanoma mouse model derived by the cooperative efforts of B-RAFV600E and ablation of PTEN [60]. Interestingly, PTEN loss in melanoma cells was accompanied by increased metastatic properties through AKT2 activation and E-cadherin downregulation [78]. Earlier studies by Robertson et al. have shown that AKT3 isoform plays a central role in melanoma development and is capable of transforming melan-a when combined with B-RAFV600E [79]. Although we had previously described elevated active AKT2 independent of PTEN phosphorylation status, it is worthwhile to question whether PTEN loss is also accompanied by AKT2 overexpression in human melanoma biopsies. Regardless of the PTEN status, the whens and whys of the preferential regulation of various AKT isoforms in melanoma development, growth and metastasis is certainly a provocative area of study.

We have extended our studies to human melanoma by examining human melanoma cell lines for mGluR1 expression. We found that 23 of 25 human melanoma cell lines expressed the human form of mGluR1 but not human melanocytes. Similar to the mouse system, MAPK signaling in mGluR1-expressing human melanoma cells can be modulated by mGluR1 agonist, L-Quisqualate (Q) and mGluR1 competitive and non-competitive antagonist, LY367385 and BAY36-7620, respectively [80]. Thus far, we have examined 175 human melanoma biopsies from primary to metastatic tumors and detected mGluR1 expression, both mRNA and protein, in approximately 60% of the tumor samples regardless of B-RAF or N-RAS genotypes. Moreover, several stable tet-R inducible siGRM1 clones were isolated from multiple mGluR1-expressing human melanoma cell lines and we observed a much reduced tumor progression in these xenografts in the presence of the inducer, doxycycline in comparison with silencing RNA to GFP [81]. Currently, we are introducing human GRM1 into immortalized human

melanocytes (hTERT/CDKR24C/ p53DD). Whether GRM1 alone is sufficient to induce transformation in human melanocytes will be investigated.

Although TG-3 tumors showed ectopic mGluR1 expression as a consequence of the disruption of intron 3 of Grm1, the precise mechanisms remain unknown. We hypothesize that the integration of the transgene clone B and the deletion of 70 kb of host intronic sequences may have disturbed the regulation of a neuronal gene expression (mGluR1) in non-neuronal cells (melanocytes) and one of the consequences of expression of an otherwise normal gene in an anomalous cell type is cell transformation and tumor formation. TG(Grm1)EPv was generated solely by targeted mGluR1 expression to melanocytes. In TG-3 and TG(Grm1)EPv, neither B-RAF or N-RAS is mutated. These results suggest that deregulation of mGluR1 expression in melanocytes does not induce mutations in B-RAF or N-RAS or mutations in either protein are not required for spontaneous melanoma development.

One mechanism utilized by mGluR1 to promote transformation involves the formation of an activating autocrine loop in mGluR1-expressing melanoma cells, a characteristic of GPCRs with oncogenic activities [22, 23]. We have demonstrated cell lines that display elevated levels of extracellular glutamate in a panel of mGluR1-positive human melanoma cell lines [80]. This is further strengthened by a threefold increase of extracellular glutamate release by mGluR1-expressing stable melanocytic clones as compared with vector control, again attributing this observation mediated by ectopic expression of mGluR1 to the presence of exogenously introduced Grm1 [75].

Earlier our group verified mGluR1-dependent but mGluR5-independent melanoma-prone phenotype in mice; however, recently Choi et al. demonstrated that overexpression of mGluR5 also induced melanoma phenotype in transgenic mouse lines in the absence of mGluR1 expression [82]. Similar to our initial derivation of TG-3, the inducible mGluR1-transgenics constructed by Ohtani et al. and the most recent finding

reported by Choi et al. were all serendipitous discoveries. Choi et al. were interested in determining the significance of mutation in the serine 901 phosphorylation site of Grm5 *in vivo*. Instead, one of the transgenic founder animals developed spontaneous melanoma. They therefore targeted wild-type Grm5 to melanocytes by a melanocyte-specific promoter, tyrosinase-related protein 1 (TRP1), which proved sufficient to drive melanoma formation within 2 months, with phenotype and progression very similar to our second transgenic line, TG(Grm1)EPv.

In light of this recent finding, we propose that ectopic or overexpression of Group I mGluRs will lead to the establishment of autocrine loops with enhanced levels of extracellular glutamate, in turn leading to constitutively activated mGluRs and downstream targets such as MAPK, which places the cells in a pro-proliferative environment that promotes cell transformation and tumorigenesis. It is noteworthy that mGluR1 may offer an edge over mGluR5 in terms of diagnostic value due to the undetectable mGluR1 expression in normal melanocytes or benign nevi. Plasma glutamate in healthy resting individuals is normally low, an average concentration of 50 μM [83]. Whether the plasma concentration of L-glutamate can provide diagnostic value in melanoma patients with altered mGluR signaling is currently under investigation.

1.3.2.C. Glutamate receptors in melanoma

Two recent reports provide additional evidence in glutamate signaling and melanoma [84, 85]. The first described a whole exome sequencing of paired normal and metastatic melanoma tumor sample DNA. As expected, 50% of the tumor samples were mutated for B-RAF. Notably, the second most mutated gene in this screening was a previously unidentified gene, GRIN2A, which encodes for NMDA receptor subunit e-1,

an ionotropic glutamate receptor (iGluR). Another frequently mutated gene is PLCB4, an enzyme that catalyzes the formation of IP3 and DAG downstream of mGluRs [84].

In the second report, the same group performed a mutational analysis in 11 melanoma tumor DNA samples, this time enriching for GPCR exons only [85]. From the initial screen, 11 genes that harbored at least two somatic mutations were chosen. Of the 11 genes probed, GRM3 and GPR98 were identified as having the highest mutation rate in a cohort of 80 melanoma samples. GRM3 encodes for mGluR3 and had a 16.3% mutation rate. Interestingly, the original cohort along with a second cohort consisting of 57 melanoma specimens revealed a GRM3 mini-hotspot (Glu870Lys) in four individuals. To characterize the functional significance of this mutation, they generated several stable clones using melanoma cell lines harboring mutated B-RAFV600E with each of the four somatic mutations identified in GRM3. These cell lines with mutated GRM3 exhibited anchorage-independent growth and increased migration mediated by MAPK signaling.

Although Vemurafenib/Zelboraf (PLX4720/PLX4032) showed remarkable clinical activity in patients harboring mutant BRAFV600E, this is marred by patient relapse within 8–12 months [58, 59, 86]. Increased efforts to understand resistant melanoma cells and this eventual BRAF bypass have identified multiple mechanisms of resistance involving the reactivation of MAPK. Among them are RAF isoform switches, up-regulation of COT (functions upstream of MEK) and RTKs [PDGFR and insulin-like growth factor 1 receptor (IGF-1R)] and, most recently, the dimerization of aberrantly spliced B-RAFV600E, p61B-RAFV600E [87-90]. Previously, mutant B-RAF but not RAS was shown to predict sensitivity to MEK inhibitors [91]. Regardless, MEK inhibitors alone have yet to generate favorable responses in the clinic. Interestingly, melanoma cells harboring mutated GRM3 clones are more susceptible to MEK inhibitor, AZD-6244 [92]. These investigators hypothesize that in some cases, previous failure of MEK inhibitors to generate significant

response was due to a lack of enrichment in tumor samples for GRM3 mutations that are also highly dependent on MAPK signaling. Both Group I and Group II mGluRs rely on two separate intracellular second messengers but downstream signals eventually feed into the MAPK pathway. Given the convergence on MEK, we postulate that general GRM alterations may be instrumental in enhancing sensitivity to MEK inhibitors.

These recent reports strongly implicate putative roles of glutamatergic pathway in the pathogenesis of melanoma. However, given that each of these glutamate receptor subtypes signal through distinct effector proteins, a number of important additional questions need to be addressed. It is especially noteworthy that the mechanism by which mGluR1-transformed melanocytes may utilize to promote growth is through increasing the production of their ligand, glutamate, leading to autocrine and paracrine loops. Whether this property is the main driving force in the oncogenic transformation of other glutamate receptor subtypes has yet to be determined. In particular, future studies will need to address whether mutation of GRM3 or GRIN2A is sufficient to induce malignant transformation. The implication of GRIN2A in melanoma is certainly provocative, although not entirely surprising, as other iGluR subtypes have been found to play functional roles in non-neuronal cells. Indeed, in a recent gene expression profiling of two molecular subsets of lung adenocarcinomas [anaplastic lymphoma receptor tyrosine kinase (ALK)-positive adenocarcinoma and triple-negative adenocarcinoma], GRIN2A was identified as the gene with the highest level of upregulation observed in addition to ALK in ALK-positive adenocarcinoma tumor samples [93]. Collectively, these findings make the glutamatergic pathway and their downstream effectors attractive candidates for therapeutic intervention in melanoma (Figure 1).

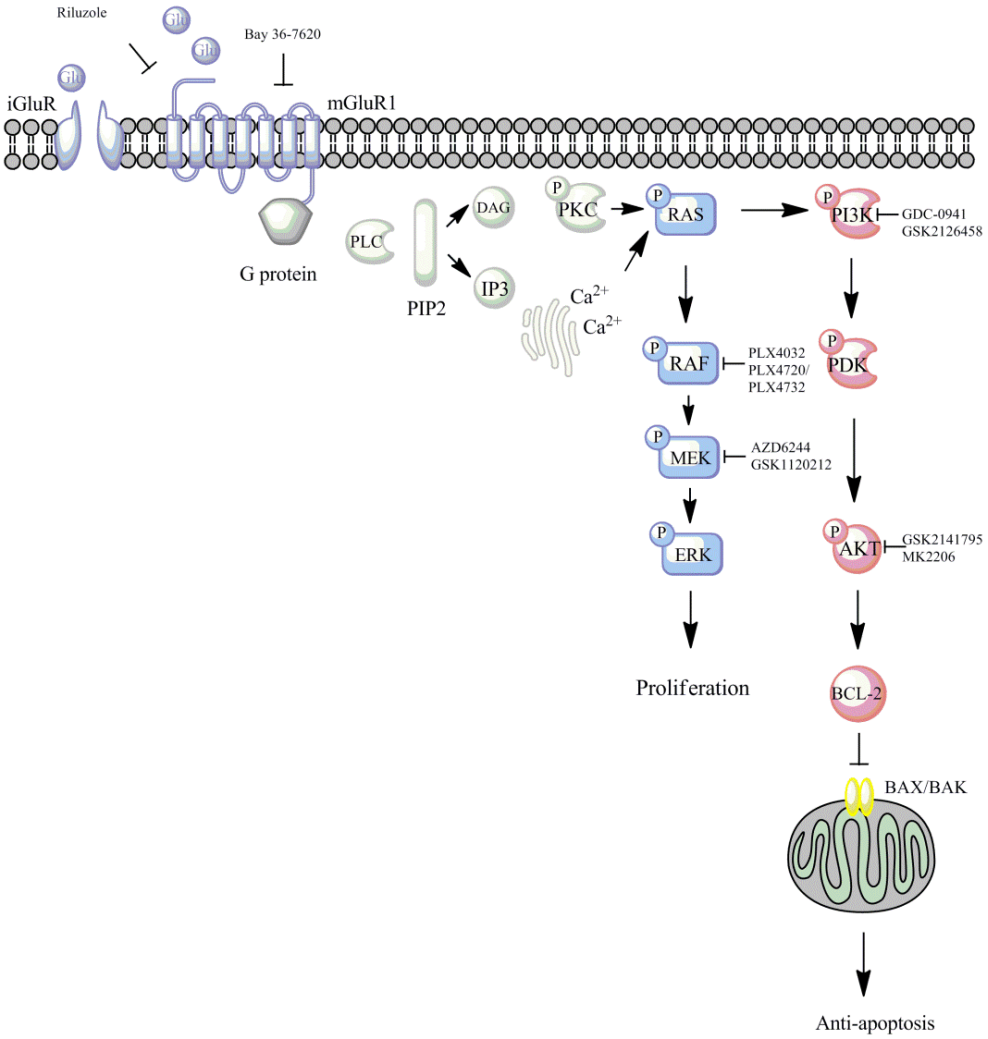

Figure 1. Signal transduction pathways affected by mGluR1 alterations.

Upon ligand binding, mGluR1 activates two major signaling cascades implicated in melanoma, MAPK and PI3K/AKT. Compounds currently tested in clinical trials that target these pathways are indicated.

1.3.3. mGluRs in breast cancer

1.3.3.A. An introduction to breast cancer

Breast cancer is a molecularly heterogeneous disease currently categorized based on their histological origin and therapeutic groups. Sporadic breast cancer is more widespread compared to the hereditary form encompassing 90% of all cases but is also the least understood malignancy. Current classification of breast cancer divides the disease in three distinct molecular subtypes: luminal tumors which are hormone receptor (estrogen receptor and/or progesterone receptor) positive and HER2 negative, HER2 amplified tumors and tumors that lack the expression of the three receptors frequently referred to as triple-negative breast cancer [94-96]. Although tumors within each division have similar gene expression patterns and clinical outcomes, novel subgroups within these groups are beginning to be identified through genomic and transcription analyses, further redefining our current understanding of the disease.

Recently, investigators from the Cancer Genome Atlas published the most comprehensive molecular portrait of human breast tumors known to date and the top (>10%) three somatic mutations were previously implicated genes, TP53, PIK3CA and GATA3 [97]. Basal-like (triple negative) breast tumors in particular displayed multiple amplifications (not mutations) of components in both PI3K/AKT and RAS-RAF-MEK pathways. Furthermore, another study has clustered a combined dataset including germline and somatic copy number variation, SNP information and gene expression data for 2000 breast tumors, finding 10 molecularly defined subgroups with distinct biology and disease-specific survival characteristics [98]. Putative cancer genes were found to include deletions in PPP2R2A, MTAP and MAP2K4.

It has been suggested that cutaneous melanoma and breast cancer observe a bidirectional correlation through germline mutations found in BRCA2 and CDKN2A, breast cancer and melanoma susceptibility genes, respectively [99, 100]. BRCA proteins are encoded by tumor suppressor genes that are involved in DNA double stranded break repair. Carriers of BRCA2 mutations have not only been shown to be at high risk for breast and ovarian cancer but for other malignancies as well including prostate, pancreatic and melanoma [101]. Goggins et al. particularly noted that younger breast cancer patients and those that have undergone radiation therapy exhibited elevated risk of a second primary cutaneous melanoma [99]. Furthermore, population-based analysis of 16,591 cutaneous melanoma survivors in the Surveillance, Epidemiology, and End Results (SEER) program data from 1973 to 2003 reported significantly elevated risks for 13 different types of primary cancers including female breast cancer [102].

1.3.3.B. Glutamate signaling in breast cancer

Recent findings of Speyer et al. were consistent with ours; they described mGluR1 as a potential target in breast cancer [103]. mGluR1 expression was found in several triple-negative breast cancer cell lines (TNBC). TNBC cell growth was inhibited when only mGluR1 utilizing shRNA-mediated knockout and mGluR1 antagonist, Bay 36-7620, were targeted. In addition, one of the TNBC lines, MDA-MB-231, has been shown to release glutamate into the extracellular environment *in vitro* [104]. Breast cancer cells have a high propensity to metastasize to bone [105]. Given that glutamate can alter bone homeostasis by suppressing osteoblastogenesis, secreting glutamate may be advantageous for the migration of tumor cells to bone [106].

Three SNPs in GRM1 have been evaluated for genotype associations with breast cancer clinicopathologic variables using DNA isolated from peripheral blood of 1,096

breast cancer patients [107]. A SNP in GRM1 resulting in a proline to serine substitution correlates with age of diagnosis highly dependent on the hormone receptor status of the tumor. Moreover, mGluR1 expression was detected not only at higher levels in breast tumors compared to normal tissue, but also in ER-positive breast cancers compared to ER negative breast cancers. Analysis of breast cancers treated with tamoxifen from an independent cohort demonstrated that high expressors of GRM1 have a worse distant recurrence free survival further implicating the role of GRM1 in breast cancer particularly in luminal breast cancers.

1.3.4. mGluRs and other cancers

Other subtypes of mGluRs that have been extensively studied in cancer growth include Group II GRMs in malignant glioma. These primary CNS tumors arise from glial cells, thought to be predominantly astrocytic cells. Due to the physical constraints of the cranium, glioma cells thrive by destroying surrounding brain tissue. To achieve this, glioma cells release glutamate, mediated by the cystine-glutamate antiporter system (xCT), which causes the excitotoxic death of neurons [108]. An interesting feature of glioma cells that allows them to release rather than remove circulating glutamate from the environment is the absence of astrocytic glutamate transporter (EEAT) expression. Nicoletti et al. demonstrated the efficacy of suppressing glioma cell proliferation *in vitro* and reduced xenograft tumor volumes *in vivo* by blockade of mGluR2/3 functions with its antagonist, LY341495 [109, 110]. Moreover, mGluR3 signaling mediated by type IV bone morphogenic protein (BMP4) was found to be responsible for sustaining the population of glioma-initiating cells (GICs) [111]. Remarkably, inhibition of mGluR3 promotes differentiation of GICs into astrocytes.

In the case of medulloblastomas, the activation of mGluR4 may actually prove beneficial. Medulloblastomas are a common pediatric malignant brain tumor and similar to gliomas, current views support the presence of stem-like progenitor cells within these tumors [112]. It is thought that transformation of cerebellar granule cell neuroprogenitors (GNPs) give rise to medulloblastomas. These GNPs exist in the external granular layer of the cerebellar cortex and migrate inward to the granular layer where they finally differentiate into mature granule cells [113]. It was hypothesized that the tendency towards a differentiated phenotype is supported by glutamate that is released by surrounding cells. Interestingly, mGluR4 receptor expression was detected in cultured cerebellar granule cells enriched with GNPs [114]. Canudas and colleagues took advantage of a specific mGluR4 enhancer, PHCCC (N-phenyl-7-(hydroxyimino)/cyclopropa[b]chromen-1a-carboxamide), which interacts with a site within the seven transmembrane region in mGluR4. They found that amplified activity of mGluR4 receptors with PHCCC could effectively reduce GNP proliferation and promote them to differentiate into mature granule cells. These results suggested that mGluR4 is crucial for maintaining a mature differentiated phenotype. These observations were reinforced when it was found that the over-expression of mGluR4 in cultured cells also promoted neuritogenesis. Therefore, it is not surprising that these findings prompted the same group to investigate the role of mGluR4 in medulloblastoma, a clinically relevant malignant disease. Approximately 75% of the biopsied human medulloblastoma samples stained positive for mGluR4 and was found to correlate with improved prognosis [115]. PHCCC treatment of mGluR4-expressing medulloblastoma cell lines resulted in decreased PI3K signaling, DNA synthesis and cell proliferation. These observations were found to be independent of other signaling pathways such as Insulin-like Growth Factor 1(IGF-1), canonical Wnt and Sonic hedgehog (SHH) all of which are known to contribute to GNP proliferation and play crucial roles in the development of

medulloblastomas [116-119]. Further evidence for the benefit of enhancing mGluR4 expression/function in medulloblastoma was shown with an *in vivo* irradiated transgenic mouse model lacking Shh receptor Patched 1 (Ptc neo67/+). When Ptc neo67/+ mice are irradiated one day after birth they are predisposed to developing medulloblastomas with an incidence of >80% [120]. However, PHCCC treatment during the first eight days of life of irradiated mice led to inhibition of medulloblastoma development [115]. Taken together, results from these studies suggest an inverse correlation of mGluR4 with the progression of the disease. While the data is exciting, further investigation is warranted to examine whether later stages of medulloblastoma are sensitive to mGluR4 activation especially in metastatic stage, which was shown to have lower expression levels of the receptor.

Park et al. have found a link between mGluR4 and the pathogenesis of colorectal cancer. 5-fluorouracil (5-FU) is a standard chemotherapeutic agent for patients with colorectal cancer and resistance toward this drug is a major hurdle. Park et al. first generated a 5-FU resistant colorectal cancer cell line and identified over-expression mGluR4 mediated the 5-FU resistance phenotype in these cells [121]. In a follow up study, expression of mGluR4 was found in 54% of the malignant tissues of colorectal carcinomas, which correlated with poor prognosis [122]. In addition, the same group also showed that several mGluR4-expressing colon cancer cell lines treated with mGluR4 antagonist resulted in suppression of cell proliferation. It is apparent that mGluRs have emerged as receptors with oncogenic potentials in a vaster variety of cancers than previously expected (Table 1; note: only mGluRs are discussed).

Table 1. Implication of mGluR subtypes in various malignancies.

Malignancies	mGluR subtype	Possible mode of action	Hot spot mutation(s) in human	Mouse model	Phenotype	References
Melanoma	mGluR1	Aberrant expression		TG-3,	Hyperpigmentation Metastasis: lymph nodes, lung, muscle and brain	[71]
				TG(Grm1)Epv/ Dct::Grm1	Hyperpigmentation Metastasis: lymph nodes only	[72]
				Conditional mGluR1-transgenic mice	Hyperpigmentation Metastasis: lymph nodes, invasion to muscle	[73]
	mGluR5	Over-expression		TRP1::Grm5	Hyperpigmentation Metastasis: lymph nodes and bone, invasion to muscle	[82]
	mGluR3	Activating mutations	Mini hotspot: Glu870Lys	N/A	N/A	[85]
	mGluR8		Unknown			
Breast cancer	mGluR1	Not reported		N/A	Pharmacological intervention of mGluR1 signaling with Bay 36-7620 and Riluzole resulted in diminished breast cancer xenografts	[103]
		SNP: proline>serine substitution GRM1 expression (mRNA)			Association with age of diagnosis dependent on molecular subtype Association with breast cancer recurrence	[107]
Prostate cancer	mGluR1	Over-expression in primary and metastatic samples, High serum glutamate levels		N/A	Pharmacological intervention of mGluR1 signaling with Bay 36-7620 and Riluzole resulted in decreased cell migration and invasion	[123]
Colorectal carcinoma	mGluR4	Over-expression in tumor tissue correlates with recurrence and poor prognosis		N/A	N/A	[122]

Glioma	mGluR2/3	Not reported		N/A	Activation of mGluR3 sustained glioma-initiating cells, Pharmacological intervention of mGluR2/3 with LY341495 reduced growth *in vitro* and *in vivo*	[109-111]
Medullo-blastoma	mGluR4	Expression correlates with improved prognosis		N/A	mGluR4 activity enhancer, PHCCC led to inhibition of medulloblastoma incidence *in vivo*	[115]

N/A, non-applicable. TRP1:tyrosinase-related protein 1, Dct:Dopachrome tautomerase, PHCCC (N-phenyl-7-(hydroxyimino)/cyclopropa[b]chromen-1a-carboxamide)

1.4. Glutamate signaling as a therapeutic target

We have successfully translated our laboratory findings into the clinic with Riluzole⁄Rilutek® (2-amino-6-trifluoro-methobenzothiazole), an FDA-approved drug for the treatment of amytropic lateral sclerosis (ALS). ALS patients suffer from excessive excitation of glutamate receptors, which triggers the fatal degeneration of motor neurons. Riluzole is thought to relieve excitatoxicity by limiting glutamate release, thus decreasing the availability of the ligand and conferring neuroprotection. Similarly, we reasoned that perturbing the existing autocrine loop in melanoma cells might interfere with cell growth and invasion. *In vitro*, treatment with Riluzole led to decreased extracellular levels of released glutamate and suppressed cell proliferation [80]. mGluR1-expressing human melanoma cell lines were more sensitive to Riluzole than were mGluR1-negative human melanoma cell lines. These *in vitro* observations were confirmed in xenograft studies *in vivo*. Furthermore, we have demonstrated that Riluzole treatment promotes melanoma cells to accumulate in G2⁄M phase before proceeding to sub-G1 apoptotic phase after 24–48 h. It is known that cells arrested in the G2⁄M phase are more sensitive to ionizing radiation. In human melanoma xenograft model, we found that daily treatments of Riluzole combined with weekly ɣ-irradiation resulted in pronounced suppression in

xenografted tumor volumes [124]. Brain metastases are one of the hallmarks of Stage IV melanoma, and because Riluzole is capable of crossing the blood brain barrier, Riluzole is currently being investigated for pretreatment as a radiation sensitizer in brain metastases from late-stage-melanoma.

Due to the heterogeneous nature of most cancers including melanoma, single agent-targeted therapies are likely ineffective in the long run. Recently, we described the benefit of combining Riluzole with Sorafenib/Nexavar®, a small molecule, multi-kinase inhibitor [125]. We demonstrated that combining both reagents resulted in synergistic or additive suppression of xenograft growth regardless of the B-RAF genotypes in melanoma cells. Surprisingly, specific B-RAFV600E inhibitor, Vemurafenib/Zelboraf® (PLX4720/PLX4032), when combined with Riluzole did not lead to enhanced suppression of xenografted B-RAFV600E tumor progression in comparison with Riluzole plus Sorafenib. We attribute this to Sorafenib's mode of action of multiple targets including decreasing levels of an anti-apoptotic protein, MCL-1, leading to enhanced cytotoxicity.

Riluzole was demonstrated to target the glutamatergic pathway in patients with advanced melanoma in a Phase 0 clinical trial [126]. A total of 12 patients with Stage III/IV malignant melanoma were enrolled in the study and received a daily oral dose of 200 mg/day of Riluzole for 2 weeks. Remarkably, 33% of these patients exhibited a significant clinical and metabolic response to Riluzole administration. All four responders had varied B-RAF and N-RAS mutational status and were positive for mGluR1 expression. We showed suppression of downstream targets, MAPK and PI3K/AKT, in post-treatment tumor samples. To evaluate overall metabolic responses in tumors, we also measured standardized uptake value by pre- and post-treatment fluorodeoxyglucose (FDG)-positron emission tomography scans. Malignant melanomas

utilize glucose more avidly as opposed to normal tissues but we found a decrease in FDG-PET intensity in post-treatment tumors of responding patients.

Although the precise mode of action of Riluzole remains to be determined, there is adequate data supporting its disruption of glutamatergic signaling in various cell types. In neuronal cells, Riluzole is thought to exert its neuroprotective properties by inhibiting glutamate release partly by acting on voltage-dependent ion channels [127]. In addition, Riluzole has been shown to antagonize NMDA receptors indirectly. Another mechanism involves the enhanced uptake of glutamate by astrocytic cells, which contributes to rapid clearance of glutamate from the synaptic cleft [128]. Hence, it is not surprising that, in addition to ALS, the therapeutic benefit of Riluzole has been extended to a range of neurodegenerative diseases. Recently, the efficacy of Riluzole was also shown in TNBC cells, a basal-like molecular subtype of breast cancer with the worst prognosis due to unavailable therapeutic targets [103]. The first *in vivo* triple-negative xenograft study with the mGluR1-specific antagonist Bay 36-7620 was also shown by the same group with promising tumor-suppressive activities *in vivo*. In human melanoma cells, we have shown that Riluzole indirectly antagonizes mGluR1 by reducing the availability of its natural ligand, glutamate. While the mechanism by which iGluRs exert a tumorigenic effect in melanoma is yet unknown, it is apparent from the recent findings that limiting glutamate signaling in general by way of reducing the ligand may prove more beneficial than targeting any one receptor subtype.

1.5 Questions for the future

Although it is clear that glutamate signaling plays a significant role in the pathophysiology of cancer progression, the precise mechanisms by which mGluR transforms cells remain unknown. The recent buzz surrounding the reprogramming of tumor cell metabolism begins with the observation of the 'Warburg effect', where fast-growing cancer cells increase their glucose uptake, which is subsequently metabolized by aerobic glycolysis despite sufficient oxygen [129]. Increasing evidence also points to a glutamine addiction in cancer cells [130]. These abnormalities occur as a consequence of oncogenic transduction signals such as PI3K/AKT and Myc. In the mitochondria, glutamine is converted into glutamate by glutaminase (GLS) before entering the tricarboxylic acid (TCA) cycle. Overexpression of Myc has been shown to stimulate the activity of glutaminase. Moreover, the pharmacological intervention of glutaminase activity is capable of inhibiting oncogenic transformation [131]. Besides gaining a foothold in promoting cell growth, abnormal cell metabolism also increases the production of mitochondrial reactive oxygen species (ROS).

We hypothesize that glutamine addiction in cancer cells may disrupt the homeostasis of exported glutamate and imported cystine (Figure 2). Under normal conditions, cystine is rapidly converted to cysteine and, together with glutamate and glycine, yields glutathione (GSH). The GSH and GSH peroxidase systems are critical players in the regulation of cellular redox states. Therefore, an increase in intracellular glutamate concentrations will result in a decrease in cystine transport and therefore reduce intracellular levels of GSH, exposing cells to oxidative stress and genomic instability [132-134]. Although this concept is certainly provocative and requires further investigation, significant progress has been made since our first report on the oncogenic role of mGluR1 in melanoma development and progression. A better understanding of

the transforming properties of mGluRs at the molecular level will identify the functional role of mGluRs and the glutamatergic pathway, which will be important for the development of new therapeutic strategies.

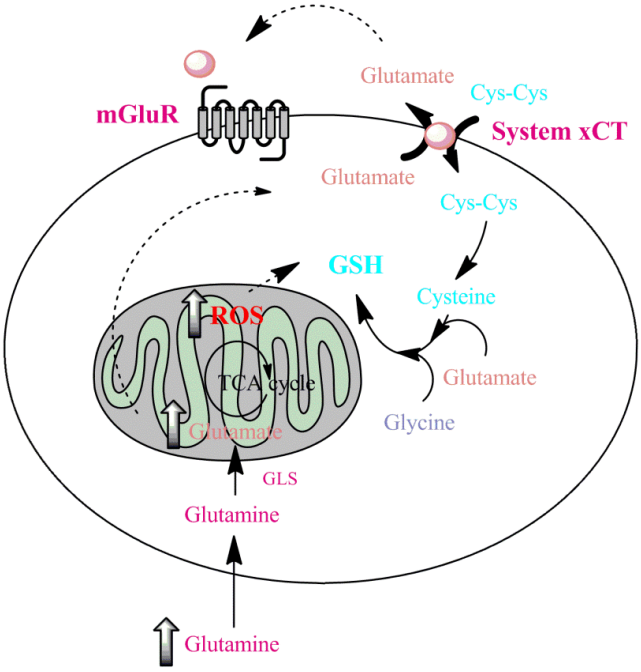

Figure 2. Proposed mechanism of mGluR transformation

Cancer cells display altered cell metabolism induced by oncogenic signals such as MAPK or PI3K/AKT, which is a downstream target of mGluR1. One of the key features includes glutamine addiction. In a transformed cell, increased uptake of glutamine is followed by a rapid conversion of glutamine into glutamate by GLS before feeding into the TCA cycle. Metabolic stress leads to elevated reactive oxygen species (ROS), which is normally neutralized by GSH. However, we speculate that the increased levels of intracellular glutamate perturbs the homeostasis of cystine-glutamate antiporter system (xCT) thus, leading to a decrease in cystine intake and impaired GSH formation exposing normal cells to oxidative stress and genomic instability. However, it is important to note that once transformed, the cancer cell takes advantage of GSH to maintain growth under hypoxic conditions thus, conferring therapeutic resistance [135, 136]. Cys, cystine. GSH, glutathione. GLS, glutaminase. ROS, reactive oxygen species. TCA, tricarboxylic acid.

CHAPTER 2

METABOTROPIC GLUTAMATE RECEPTOR 1 MEDIATES MELANOCYTE TRANSFORMATION VIA TRANSACTIVATION OF IGF-1 RECEPTOR

Abstract

Our lab previously described the oncogenic properties of metabotropic glutamate receptor 1 (mGluR1/Grm1) in melanocytes. Ectopic expression of mGluR1 transformed immortalized mouse melanocytes *in vitro* and induced vigorous tumor formation *in vivo*. Subsequently, we observed the activation of PI3K/AKT in mGluR1-mediated melanocytic tumorigenesis *in vivo*. In particular, we identified AKT2 being the predominant isoform contributing to the activation of AKT. Suppression of Grm1 or AKT2 using an inducible Tet-R siRNA system resulted in a 60% and 30% reduction respectively in *in vivo* tumorigenesis. We show that simultaneous down-regulation of Grm1 plus AKT2 results in a reduction of approximately 80% in tumor volumes suggesting that both mGluR1 and AKT2 contribute to the tumorigenic phenotype *in vivo*. The discrepancy between the mild *in vitro* transformation characteristics and the aggressive *in vivo* tumorigenic phenotypes of these stable Grm1-melanocytic clones led us to investigate the possible involvement of other growth factors. Here, we demonstrate a novel pathway for mGluR1-mediated tumorigenesis involving the transactivation of IGF-1R. Disrupted IGF-1R signaling in stable Grm1-melanocytic cells led to the ablation of mGluR1-induced AKT activation and reduced tumor growth. We propose that IGF-1R activation represents a previously overlooked key pathway involved in the mechanisms by which mGluR1 exerts its transformative properties.

2.1 Introduction

We have successfully generated several stable mGluR1-expressing mouse melanocytic clones (MASS clones), which exhibited tumorigenic characteristics in vivo [75]. Moreover, we identified two major signaling pathways that underlie Grm1-mediated melanocytic transformation. The first pathway is MAP Kinase which is specifically activated in response to L-Quisqualate (Q), a Group I mGluR agonist and suppressed by Bay 36-7620, a specific antagonist of mGluR1. Furthermore, we observed elevated levels of phosphorylated AKT/Protein Kinase B in allografts of MASS clones [76]. The AKT kinase family consists of three highly homologous isoforms, AKT1/PKB-α, AKT2/PKB-β, and AKT3/PKB-ɣ. Despite being similar in structure, all three AKT isoforms have non-overlapping function [137]. For instance, upon insulin stimulation of adipocytes, Akt2 accumulates at the plasma membrane environment at a larger degree than Akt1 [138]. Additionally, AKT2 has been shown to enhance cell migration in mammary epithelial cells both *in vitro* and *in vivo* whereas AKT1 plays an inhibitory role [139, 140].

In melanoma, Stahl and colleagues showed upregulation of AKT3 in cell lines established from various phases of primary melanoma tumors [141]. The targeting of AKT3 by siRNA was sufficient to inhibit human melanoma xenograft tumor progression. However, a recent report demonstrated that loss of PTEN promotes the invasion and migration of melanoma cells via the activation of the AKT2 isoform [78]. Interestingly, we also showed AKT2 and not AKT3 to be the predominant isoform activated in human melanoma biopsy samples [76].

While MASS clones exhibit aggressive *in vivo* phenotype which included short latency, strong angiogenic activities and invasiveness, the *in vitro* transformation properties were only modestly altered. As a clue of the discrepancy in aggressiveness

between the *in vivo* and *in vitro* phenotypes, we observed the hyperactivation of AKT in MASS tumor allografts but not in cultured cells except by stimulation of the receptor with its agonist, L-Quisqualate. In particular, the AKT2 isoform was differentially activated in the excised allografted tumors. As such, we hypothesize that the *in vivo* microenvironment may contribute in part to promote the tumorigenic phenotype via activation of the PI3K/AKT signaling cascade. It is possible that *in vivo*, there exist an excessive supply of natural ligand, glutamate, which leads to the constitutive activation of the mGluR. Alternatively, we propose the existence of a paracrine supply of growth factors from neighboring stromal cells that feeds into the PI3K/AKT pathway. We screened various exogenous growth factors/ligands including those that activate receptor tyrosine kinases for the ability of one or more of these factors to modulate the activation of ERK and/or AKT. Insulin-like growth factor (IGF-1), a known upstream regulator of AKT, was the only growth factor among those tested that was able to stimulate AKT in cultured MASS clones [76]. In this study, we set out to determine whether IGF-1 Receptor (IGF-1R) participates in mGluR1-mediated transformation of melan-a cells.

2.2 Materials and methods

Antibodies and reagents

Anti-phosphorylated AKT (Thr308, Ser473), anti-AKT2 (5B5), anti-phosphorylated ERK1/2 (Thr202/Tyr204), anti-AKT, anti-ERK1/2, and anti-IGF-1R antibodies were purchased from Cell Signaling (Davers, MA, USA); IGF-1 (Recombinant Human Insulin Like Growth Factor-1) and anti-phosphorylated IGF-1R antibody were purchased from Invitrogen (Carlsbad, CA, USA); anti-mGluR1 was purchased from BD Biosciences (Franklin Lakes, NJ, USA), monoclonal anti-α-tubulin antibody was purchased from Sigma (St. Louis, MO, USA). C-myc tag antibody, L-Quisqualate [(L)-(+)-α-amino-3,5-dioxo-1,2, 4-oxadiazolidine-2-propanoic acid] and Bay 36-7620 [(3aS,6aS)-6anaphtalen-2-ylmethyl-5-methyliden-hexahydro-cyclopental[c]-furan-1-on] were purchased from Tocris (Ellisville, MO, USA). PPP (Picropodophyllin) and PP-2 (4-Amino-5-(4-chlorophenyl)-7-(t-butyl)pyrazolo[3,4-d]pyrimidine) were purchased from Calbiochem (San Diego, CA, USA). Riluzole was obtained from Sigma and OSI-906 (Linsitinib) was generously provided by OSI Pharmaceuticals Inc. and the National Cancer Institute, National Institutes of Health.

Cell culture conditions

Stable Grm1-melanocytic transfectants (MASS clones) were produced from introduction of exogenous Grm1 cDNA into immortalized, normal murine melanocytes, melan-a that were provided by Dr. Dorothy Bennett (St. George's, University of London, UK). UACC903 cells were provided by Dr. Jeffrey Trent (The Translational Genomics Research Center, Phoenix, AZ). 1205Lu cells and WM239A cells were provided by Dr. Meenhard Herlyn (Wistar Institute, Philadelphia, PA). All cells were maintained in RPMI plus 10% FBS.

A total of 1.25 µg siAKT2-Teto and 1.25 µg Zeocin™ plasmid DNA were co-transfected into siGrm1-MASS20-TetR cells5. Selection of siGrm1-siAKT2-MASS20 stable clones was performed with 400 µg/ml of Zeocin™.

Truncated IGF-1R cDNA tagged with the c-myc epitope was kindly provided by Dr. Douglas Yee (Minnesota, University of Minnesota, USA). This construct was transfected into one of the stable-Grm1-melanocytic clones, MASS20. Selection of IGF-1RDN-MASS20 stable clones was performed with 75 µg/ml of Zeocin™.

For induction experiments, the conditions were the same as reported [75]. Briefly, cells were grown in glutamate/glutamine free RPMI plus 10% dialyzed fetal bovine serum with the supplement of GlutaMax™ (Gibco Life Technologies, Invitrogen, Carlsbad, CA, USA) to minimize the effect of glutamate, the natural ligand of Grm1 for 3 days before the cells were plated out in glu/gln free RPMI medium for induction experiments.

Western immunoblots

Protein lysates were prepared as described previously [142]. Briefly, media was removed and cells were washed once with ice-cold phosphate buffered saline (PBS). After removal of PBS, extraction buffer was added directly to the plates and cells were collected with a cell scraper. Cell extracts were incubated on ice for 20 min. Cell debris was removed by centrifugation at 14000xg at 4°C for 20 min and supernatant was collected to measure protein concentration and for Western immunoblot analysis.

MTT assays

Each cell line was cultured in 96 well plates at $2x10^3$ per well with the following conditions; no treatment, vehicle (dimethyl sulfoxide, DMSO), Riluzole and OSI-906 or a combination of both Riluzole and OSI-906. Concentration of each treatment group is stated in the figure legends. Viable cells were measured at Day 4 and Day 7. At designated time points, 0.1 volumes of 5 mg/ml Thiazolyl Blue Tetrazolium Bromide (Sigma, St. Louis, MO, USA) in 1x phosphate-buffered saline were added to growth

medium, incubated for 4h at 37°C and then solubilized overnight with equal volume of 10% sodium dodecyl sulfate/0.1N HCl. A 96 well plate reader (Infinite 200 Tecan USA, Durham, NC, USA) was used to measure absorbance at 550 nm with a reference wavelength of 750 nm. The graphs represent the average of three independent experiments.

Immunoprecipitation

For immunoprecipitation, protein-A/G-agarose beads were used (Santa Cruz Biotechnology, Santa Cruz, CA, USA). Procedures were performed as per manufacturer's instructions. Briefly, lysate was incubated with rabbit anti-IGF-1R for 1 hr in 4°C. 20 µL of Protein-A/G agarose beads were added and incubated overnight at 4°C. After collecting the pellets by centrifugation at 2500 rpm for 5 min at 4°C, the pellets were washed four times with Triton-X-100 buffer. Washed pellets were then mixed with 40 µl of 1X electrophoresis buffer and boiled for 5 min. Samples were centrifuged and loaded for SDS gel electrophoresis.

Allograft assay

The Institutional Animal Care and Use Committee at Rutgers University approved all animal studies. To assess the effect of siGrm1 and siAKT2 on Grm1-induced tumorigenesis of MASS clones, 10^6 cells from each stable siGrm1siAKT-MASS clone were injected subcutaneously into each of the dorsal flanks of 6 week-old male immunodeficient nude mice (Taconic, Hudson, NY, USA). Appearance of the tumor was monitored daily and measured twice a week. When the tumor volumes reach $10mm^3$, mice were divided randomly into experimental and control groups. Mice in the experimental group were fed with doxycycline (0.2% w/v) containing drinking water and the control group was fed with regular drinking water. Drinking water was changed twice a week. Tumor volumes were measured twice a week with a vernier caliper and calculated by the formula (d^2 x D/2), D is the large number and d is the smaller one.

Similarly, to determine the effect of disrupted IGF-1R signaling in MASS clones, 10^6 cells from two stable IGF-1RDN-MASS20 clones were injected subcutaneously into each of the dorsal flanks of 6 week-old male immunodeficient nude mice (Taconic, Hudson, NY, USA). Tumors were monitored and measured as described above.

For the xenograft studies with Riluzole and OSI-906, human melanoma cells were injected into both dorsal sites of each mouse at 10^6 cells per site. Once tumor volumes reached $10mm^3$, mice were divided into no treatment and treatment groups. The treatment groups received vehicle (DMSO), Riluzole (10 mg/kg), OSI-906 (30 mg/kg) or the combination of Riluzole (5 mg/kg) and OSI-906 (15 mg/kg) by oral gavage daily. The doses of oral Riluzole and OSI-906 were based on published reports [143, 144].

2.3 Results

2.3.1 Both mGluR1 and AKT are required for the transformed phenotype of mGluR1-melanocytic clones

First, we evaluated whether AKT activation is solely contributed by mGluR1 *in vivo*. To test this, we generated stable inducible siGrm1-siAKT2-MASS clones utilizing a tetracycline-inducible siRNA system. TetO-siAKT2 recombinant DNA was transfected into inducible siGrm1-MASS20 clones from previous studies [76] and several stable clones harboring both siGrm1 and siAKT2 were isolated. Modulation of levels of mGluR1 and AKT2 expression in the presence of doxycyline (analog of tetracycline) was assessed by Western immunoblots (Figure 3A). Previously, suppression of mGluR1 expression in siGrm1-MASS clones led to a 60% reduction in allografted tumors in the presence of the inducer, doxycycline. These *in vivo* studies suggest that mGluR1 is required in part for the maintenance of tumorigenicity but also points to the involvement of additional factors in promoting melan-a transformation. Suppression of AKT2 isoform in MASS allografts resulted in a decrease in tumor volume *in vivo* of approximately 30% [76]. Here, we show that simultaneous down-regulation of Grm1 plus AKT2 leads to approximately 80-90% suppression of allografted tumors, these results strongly suggesting that both mGluR1 and AKT2 are involved in the tumorigenic phenotype *in vivo* (Figure 3B). Furthermore, these findings support our hypothesis that there exists at least one additional factor contributing to AKT2 activation *in vivo*.

Receptor tyrosine kinases (RTKs) are well-known key constituents of GPCR signaling which facilitates tumor progression in various malignancies by enhancing proliferative and/or cell survival signals [24, 145]. Previously, we identified IGF-1 as being able to activate AKT in cultured MASS20, suggesting the expression and

functionality of IGF-1R (or related receptor) in MASS cells [76]. Now we confirm the expression of IGF-1R in MASS20 allografts. Interestingly, not only was IGF-1R expressed in MASS20 allografts, the activation of the receptor occurred in a time-dependent manner peaking at Day 10 post initial appearance of tumor (Figure 3C).

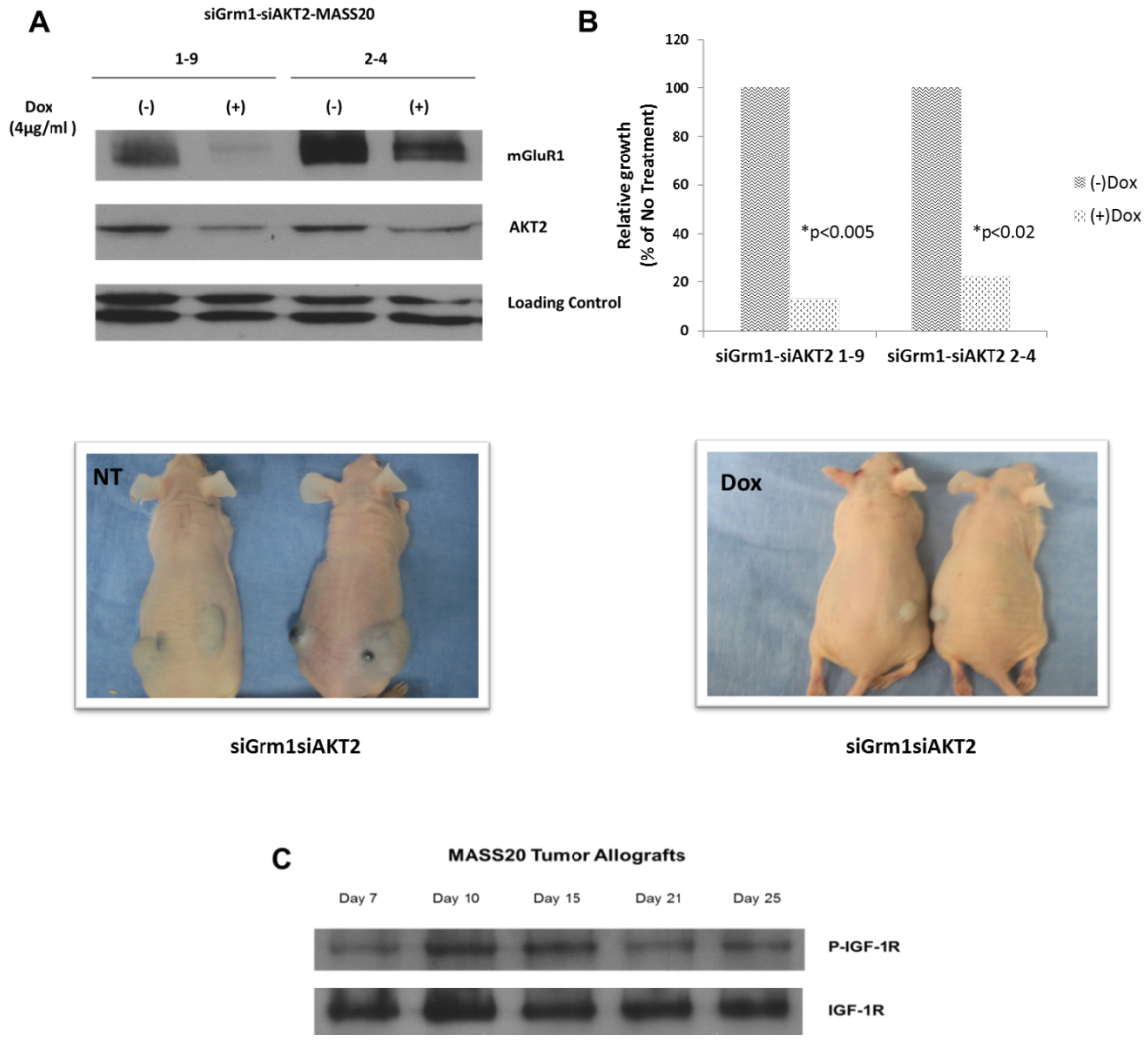

Figure 3. Reduced tumorigenicity in MASS20 cells by siRNA to Grm1 plus AKT2.

(A) siGrm1-siAKT2-MASS20 clones were grown in the presence or absence of the inducer of siRNA, doxycycline, for the indicated time points up to 7 days. Expression of mGluR1 and AKT2 was suppressed in the presence of doxycycline (4 µg/ml). (B) Simultaneous suppression of mGluR1 and AKT2 were assessed by inoculating two different inducible siGrm1-siAKT2-MASS20 clones (10^6 cells/site) into immunodeficient nude mice. The inducer, doxycycline (0.2% w/v) was supplied in the drinking water. Approximately, 80-90% of tumor volumes were suppressed in siGrm1-siAKT2-MASS20 clones ($p<0.02$, t-test, n=10). (C) Levels of phosphorylated IGF-1R peaked at Day 10 post-initial appearance of MASS20 allografts.

2.3.2 mGluR1 activation induces IGF-1R transactivation

Furthermore, induction of mGluR1 with a Group I mGluR agonist, L-Quisqualate (10 μM) in cultured cells caused a rapid transient activation of IGF-1R, which is abolished by pre-incubation with mGluR1-specific antagonist, Bay 36-7620 (10 μM) (Figure 4A). Because the antibody used to assess IGF-1R phosphorylation cross-reacts with insulin receptor, an immunoprecipitation approach was employed to verify that the 95kD band is indeed IGF-1R. MASS20 cells were induced with L-Quisqualate (10 μM) for 30 minutes and extracts were prepared and first immunoprecipitated with IGF-1R antibody followed by immunoblotting using p-IGF-R antibody (Figure 4B).

Next, we examine whether transactivation of IGF-1R contributes to mGluR1-mediated transformation of mouse melanocytes. First we confirmed our earlier observation that incubation of MASS20 cells with a Group I mGluR agonist, L-Quisqualate (Q) for 30 min led to activation of AKT (Figure 4C). Inclusion of IGF-1R specific inhibitor, PPP, resulted in the absence of AKT phosphorylation above basal levels even in the presence of mGluR1 agonist (Q), suggesting that both mGluR1 and IGF-1R contribute to stimulation of AKT (Figure 2C). Several earlier studies have postulated that Src-family tyrosine kinases serve as intermediates between GPCR and RTKs [146]. Src is a well-established player in EGFR signaling, directly phosphorylating two key tyrosine residues and allowing mitogenic signals. We assessed the possibility that intracellular tyrosine kinase Src participates as a signaling intermediate for mGluR1-induced IGF-1R tyrosine phosphorylation. Pretreatment of MASS20 with a Src inhibitor, PP2 for 15 minutes (10 μM), followed by stimulation with Q for 15 minutes resulted in the ablation of IGF-1R tyrosine phosphorylation (Figure 4D), suggesting that Src is upstream of IGF-1R transactivation. As expected, mGluR1-induced AKT phosphorylation was also suppressed with PP2 pre-treatment. Interestingly, MAPK signaling was also disrupted

suggesting a divergent pathway following Src kinase activation before reaching IGF-1R (Figure 4D).

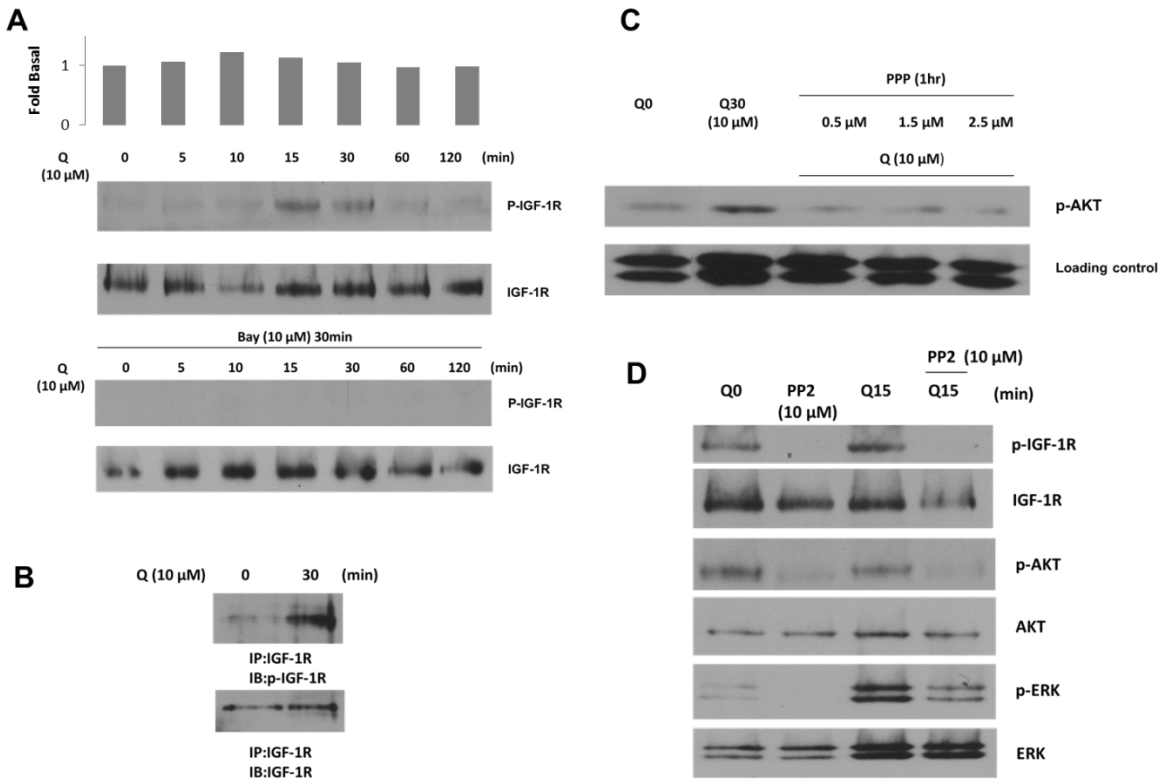

Figure 4. Activation of mGluR1 transactivated IGF-1R.

(A) Time-course of L-Quisqualate-(10 μM) induced IGF-1R phosphorylation in MASS20 (top panel). Pre-treatment with mGluR1-specific antagonist, Bay 36-7620 (10 μM) abolished this transactivation (middle panel). (B) MASS20 cells treated with or without L-Quisqualate (10 μM) for 30 min then lysed with Triton-X100 buffer and immunoprecipitated with IGF-1R specific antibody followed by immunoblot with phosphorylated IGF-1R antibody (bottom panel). (C) MASS20 cells were pre-treated with IGF-1R inhibitor, PPP for 1 hr at indicated concentrations before treatment with L-Quisqualate (10 μM). (D) MASS20 cells were pretreated with Src inhibitor PP2 (10 μM) for 1hr, and then treated with L-Quisqualate (10 μM) for 15 min.

2.3.3 IGF-1R is required for mGluR1-mediated tumorigenesis

We further confirm the involvement of IGF-1R signaling, by taking advantage of a Myc-tagged dominant-negative IGF-1R construct. MASS20 cells were stably transfected with either empty vector or the truncated IGF-1R mutant. The truncated receptor retains the ligand binding site but lacks the autophosphorylation domain [147]. Several IGF-1RDN-MASS20 clones were isolated (Figure 5A) and the consequences of the mutated IGF-1R on AKT signaling were assessed. In contrast to the parental MASS20 cells, IGF-1 (5 ng/ml) was unable to activate AKT in IGF-1RDN-MASS20 cells (Figure 5B). Furthermore, confirming our previous observation, dominant negative IGF-1R expression inhibited mGluR1-mediated activation of AKT (Figure 5C).

To verify that IGF-1R participates in the tumorigenic phenotype of MASS clones, we subcutaneously injected one vector control-MASS20 and two IGF-1RDN-MASS20 clones into immunodeficient nude mice. Although tumors were detectable in both Vector-MASS20 and IGF-1RDN-MASS20 clones, there was a significant reduction (approximately 40%) in IGF-1RDN-MASS20 tumor volumes by day 31 in comparison to Vector-MASS20 (Figure 5C). Taken together, our *in vivo* data put forth the notion that functional IGF-1 signaling is indeed required for mGluR1-mediated tumorigenesis potentially mediated via the functional transactivation of IGF-1R.

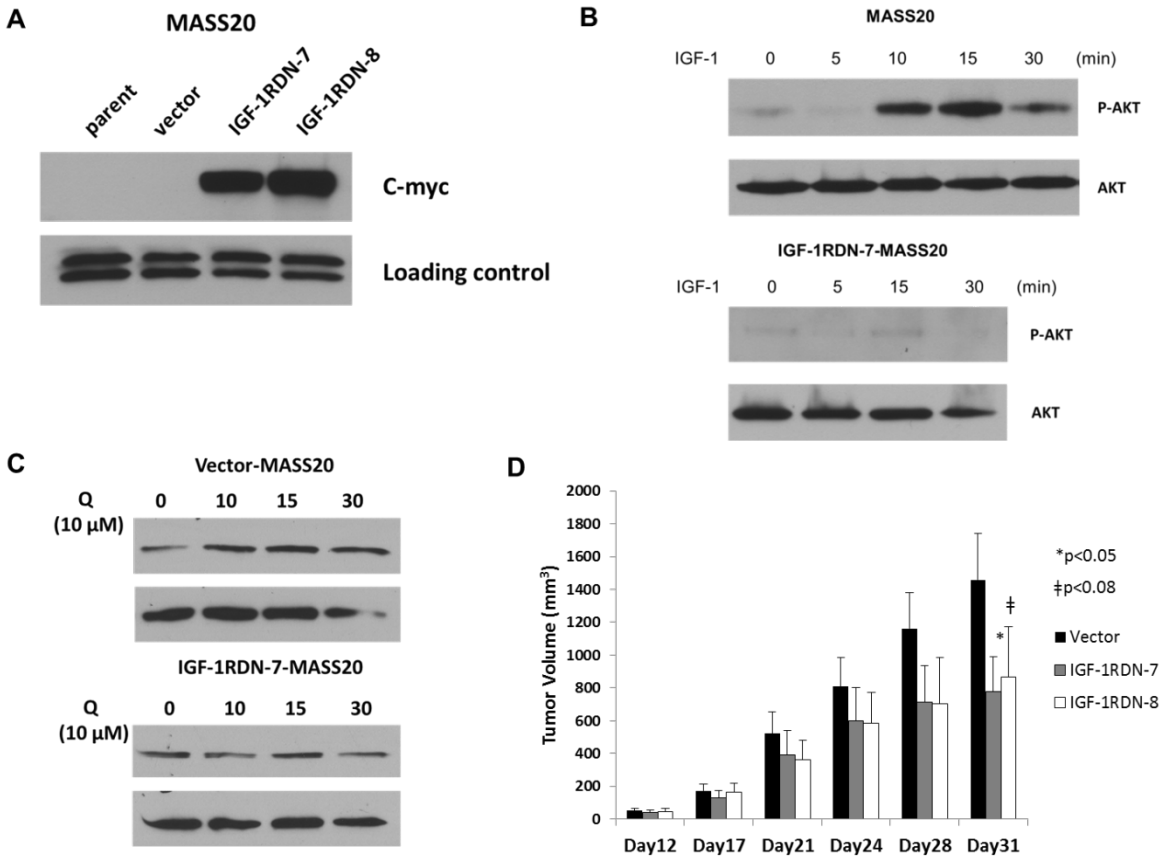

Figure 5. Functional IGF-1R is required for mGluR1-mediated tumorigenicity.

(A) Expression of c-Myc-tagged truncated IGF-1R mutant in IGF-RDN-MASS20 clones was visualized by immunoblotting for c-Myc tag. (B) Activation of AKT in IGF-1 treated parental MASS20 cells. Truncated IGF-1R mutant in MASS20 cells inhibits IGF-1 (5 ng/ml)-induced AKT activation (bottom panel). (C) Expression of truncated IGF-1R inhibits mGluR1-mediated activation of AKT. (D) One vector control and two different IGF-1RDN-MASS20 clones were inoculated into immunodeficient nude mice. Approximately, 35% of tumor volumes were suppressed in IGF-1RDN-MASS20 clones as compared to Vector-MASS20 ($p<0.05$ for IGF-1RDN-7 clone and $p<0.08$ for IGF-1RDN-8 clone, t-test, n=10).

2.3.4 Co-inhibition of glutamate signaling and IGF-1R signaling in human melanoma cells leads to decreased tumor growth

Finally, to evaluate the potential clinical implications in our findings, we explored the efficacy of combining Riluzole, an inhibitor of glutamate release and an inhibitor of IGF-1R, Linsitinib (OSI-906) using human melanoma cell lines. B-RAF and N-RAS are among the most common mutations in cutaneous melanoma encompassing 75% and 15% of malignant melanoma cases respectively [56, 148]. The constitutive activation of MAPK pathway in tumors harboring B-RAF and N-RAS mutations are thought to render tumor cells refractory to targeting upstream signaling elements such as mGluR1 or receptor tyrosine kinases. However, we have shown in completed Phase 0 and II trials of single-agent Riluzole, an FDA-approved drug for amyotrophic lateral sclerosis, to have anti-tumor activity in patients with advanced melanoma regardless of their BRAF/NRAS status [126]. We selected a potent inhibitor of IGF-1R that is orally efficacious in pre-clinical models, OSI-906, currently in clinical development for advanced solid tumors [149-151]. In *in vitro* MTT assays all three mGluR-expressing human melanoma cell lines, C8161 (B-RAF wild-type), 1205Lu (B-RAFV600E mutant) and WM239A (B-RAFV600D mutant) displayed enhanced efficacy in suppressing cell growth in the presence of both Riluzole and OSI-906 as compared with single agent alone regardless of their B-RAF genotypes (Figure 6A). Previously, we showed a reduction in MAPK signaling in Riluzole treated human melanoma cells. Here, we demonstrate enhanced suppression of both phospho-AKT and phospho-ERK with the combination of Riluzole and OSI-906 compared to either agent alone (Figure 6B). Given these encouraging *in vitro* findings, we next assessed the combined efficacy of Riluzole and OSI-906 on established xenografted tumors *in vivo*. Remarkably, the *in vivo* combinatorial application using only half the optimal dose for single agents showed a synergistic

reduction of tumor progression as evident by the decrease in tumor volumes in both B-RAF-wild type and B-RAF-mutant xenografts as compared with vehicle controls (Figure 6C).

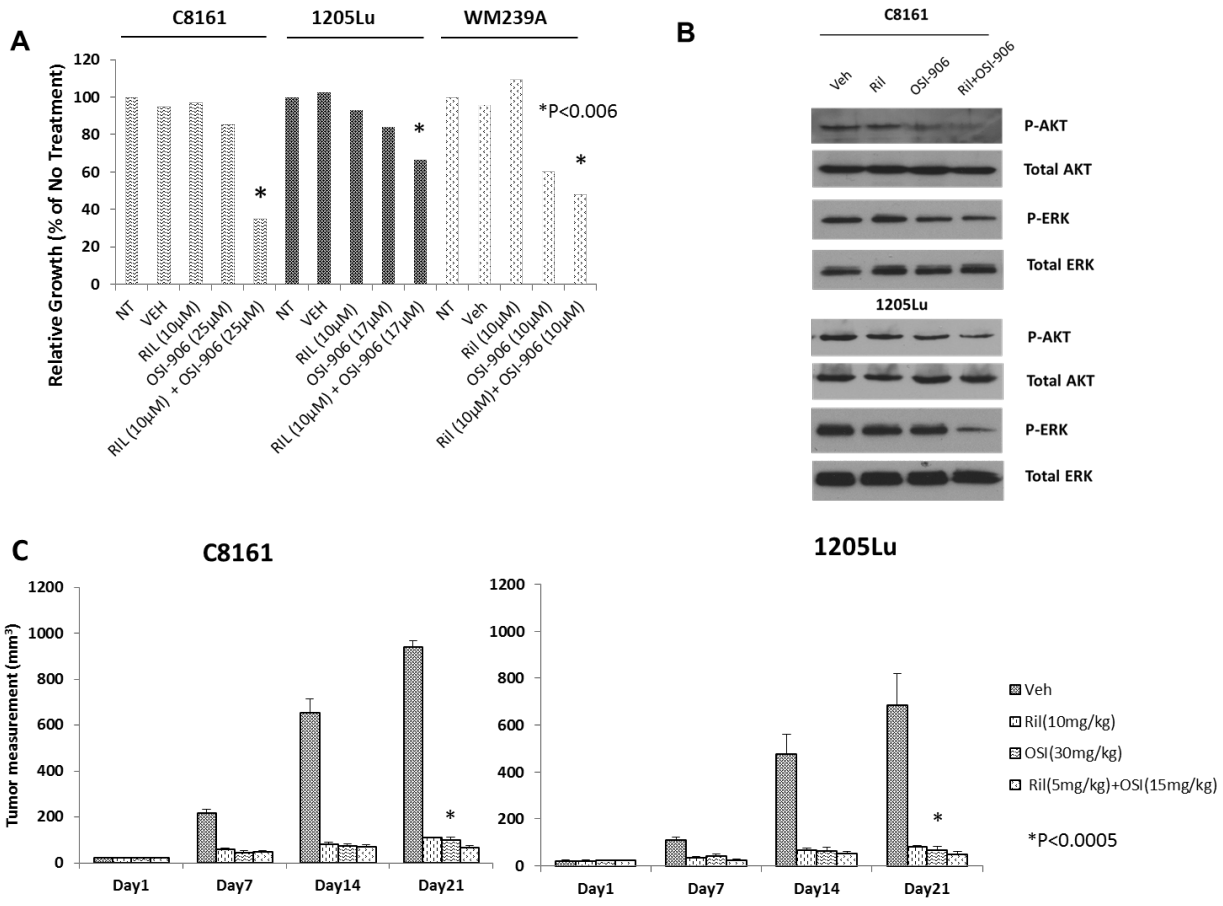

Figure 6. Suppression of growth of mGluR1-expressing human melanoma cells with Riluzole and OSI-906.

(A) MTT assays of C8161 (B-RAFwild-type), 1205Lu (B-RAFV600E), WM239A (B-RAFV600D) with glutamate release inhibitor, Riluzole and IGF-1R inhibitor, OSI-906 or combination of both compounds. (B) Effects of Riluzole and OSI-906 on phosphorylated-AKT and phosphorylated-ERK levels. C8161 (Ril; 10 μM, OSI; 25 μM) and 1205Lu (Ril;10 μM, OSI;10 μM). (C) Xenografts of C8161 (B-RAFwild-type) and 1205Lu (B-RAFV600E). The groups were no treatment (NT), vehicle (Veh; DMSO), Riluzole (10 mg/kg), OSI-906 (30 mg/kg), or the combination of Riluzole (5 mg/kg) and OSI-906 (15 mg/kg). All agents were given daily by p.o. gavage. Each treatment group was compared to vehicle group, $p<0.0005$, t-test, n=10. The combinatorial treatment groups were also

compared to single agent Riluzole and single agent OSI-906, $p<0.05$, t-test, n=10, (except combinatorial treatment group for 1205Lu xenografts was not statistically significant when compared to single agent OSI-906, $p=0.17$).

2.3.5 Increased p-IGF-1R expression in non-responders from Phase 0 and Phase II Riluzole trial

Additionally, we examined tumor biopsies from five patients with advanced metastatic melanoma from both completed Phase 0 and II trials treated with Riluzole [126]. The tumors of all five responders and non-responders patients were positive for mGluR1 expression. Five sets of paired tumor samples (pre-treatment and post-treatment) were analyzed for phospho-IGF-1R and phospho-AKT levels. Interestingly, reduced phospho-IGF-1R and phospho-AKT levels were detected in responder from both Phase 0 and stable disease in Phase II trials (Patient 9 and Patient 1 respectively) (Figure 7). In contrast, increased levels of phospho-IGF-1R were detected in tumor biopsies of non-responders, Patient 6 and 12 from Phase 0 and Patient 3 from Phase II (Figure 7). Correspondingly, phospho-AKT levels were also increased in non-responders (Patient 12 from Phase 0 and Patient 3 from Phase II). Patient 6 from Phase 0 trial displayed unchanged phospho-AKT levels but elevated phospho-IGF-1R, suggesting that activation of the IGF-1R/PI3K/AKT axis may be associated with resistance to Riluzole.

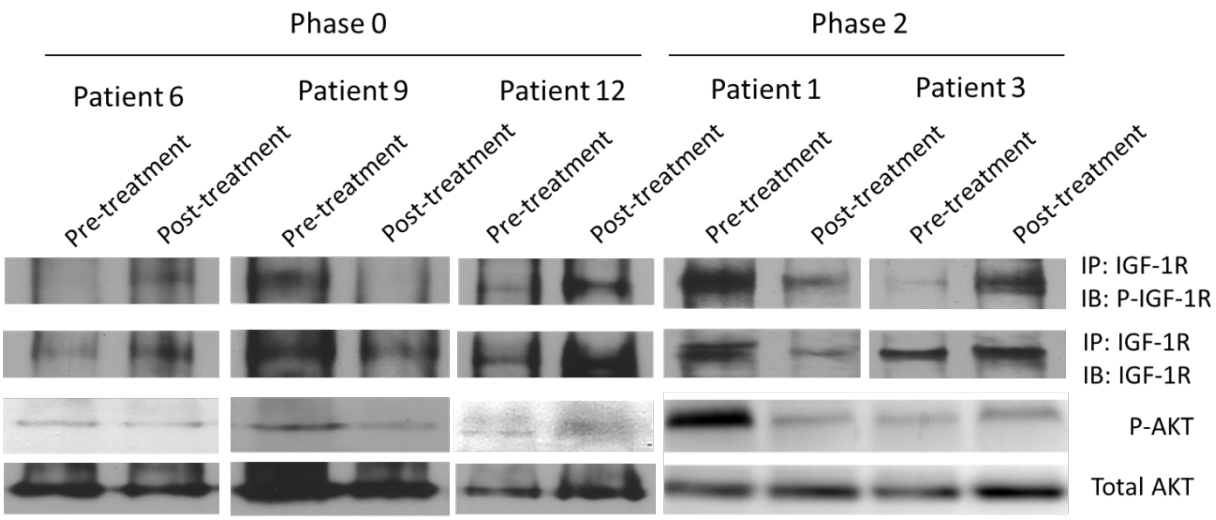

Figure 7. Increased phospho-IGF-1R expression in non-responding patients of Phase 0 and Phase II Riluzole trials.

Paired tumor samples from pre-treatment and post-Riluzole treatment were analyzed for P-IGF-1R or P-AKT expression by Western immunoblots. A reduction in levels of P-IGF-1R and P-AKT was detected in Phase 0 responder (Patient 9) and Phase II patient with stable disease (Patient 1). In contrast, non-responders in Phase 0 (Patient 6 and 12) and Phase II (Patient 3) Riluzole trials showed elevated P-IGF-1R and P-AKT levels or unaltered P-AKT in Patient 6. The blots were subsequently stripped and probed with IGF-1R and AKT antibodies as control.

2.4 Discussion

Several recent reports by other groups implicate both ionotropic and metabotropic glutamate receptors in oncogenesis; overexpression of mGluR5 and activating mutations in GRIN2A and GRM3 in melanoma [82, 85]. Other noteworthy findings include the identification of over 20 missense mutations in GRM1 in various tumor types, some of which has been characterized to have multiple downstream consequences [152]. Our group was the first to show through insertional mutagenesis resulting in the disruption of intron 3 of Grm1 and the ectopic expression of mGluR1 in melanocytes which ultimately produced spontaneous metastatic melanomas with 100% penetrance [72]. Conventionally, GPCRs and RTKs were thought to represent distinct signaling units converging only further downstream in the signaling cascade [153]. Recently, it is becoming more apparent that they do not operate exclusively but rather cross-communicate with G protein activity occurring either upstream or downstream of RTKs [153, 154]. Although crosstalks between GPCRs and RTKs are not novel, this is the first report, which demonstrates the functional transactivation of IGF-1R by mGluR1 in Grm1 transformed mouse melanocytic cells (Figure 8). Some other well characterized examples demonstrating IGF-1R transactivation by GPCRs include angiotensin II type 1 (AT1) receptor in smooth muscle cells and GABAβ receptor in neuronal cells [155, 156]. Results from our studies suggest that the mechanism involved is more similar to that exerted by AT1 receptor which is dependent on Src kinase activation [156]. In addition, we also present evidence that activation of the PI3K/AKT pathway occurs via IGF-1R, which in turn contributes to mGluR1-mediated tumorigenesis. This substantiates earlier reports on the cross-coupled signaling between mGluRs and epidermal growth factor receptors (EGFR) with significant implications in glial cell physiology and pathogenesis [25, 157].

Whether or not melanoma cells produce IGF-1 is controversial. It has been speculated that IGF-1R expressing melanoma cells receive signal from paracrine sources of IGF-1 such as neighboring keratinocytes and fibroblasts because IGF-1R expression correlates with melanoma progression [158, 159]. However, Molhoek and colleagues recently showed the expression of IGF-1 mRNA in melanoma cells [160] thus, the possibility that melanoma cells produce IGF-1 and create autocrine loops cannot be ruled out. Human relevance of our current studies was put forth in the *in vivo* tumorigenesis studies with reduced tumor progression by inhibitors to glutamate and IGF-1R signaling. Interestingly, we also observed that biopsies from our completed Phase 0 and II trials, non-responders showed elevated levels of phosphorylated IGF-1R in post-treatment samples in comparison to pre-treatment biopsies (Figure 7). In contrast, samples from one responder in the Phase 0 trial and one patient with stable disease in the Phase II trial did not show amplified P-IGF-1R in post-treatment samples. Despite the small sample size, these promising results suggest the merit of combining Riluzole and OSI-906 to circumvent the challenge of drug resistance. This is in line with our previous observation of patients who did not show clinical or radiologic response in the Phase 0 trial but exhibit high or similar levels of phosphorylated AKT in their post-treatment tumor biopsies [126]. Similarly, IGF-1R/PI3K signaling was shown to be enhanced in B-RAF-inhibitor resistant melanomas [90]. Presence of IGF-1 ligand has also been shown to override the suppression of AKT activity by B-RAF inhibitor, PLX4720 [161]. Taken together, we propose that IGF-1R activation represents a previously overlooked key pathway involved in the mechanisms by which mGluR1 exerts its transformative properties and warrants further investigation.

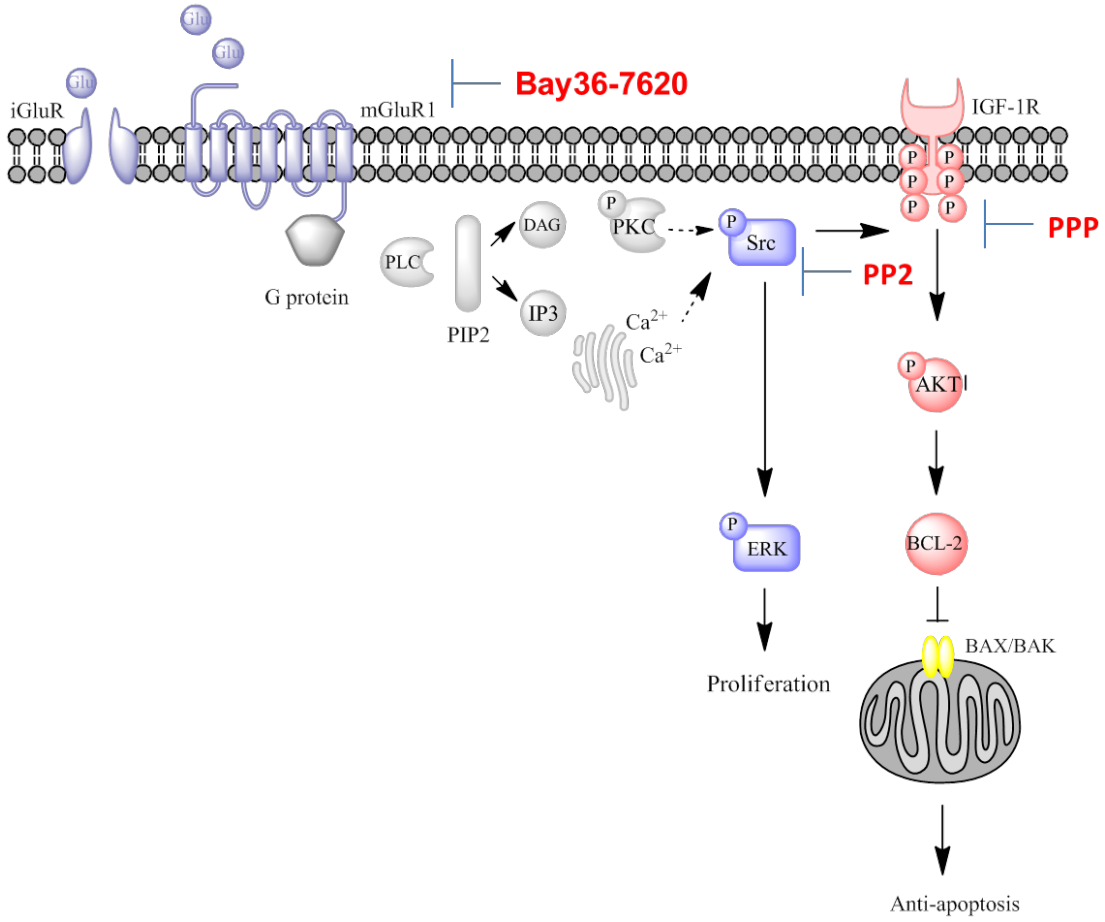

Figure 8. Proposed signaling pathways activated by mGluR1 and mediated by IGF-1R transactivation.

CHAPTER 3

METABOTROPIC GLUTAMATE RECEPTOR 1 DISRUPTS MAMMARY ACINAR ARCHITECTURE AND PROMOTES MAMMARY TUMORIGENESIS

Abstract

Metabotropic glutamate receptor 1 (mGluR1/Grm1) is a member of the G-protein coupled receptor superfamily, which was once thought to only participate in synaptic transmission and neuronal excitability, but has more recently been implicated in non-neuronal tissue functions. We previously described the oncogenic properties of Grm1 in cultured melanocytes *in vitro* and in spontaneous melanoma development with 100% penetrance *in vivo*. As most human cancers are of epithelial origin, we utilized immortalized mouse mammary epithelial cells (iMMECs) as a model system to study the transformative properties of Grm1. We introduced Grm1 into iMMECs and isolated several stable mGluR1-expressing clones. Phenotypic alterations in acinar architecture were assessed using three-dimensional (3D) morphogenesis assays. We found that mGluR1-expressing iMMECs exhibited delayed lumen formation in association with decreased central acinar cell death, disrupted cell polarity, and a dramatic increase in the activation of the mitogen-activated protein kinase (MAPK) pathway. Orthotopic implantation of mGluR1-expressing iMMEC clones into mammary fat pads of immunodeficient nude mice resulted in mammary tumor formation *in vivo*. Persistent mGluR1 expression was required for the maintenance of the tumorigenic phenotypes *in vitro* and *in vivo*, as demonstrated by an inducible Grm1-silencing RNA system. Our results are likely relevant to human breast cancer, as mGluR1 was found to be expressed in human breast tumor biopsies and breast cancer cell lines. Taken together, our findings demonstrate that mGluR1 is oncogenic in mammary epithelial cells and may play a role in the pathophysiology of breast cancer.

3.1 Introduction

Recent studies have implicated mGluR1 in epithelial tumorigenesis, as mGluR1 was reported to regulate proliferation in triple negative breast cancer cells and the tumor inhibitory effects of mGluR1 antagonists were shown in an MDA-MB-231 xenograft tumor model [103]. Furthermore, two polymorphic variants of GRM1, rs6923492 and rs362962 were found to associate with breast cancer phenotypes [107]. Interestingly, low mGluR1 expression level appears to correlate with a longer distant metastasis-free survival (DMFS) in patients with estrogen receptor (ER)- positive breast cancers treated with tamoxifen suggesting a functional role for mGluR1 in the setting of active hormone signaling [107]. In patients with prostate cancer, serum glutamate levels correlated with Gleason score and high levels of mGluR1 expression was detected in primary and metastatic tissues [123]. In addition, we demonstrated the transformation of immortalized primary baby mouse kidney (iBMK) cells with exogenous Grm1 *in vitro* and tumorigenesis *in vivo* as well as functional glutamate signaling in corresponding human tumor type, renal cell carcinoma [162]. These reports indicate an important role for mGluR1 in various malignancies and thus provide clear clinical implications. However, neither the mechanism by which Grm1 mediates mammary epithelial cell transformation nor whether the sustained mGluR1 expression is required in breast mammary tumorigenesis is well understood.

Currently, breast cancer is the most common malignancy afflicting women in the United States with over 232,000 cases diagnosed every year, also ranking second in the number of cancer deaths among women, preceded only by lung cancer [163]. The normal breast comprises a network of ducts and lobules, which ultimately give rise to terminal ductal lobular unit (TDLU) structures. It is within the epithelium of these units that the most invasive form of breast cancer is thought to arise. The TDLU is made up of

a collection of acinar structures consisting of a single layer of polarized luminal epithelial cells surrounding a hollow lumen. Three-dimensional (3D) epithelial culture systems, which allow epithelial cells to organize into structures that resemble *in vivo* architecture, are useful for elucidating the functions of cancer genes and pathways in a biologically relevant context. One such model involves the use of immortalized mouse mammary epithelial cells (iMMECs) which form polarized solid acini in the presence of extracellular matrix similar to the well-characterized nonmalignant human mammary epithelial cell line MCF10A [164, 165]. Due to the predictable, chronologic changes in morphology with mammary epithelial cells, the iMMEC model has been used to evaluate altered morphologic and developmental patterns as a result of the expression of oncogenic signals [166, 167]. To directly investigate the possible role of Grm1 in regulating breast tumorigenesis, we examine the consequences of introducing exogenous Grm1 into iMMECs. We now report that by disrupting acinar morphogenesis, Grm1 induces transformation of mammary epithelial cells *in vitro* by disrupting acinar morphogenesis and promotes mammary tumorigenesis *in vivo*. Furthermore, modulation of GRM1 signaling suppresses tumor growth of ER-positive human breast cancer cell xenografts in nude mice, suggesting that this pathway plays an important role in breast cancer pathogenesis and can be pharmacologically targeted for breast cancer treatment.

3.2 Materials and Methods

Antibodies, reagents and Western immunoblots

Anti-phosphorylated AKT (Ser473), anti-AKT, anti-phosphorylated ERK1/2 (Thr202/Tyr204), anti-ERK1/2 antibodies were purchased from Cell Signaling (Danvers, MA, USA). Anti-Grm1 antibody (mouse) was purchased from BD Biosciences (Franklin Lakes, NJ, USA), anti-GRM1 antibody used for Western immunoblots (human) was purchased from Novus Biologicals (Littleton, CO, USA), anti-GRM1 used for immunofluorescent staining was purchased from Upstate (now Milipore, Billerica, MA, USA). Monoclonal anti-α-tubulin antibody, doxycycline hyclate and Riluzole were purchased from Sigma (St. Louis, MO, USA). Anti-53BP1 antibody was purchased from Bethyl Laboratories Inc. (Montgomery, TX, USA), phospho H2AX antibody was purchased from EMD Milipore Corporation (Temecula, CA, USA). Alexa fluor 488 goat anti-mouse IgG, alexa fluor 546 goat anti-rabbit IgG were purchased from Life Technologies (Carlsbad, CA). Secondary antibodies, donkey anti-Rabbit IgG Antibody,-HRP conjugate and Goat Anti-Mouse IgG,-H&L Chain Specific Peroxidase Conjugate and Luminata Western HRP substrates were purchased from Milipore (Billerica, MA, USA). MK-2206 was generously provided by Merck & Co., Inc. and the National Cancer Institute, National Institutes of Health.

Protein lysates were prepared as described previously [142]. Briefly, media was removed and cells were washed once with ice-cold phosphate buffered saline (PBS). After removal of PBS, extraction buffer was added directly to the plates and cells were collected with a cell scraper. Cell extracts were incubated on ice for 20 min. Cell debris was removed by centrifugation at 14000xg at 4°C for 20 min and supernatant was collected to measure protein concentration with Detergent Compatible Protein Assay

(Bio-Rad Laboratories, Hercules, CA, USA) and 25 µg of protein is routinely used for Western immunoblot analysis.

Cell culture, transfection and generation of stable cell lines

iMMECs were produced from mouse mammary epithelial cells isolated from young, C57BL/6 virgin female mice and immortalized through the inactivation of Rb and p53 pathways as described [164, 168]. Cells were maintained in regular iMMEC growth medium (F12 medium supplemented with 5 µg/ml insulin, 1 µg/ml hydrocortisone, 5 µg/ml EGF) with 10% FBS. MCF7 cells were maintained in RPMI supplemented with 10% FBS.

Coding sequence for the full-length α form of Grm1 was subcloned from mouse-brain cDNA library [169] into mammalian expression vector pCI-neo (Promega, Madison, WI, USA). A total of 2.5 µg Grm1 cDNA was transfected into iMMECs ($3X10^5$ cells) using DOTAP transfection reagent (Roche, Mannheim, Germany). Stable Grm1-transfectants were selected using 100 µg/ml neomycin in regular iMMEC growth medium.

TetR plasmid (neomycin-resistant) was co-transfected with Zeocin plasmid and TetR clones were selected with Zeocin (Invitrogen) at a concentration of (300 µg/ml). siGrm1 or siGFP sequence was cloned into the inducible siRNA expression vector pRNATin-H1.1/Hygro (GenScript, Piscataway, NJ, USA). Stable siRNA/TetR-transfected iMMEC-Grm1 clones were selected in Hygromycin B (Invitrogen, Grand Island, NY, USA) at a concentration of (50 µg/ml). siGRM1-MCF7 clones were selected in neomycin (300 µg/ml) and Hygromycin B (50 µg/ml). For induction of siGrm1, 4 µg/ml of doxycycline was added a day after plating and medium was replaced every 4 days in 2D or 3D cultures.

The 3D cultures of iMMECs were generated as described [164]. Mammary acini were grown in iMMEC growth medium and 2% growth factor reduced matrigel (BD Biosciences, Franklin Lakes, NJ, USA). The medium was replaced every 4 days.

3D morphogenesis

Mammary acini were fixed and processed for immunofluorescence as previously described [164]. Acini were incubated with primary antibodies overnight at 4°C, washed and then incubated with fluorescein- or rhodamine-coupled secondary antibodies for 2h at room temperature. Finally acini were stained with TO-PRO-3, washed and mounted with Prolong anti-fade. Confocal laser scanning was carried out with a Nikon Eclipse C1 Confocal Microscope.

Antibody	Function	Normal localization	Source	Species
Cleaved Caspase-3	Apoptosis maker	Apoptotic cells in luminal space	Cell Signaling	Rabbit
B-Catenin	Cell-cell junction	Basolateral	Zymed Lab	Mouse
TO-PRO-3	Nuclear counterstain	Nuclei	Invitrogen	NA
GM130	Apical polarity	Golgi (apically located)	BD	Mouse
Ki-67	Proliferation marker	Nuclei of proliferating cells	Dako Cytomation	Rat
Phospho-ERK	ERK activation	Cytosol and nucleus	Cell Signaling	Rabbit
Total ERK	ERK activation control	Cytosol and nucleus	Cell Signaling	Rabbit

Tumorigenicity assays

iMMECs expressing mGluR1 or empty vector were harvested by trypsinization and resuspended in PBS (10^7cells/ml). Orthotopic mammary gland implantation of iMMECs was performed according to our Institutional Animal Care and Use Committee approved protocol. Immunodeficient nude female mice at 5-6 weeks old were anesthetized with

Avertin. A small incision was made to expose the second pair of mammary fat pads on both sides and each mammary gland pad was subjected to implantation with 10^6 cells. The incision was closed with surgical clips that were removed 10 days later. Tumor growth was monitored weekly with a vernier caliper and calculated with the formula (d^2 x D/2) as described [170]. Studies were terminated as soon as tumor volumes reached maximally permissible size. Similar protocol was carried out for the following *in vivo* studies: siGrm1/TetR iMMECs (10^8 cells/ml) and MCF7 ($5x10^7$ cells/ml). For the siGrm1/TetR studies, once tumor volumes reached $10mm^3$, mice were divided into two treatment groups. Doxycycline (0.2% w/v) was included in the drinking water of doxycycline treatment groups to induce siGrm1 expression in siGrm1/TetR iMMEC cells and replaced twice a week.

For the MCF7 xenograft study, once MCF7 tumor volumes reached 10 mm^3, mice were divided into treatment groups. The treatment groups received vehicle (DMSO), Riluzole (10 mg/kg), MK-2206 (30 mg/kg), or the combination of Riluzole (10 mg/kg) and MK-2206 (15 mg/kg) by oral gavage daily for Riluzole and twice a week for MK-2206. The experiments were terminated when the xenografts on the no-treatment or vehicle group reached the maximum permitted size.

Immunofluorescent staining

Cells were grown on glass coverslips to the appropriate density and synchronized by serum starvation for 48 hours. Following synchronization, cells were treated with Riluzole (25 μM). At each time point, cells were fixed with 4% paraformaldehyde in PBS and permeabilized for 10 minutes in 0.5% Triton X-100 in PBS at room temperature. Cells were then washed with PBS and blocked in 5% goat serum/PBS. Primary antibodies (53BP1 anti-rabbit IgG and phospho H2A anti-mouse IgG) were incubated at room temperature in blocking solution. Cells were washed with PBS for 5 min and incubated with Fluorophore-conjugated secondary antibody (Alexa Fluor 488 goat anti-

mouse IgG and Alex Fluor 546 goat anti-rabbit IgG, for 1 h in blocking solution. Cells were washed with PBS for 5 min and mounted using Vectashield (Vector Laboratories, Burlingame, CA). Images were captured using a Nikon Eclipse microscope coupled with a Coolsnap EZ camera powered by NIS-Elements BR 3.1 software.

A similar method was used to detect mGluR1 expression in breast cancer cells. Cells were fixed immediately after serum starvation and incubated with mGluR1 anti-rat IgG, Upstate (now, Milipore, Billerica, MA, USA).

Immunohistochemistry

The human tissues were obtained from the Biospecimen Retrieval Services at Rutgers Cancer Institute of NJ. CINJ Histopathology and Imaging Core performed the IHC for mGluR1 and unbiased quantitative assessment of IHC staining was completed using a digital Aperio ScanScopeGL system and ImageScope software (v10.1.3.2028) (Aperio Technologies Inc., Vista, CA, USA) as described [171].

Cell proliferation/viability (MTT) assay

Each cell line was cultured in 96 well plates at $2x10^3$ per well with the following conditions: no treatment or doxycycline (4 µg/ml). Viable cells were measured at Day 4 and Day 7. At designated time points, 0.1 volumes of 5mg/ml Thiazolyl Blue Tetrazolium Bromide (Sigma) in 1x phosphate-buffered saline were added to growth medium, incubated for 4h at 37°C and then solubilized overnight with equal volume of 10% sodium dodecyl sulfate/0.1N HCl. A 96 well plate reader (Infinite 200 Tecan USA, Durham, NC, USA) was used to measure absorbance at 550 nM with a reference wavelength of 750 nM.

Glutamate release assay

Cells were seeded at $4x10^3$ per well and cultured in 200 µl glutamate/glutamine-free medium with 10% dialyzed FBS. At measurement, half of the volume was removed from each well for glutamate assay and cell-viability immediately assessed by MTT assay.

Glutamate concentration in culture medium was measured by Amplex Red Glutamic Acid/Glutamate Oxidase Assay Kit (Invitrogen, Carlsbad, CA, USA).

Cell cycle analysis

Cells were plated at 1 x 10^6 per 100 mm dish and treated with 50 μM Riluzole or vehicle (dimethyl sulfoxide) for 24-48 hours. Adherent and floating cells were pooled, pelleted, washed twice with ice-cold 1X phosphate-buffered saline, fixed by drop-wise addition of ice-cold 70% ethanol while mixing and stored at 20°C. Fixed cells were washed twice with and resuspended in 1X phosphate-buffered saline, treated with RNase A solution (Sigma) at 100 mg/ml and stained with propidium iodide (Sigma) at 10 mg/ml for 30 min. Cell-cycle analysis was performed on a Coulter Cytomics FC500 Flow Cytometer (Beckman Coulter, Fullerton, CA, USA) at the Analytical Cytometry Core Facility, Rutgers University.

Analysis of *in vivo* Synergy Data.

The nature of the interaction between Riluzole and MK-2206, was analyzed by the combination index method [172]. The combination index was calculated using eq.:

Combination Index= $[IC_{Ril,\ Comb}/IC_{Ril}] + [IC_{MK,\ Comb}/IC_{MK}]$

where IC_{Ril} and IC_{MK} are the concentrations of Riluzole and MK-2206 needed to produce a given level of cytotoxicity when used alone, and $IC_{Ril,\ Comb}$ and $IC_{MK,\ Comb}$ are the concentrations needed to produce the same effect when used in combination. A combination index value of 1 indicates additive interaction, values less than 1 indicate synergistic interaction, and values greater than 1 indicate antagonistic interaction.

3.3 Results

A. Grm1 in mouse mammary epithelial cells

3.3.1 Ectopic expression of mGluR1 promotes cell proliferation and attenuates luminal apoptosis in 3D morphogenesis

To study the consequence of the ectopic expression of mGluR1 in mammary epithelial cells, several stable mGluR1-expressing iMMEC clones were generated using Grm1 cDNA [169]. Expression of mGluR1 in several independent iMMEC-Grm1 clones was verified through Western immunoblots (Figure 9A). Empty vector-transfected iMMEC clones showed undetectable levels of mGluR1 (Figure 9A).

We measured the levels of extracellular glutamate in these independent iMMEC-Grm1 clones as our previous studies suggest that aberrantly expressed mGluR1 behave similarly to GPCRs with oncogenic activity, displaying enhanced levels of locally produced ligands [80, 162]. These measurements were done in parallel with MTT cell proliferation/cell viability assays to ensure that any increases in extracellular glutamate was not due to release of intracellular glutamate by cell death. Two independent iMMEC-Grm1 clones showed excess in the levels of extracellular glutamate compared with control iMMEC-vector cells when adjusted for difference in growth rate over the course of the experiment as measured by MTT (Figure 9B).

iMMEC-Grm1 and vector clones were grown on a reconstituted basement membrane in a 3D cell culture system as previously described [164]. The 3D culture of mammary epithelial cells in basement membrane gel promotes the organized development of single-cell acinar structures that mimics mammary morphogenesis

during mammary gland development. Oncogenic events perturb this morphogenetic process leading to a distorted phenotype [166, 167].

We first investigated whether ectopic expression of mGluR1 affected the induction of apoptosis in central acinar cells during normal mammary morphogenesis by immunostaining with an antibody against the activated form of caspase-3, cleaved-caspase-3. In vector-expressing acini, apoptosis was visualized in the centrally located cells by day 14 (Figure 10A). By day 21, we observed the classical formation of a hollow lumen as previously described [164]. Remarkably, forced expression of mGluR1 significantly delayed lumen formation indicated by the reduced number of apoptotic cells in the luminal space. The amount of empty lumen in the different clones is expressed as a percentage of whole acini (Figure 10A).

Next, to determine whether mGluR1 expression affects cellular proliferation during morphogenesis, acinar structures were immunostained with a proliferation marker, Ki-67. At an early time-point (Day 7), both vector and mGluR1-expressing acini exhibited similar levels of Ki-67. At Day 14, compared to vector-expressing acini, which were mostly hollow, more cells were Ki-67-positive in acini generated by iMMEC-Grm1 clones (Figure 10B), even within the region of anticipated acinar luminal space. β-Catenin stains cell-cell junctions and was used to visualize epithelial cells.

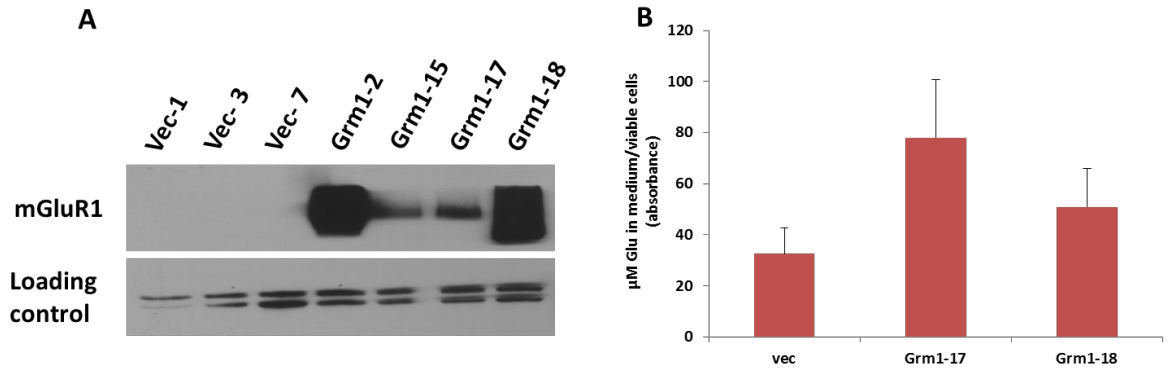

Figure 9. Isolation of stable mGluR1-expressing mammary epithelial cells.

(A) iMMECs were transfected with the full-length Grm1 α-form in pCI-neo or empty vector pCI-neo alone (vec). Independent stable clones exhibited varying levels of mGluR1 expression shown by immunoblotting. (B) iMMEC-Grm1 clones release glutamate. At the time of measurement (Day 4), half the volume of medium was removed for glutamate assay and the other half for cell-viability assessed by MTT. iMMEC-Grm1 clones released increased levels of extracellular glutamate when compared to iMMEC-vector even when adjusted for difference in growth rate over the course of the experiment as measured by MTT. Glutamate release is expressed as µM Glu per number of viable cells.

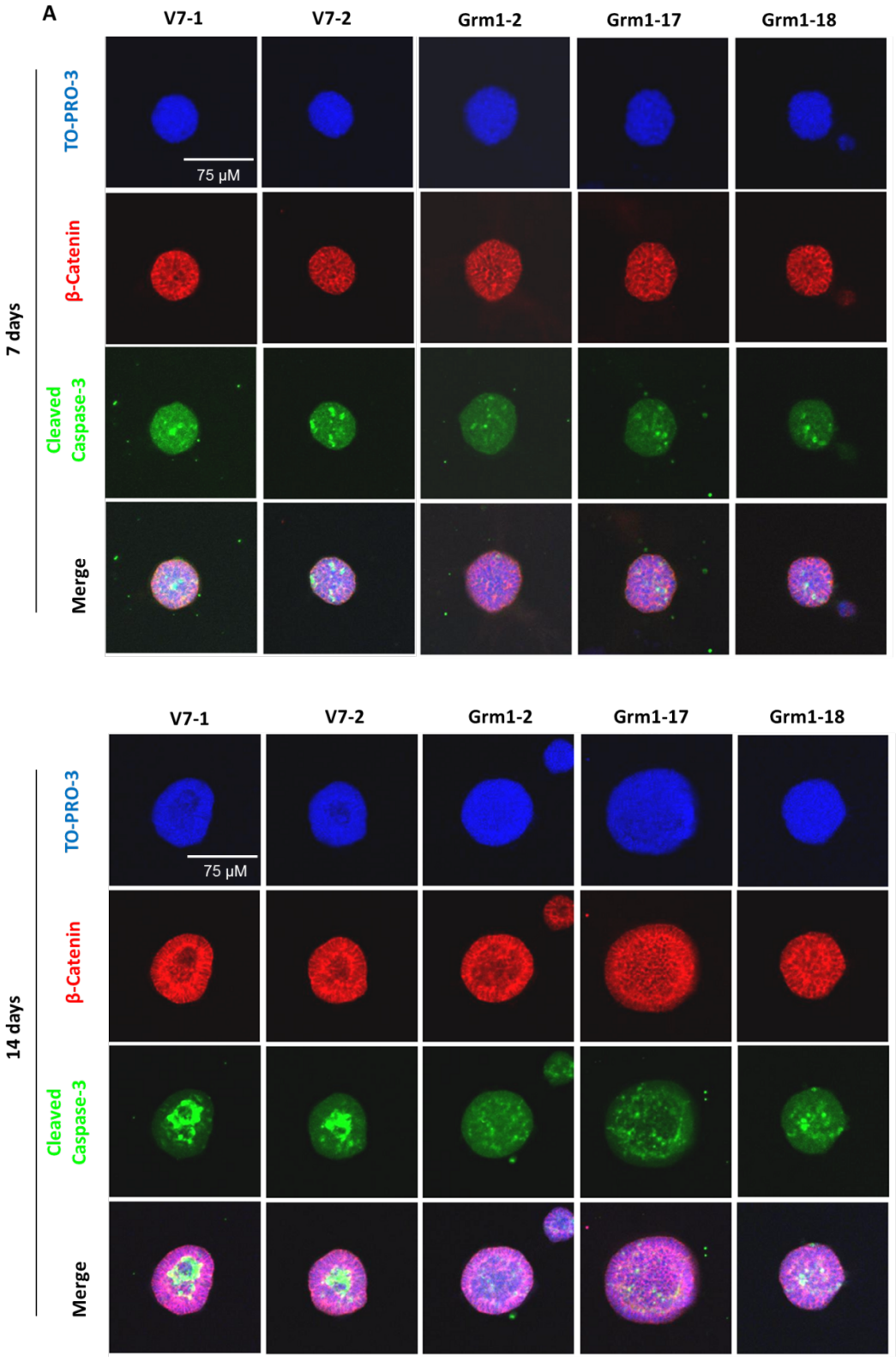
A
V7-1
V7-2
Grm1-2
Grm1-17
Grm1-18
7 days
TO-PRO-3
β-Catenin
Cleaved Caspase-3
Merge
75 μM
14 days
TO-PRO-3
β-Catenin
Cleaved Caspase-3
Merge
75 μM

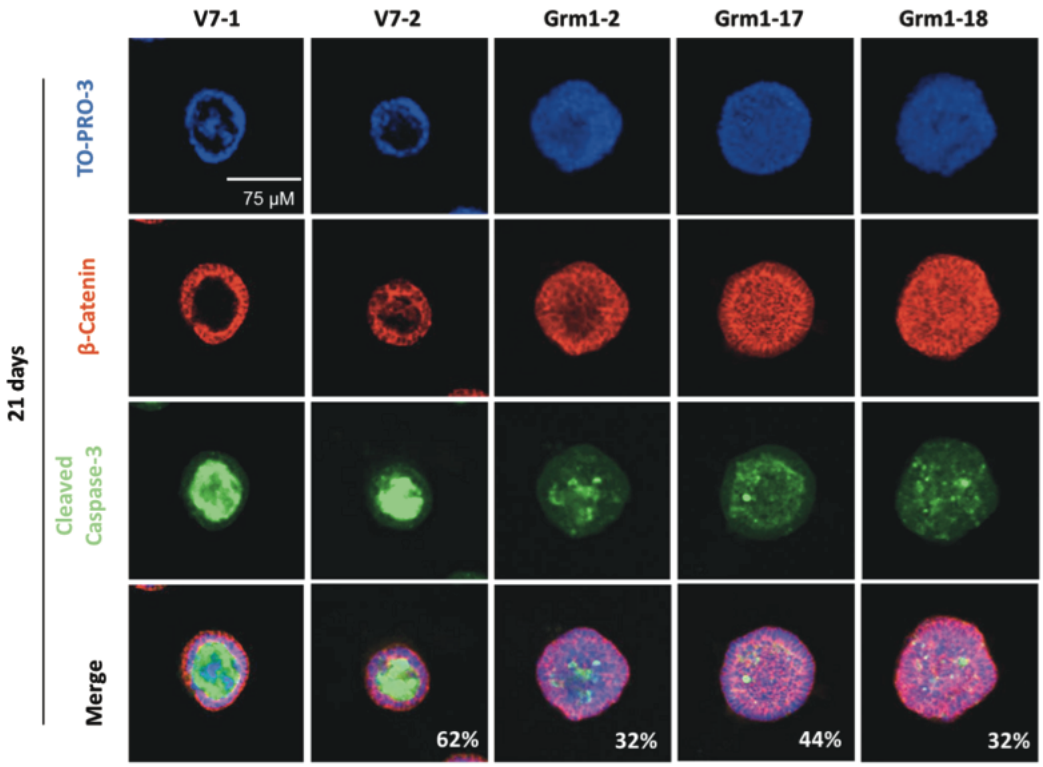

Figure 10. mGluR1 reduces apoptosis and promotes proliferation in iMMEC-Grm1 in 3D cultures. (A) Inhibition of apoptosis in iMMEC-Grm1. iMMECs stably expressing either empty vector (vec-7) or mGluR1 were grown in 3D culture. Acini were stained with TO-PRO 3 (blue; for nuclear counterstaining), β-catenin (red; to visualize epithelial cells) and cleaved-caspase 3 (green). Acini morphology at day 7, 14 and 21 after plating are shown. Images are representative of the majority of acini for a specific genotype at a given time point and the number indicated at the bottom right corner (day 21) is the percentage of acini with hollow lumens. A total of 300 acinar structures were evaluated for lumen formation.

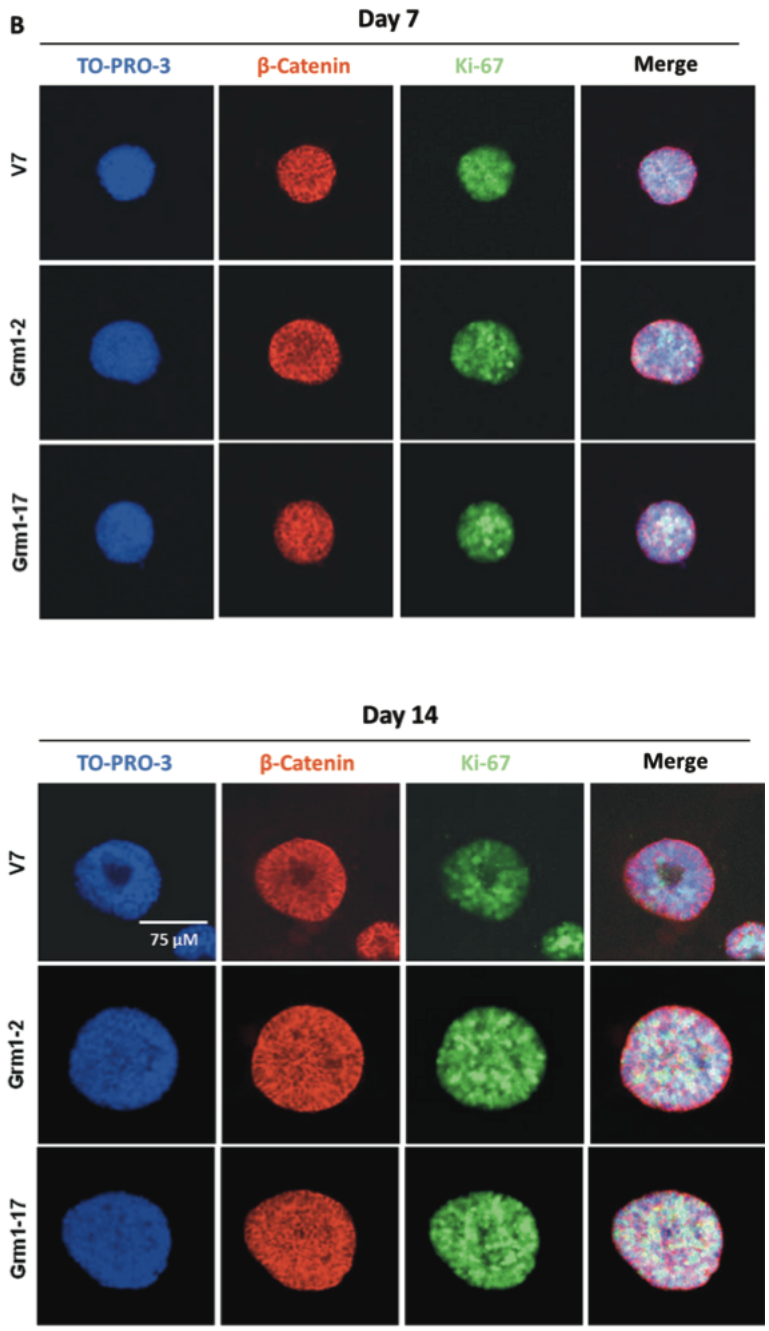

(B) Ectopic expression of mGluR1 promotes proliferation in iMMECs. Ki-67 (green) is used to visualize proliferating cells, TO-PRO 3 (blue; for nuclear counterstaining), β-catenin (red; to visualize epithelial cells). By Day 14, proliferating cells could be seen in the lumens of acini generated by iMMEC-Grm1, whereas Ki-67 signals were reduced and absent in the lumen of V7 acini.

3.3.2 Ectopic expression of mGluR1 leads to sustained activation of the MAPK/extracellular signal-regulated kinase

Based on our early observations [75, 80] and the hyperactivation of MAPK/ERK in many human neoplasms [173], we investigated the involvement of the MAPK/ERK pathway in mediating the proliferative effects of mGluR1. We probed the acinar structures for the phosphorylated form of ERK and total ERK. At an early time-point (Day 7), ERK is highly activated in both vector- and mGluR1-expressing iMMEC (Figure 11). This parallels the early events of mammary morphogenesis, which involves robust proliferation before undergoing growth arrest following lumen formation. As expected, we observed a loss of phosphorylated-ERK expression in iMMEC-vector at 14 days. In contrast, the signal was continually sustained in iMMEC-Grm1 acini suggesting that mGluR1 exerts its signals in mammary epithelial cells in part through the activated MAPK pathway.

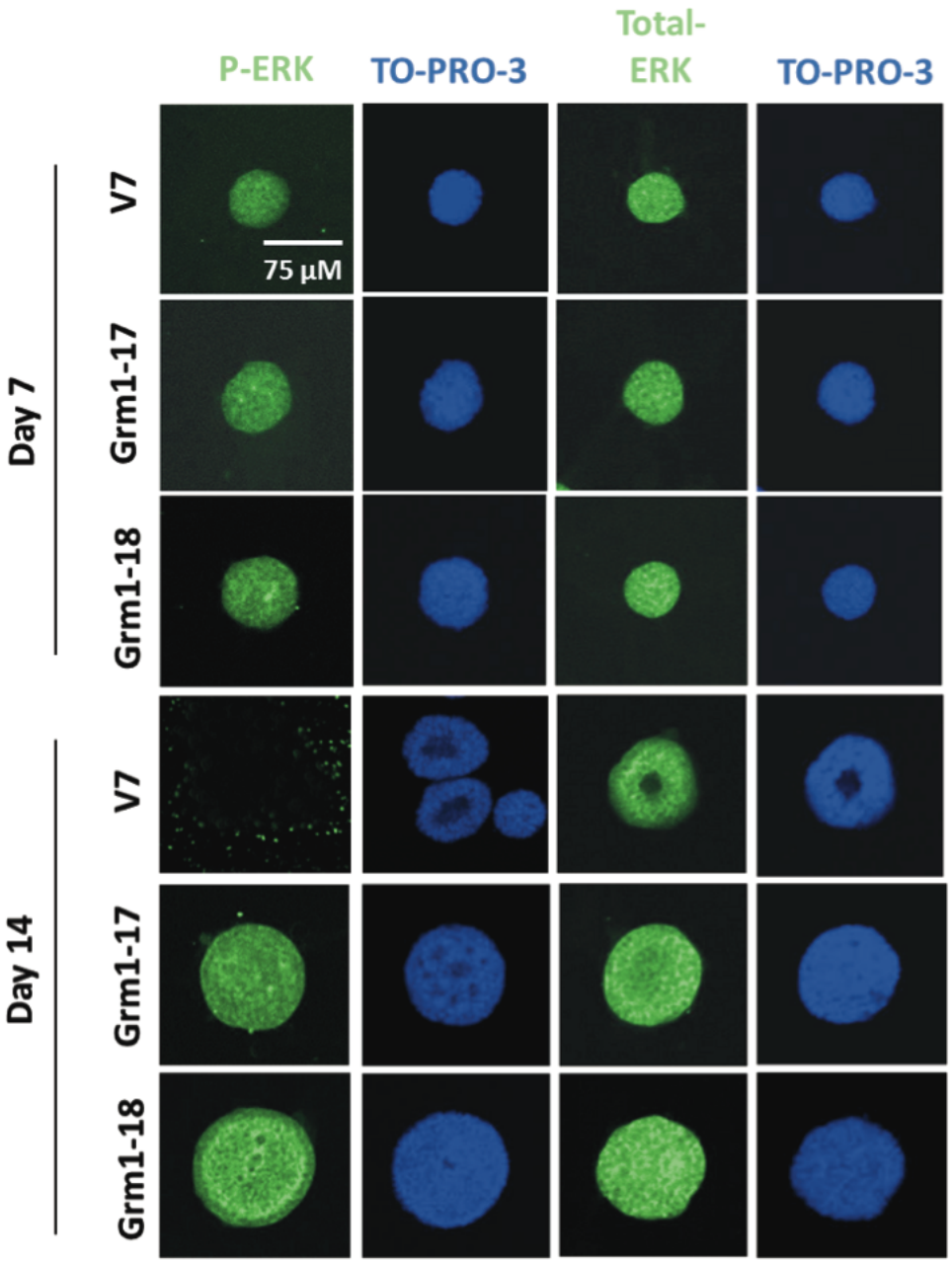
P-ERK
TO-PRO-3
Total-ERK
TO-PRO-3
Day 7
Day 14
V7
Grm1-17
Grm1-18
V7
Grm1-17
Grm1-18
75 µM

Figure 11. Ectopic expression of mGluR1 sustains ERK activation.

iMMECs-expressing empty vector clone (V7) or two independent mGluR1-expressing clones (Grm1-17 and Grm1-18) were plated in 3D cultures. Acini are shown at day 7 and day 14 after plating. 3D cultures were stained with phosphorylated-ERK or total-ERK (green) to visualize ERK activation and TO-PRO-3 (blue) to visualize nuclei. At day 7, phosphorylated-ERK levels were very similar among all clones but at day 14, phosphorylated-ERK staining was completely absent in V7, but still very prominent in two mGluR1-expressing clones. Total ERK levels were similar in all clones.

3.3.3 Ectopic expression of mGluR1 triggers changes in cell polarity

Establishment of apical-basal polarity in mammalian epithelia during mammary morphogenesis is an early event preceding both apoptosis of the central acinar and lumen formation [174]. To assess possible changes in polarity by exogenous Grm1, we monitored the orientation of the Golgi apparatus which is normally oriented toward the acinar lumen. Immunostaining with an apical polarity marker, GM130, showed that iMMEC-Grm1 acini at 21 days post-culture were depolarized with a disorganized pattern of GM130 staining (Figure 12). On the other hand, iMMEC-vector acini had a well-developed lumen and polarized Golgi apparatus suggesting that mGluR1 also affects the ability of mammary epithelial cells to maintain normal polarized organization

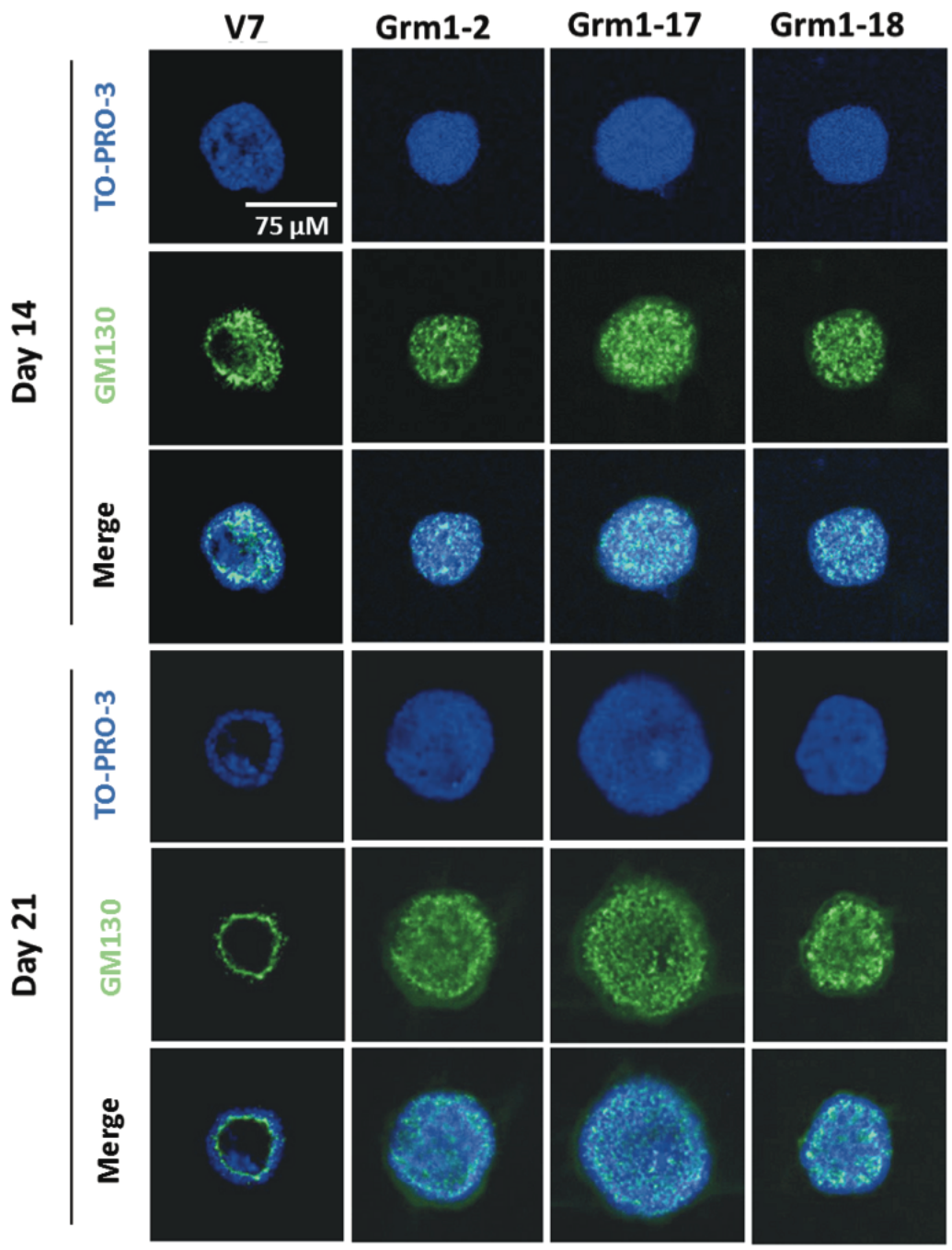

Figure 12. Ectopic expression of mGluR1 induces disruption in cell polarity.

Acini are shown at day 14 and day 21 after plating in 3D culture conditions. GM130 (green) stains the apical orientation of the Golgi apparatus toward the lumen of the acini, a marker for cell polarity. TO-PRO-3 (blue) is utilized to visualize nuclei of all cells.

3.3.4 Ectopic expression of mGluR1 induces mammary tumors

The ability to form tumors in *in vivo* tumorigenicity assays is the ultimate test of oncogenic transformation. To investigate whether glutamatergic signals provided solely by the exogenous expression of mGluR1 in mammary epithelial cells promoted tumorigenesis *in vivo*, we performed orthotopic implantation of both iMMEC-vector and iMMEC-Grm1 clones into the mammary fat pads of immunodeficient nude mice. The formation of palpable mammary tumors was monitored weekly. iMMEC-Grm1 clones developed tumors as early as 6 weeks post-implantation and a representative of the tumor growth kinetics is shown (Figure 13A). Excised iMMEC-Grm1 allografts displayed mGluR1 expression at various levels as demonstrated in immunoblots (Figure 13B). Interestingly, AKT was activated in a majority of the iMMEC-Grm1 allografts but not in the corresponding *in vitro* cultured cells. This observation is similar to our previous report in Grm1-mouse melanocytic clones [76]. P-ERK levels in the excised tumors were overall stable as shown by the quantification of immunoblot bands by densitometry. Representative high magnification of hematoxylin and eosin (H&E) staining of formalin-fixed sections of the excised allografts are also shown (Figure 13C). Tumors formed by two independent clones, IMMEC-Grm1-2 and -Grm1-17 displayed a “ribbon and gland” pattern characteristic of moderately differentiated adenocarcinoma with extensive tumor necrosis. The tumor representative of iMMEC-Grm1-18 also showed neoplastic epithelial cells attempting to form glands with an abortive ribbon pattern, that are much less organized than that of iMMEC-Grm1-2 and Grm1-17. Additionally, blood vessels were identified within iMMEC-Grm1-18-generated tumors.

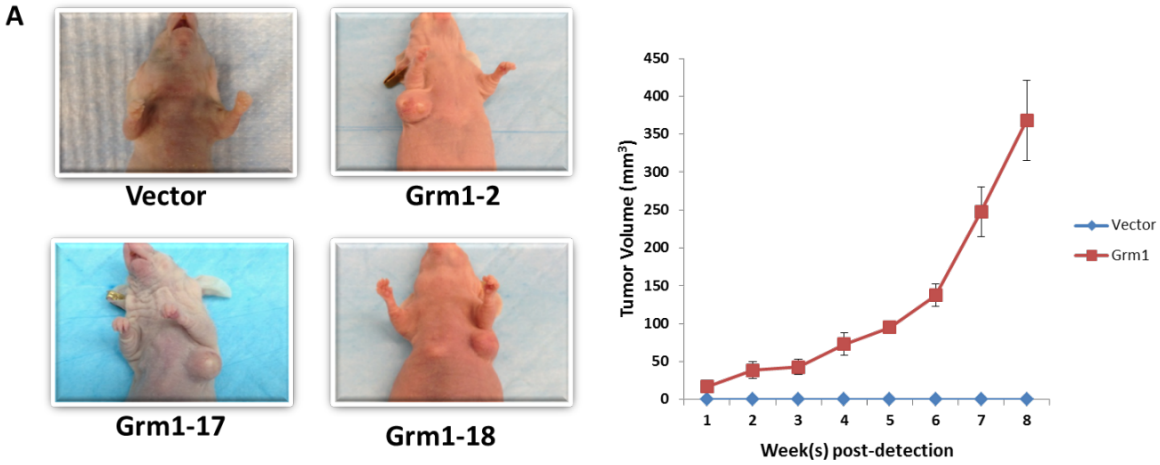
A
Vector
Grm1-2
Grm1-17
Grm1-18
Tumor Volume (mm3)
Week(s) post-detection
Vector
Grm1

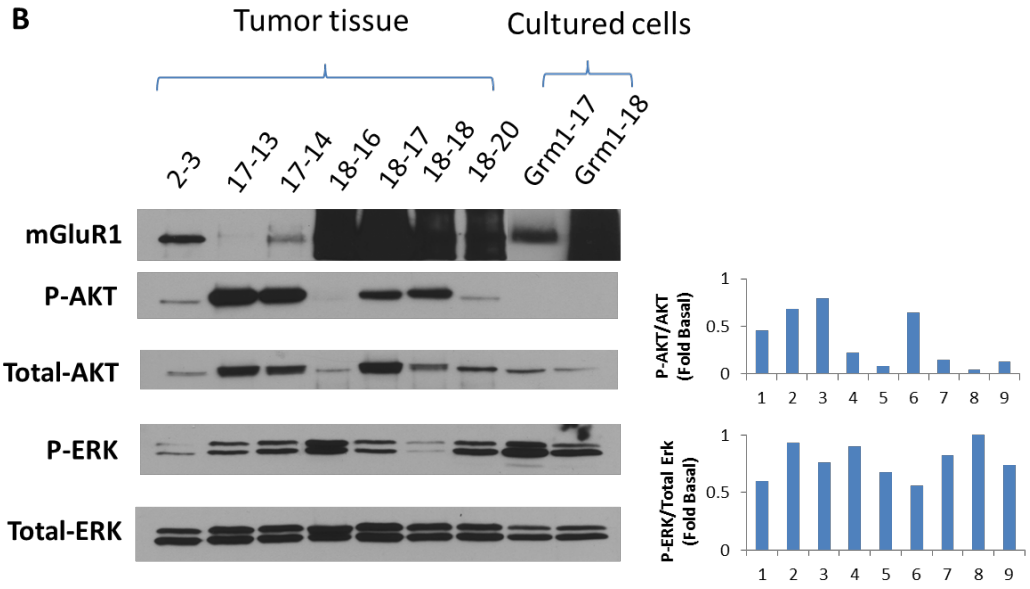
B
Tumor tissue
Cultured cells
2-3
17-13
17-14
18-16
18-17
18-18
18-20
Grm1-17
Grm1-18
mGluR1
P-AKT
Total-AKT
P-ERK
Total-ERK
P-AKT/AKT (Fold Basal)
P-ERK/Total Erk (Fold Basal)

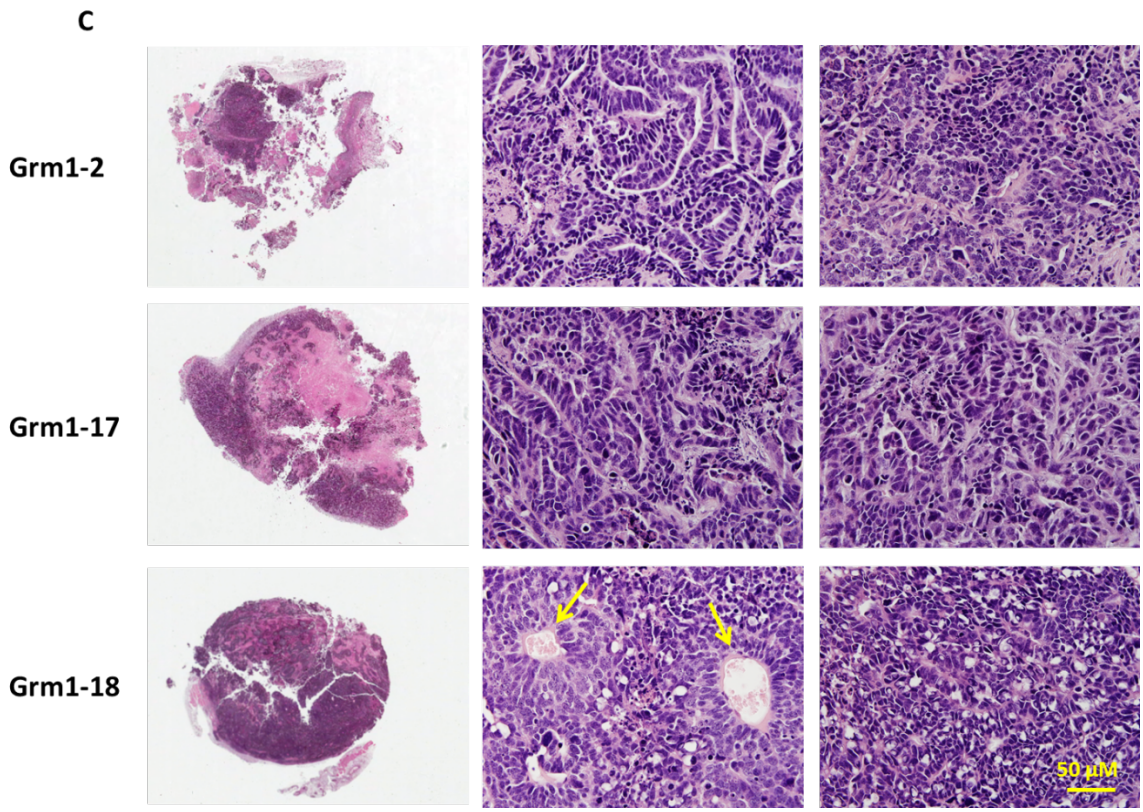

Figure 13. mGluR1 ectopically expressed in iMMECs promotes mammary tumor formation in athymic nude mice.

(A) At 6 weeks after implantation of iMMEC-Grm1 cells, palpable tumors were detected. All three iMMEC-Grm1 clones tested were tumorigenic *in vivo* (left panel). A representative of growth kinetics of implanted allografts is shown (right panel). (B) Levels of mGluR1, phosphorylated-AKT and phosphorylated-ERK in cultured iMMEC-Grm1 clones and corresponding excised allografts were examined by Western immunoblots. mGluR1 expression was detected in cultured and excised tumor samples. Various levels of phosphorylated-ERK were observed in all samples, phosphorylated-AKT was detected only in excised allograft tumor samples but not in iMMEC-Grm1 under normal culture conditions. Ratio of phospho to total AKT by densitometry. (C) H&E staining of tumors generated by iMMEC-Grm1 clones. Grm1-18 clone formed adenocarcinomas that are much less organized than specimens Grm1-2 and Grm1-17. Blood vessels are

identified within the tumor formed by Grm1-18. Images taken at magnification of 10 x and 400 x.

3.3.5 Grm1 suppression leads to phenotypic reversion *in vitro* and *in vivo*

To determine whether sustained expression of mGluR1 was required to maintain the observed transformed phenotype, iMMEC-Grm1 clones were engineered to express a tetracycline-inducible siRNA construct targeting Grm1 (siGrm1-iMMECs) or green fluorescent protein (GFP)-control (siGFP-iMMECs). Several independent siGrm1-iMMEC clones were isolated and evaluated by immunoblotting. siGrm1-iMMECs demonstrated consistent suppression of mGluR1 expression in the presence of the inducer, doxycycline (dox), whereas mGluR1 expression remained unchanged in the negative control siGFP clones (Figure 14A). Next, we assessed if reduced mGluR1 expression modulated cell growth *in vitro* as measured by the standard MTT cell proliferation/viability assays. Dox-treated siGrm1-iMMEC clones displayed a significant decrease (≈ 80%) in the number of viable cells (Figure 14B).

We were also interested in the consequences of reduced mGluR1 levels in 3D acinar morphogenesis. siGrm1-iMMEC clones were grown in 3D culture and at 24 hours after plating, doxycycline was added to induce the expression of siGrm1. Mammary morphogenesis was assessed after 14 or 21 days of treatment. Consistent with our earlier findings (Figure 10A), the majority of siGrm1-iMMEC (75%) formed solid acini with a central hollow lumen when cultured in the presence of doxycycline whereas much reduced (<30%) lumen formation was detected in non-dox-induced siGrm1-iMMEC (Table 2). Suppression of mGluR1 expression also led to the generation of acini that were approximately 60% smaller than non-dox-induced siGrm1-iMMEC-clones (Figure 14C). We next examined the effects of diminishing Grm1 expression in growth properties

of cells in 3D culture system. In acini not-treated with doxycycline, similar to our earlier findings (Figures 10A and 10B), mGluR1 expression significantly promoted cell proliferation (as assessed by Ki-67 staining) and attenuated apoptosis (as assessed by cleaved-caspase 3 staining) (Figure 14D). In contrast, suppression of Grm1 by siRNA led to reduced proliferating cells in the central acinar and increased levels of apoptotic cells in the lumen of the acinar structure (Figure 14D). Inclusion of the inducer, doxycycline, in the culture medium led to significant attenuation of ERK phosphorylation similar to levels detected in clones of iMMEC-vector (Figure 14D). To ensure that the observed morphology was not an artifact of doxycycline, siGFP-iMMEC clones were subjected to the same 3D-culture conditions and two treatment groups (dox or no treatment). Both groups were analyzed with the same set of antibodies to Ki-67, cleaved caspase-3 and phosphorylated-ERK (Supplemental Figure 1, Table 2). There were no obvious differences between dox and no treatment groups as both groups exhibited similar patterns of staining as the parental iMMEC-Grm1 cells.

Next, we assessed by orthotopic allografts whether a reduction of iMMEC-Grm1-driven mammary levels modulated tumorigenesis *in vivo*. Again, siGrm-iMMEC-18-4 and siGrm-iMMEC-18-8 clones were orthotopically implanted into immunodeficient nude mice. Upon initial appearance of palpable mammary tumors, mice were randomly segregated into two groups with similar tumor volumes and doxycycline was administered in the drinking water of the treated group (0.2%w/v). Doxycycline-induced Grm1 knockdown suppressed tumor progression of mGluR1-expressing iMMEC allografts, as mammary tumors generated by both siGrm-iMMEC-18-4 and siGrm-iMMEC-18-8 clones in dox-treated mice were about 60% smaller in volume compared to tumors in untreated mice ($p<0.05$, t-test, n=5 Figure 15A), thus indicating that Grm1 expression is required for the tumorigenic phenotype exhibited by mGluR1-expressing iMMECs in nude mice *in vivo*.

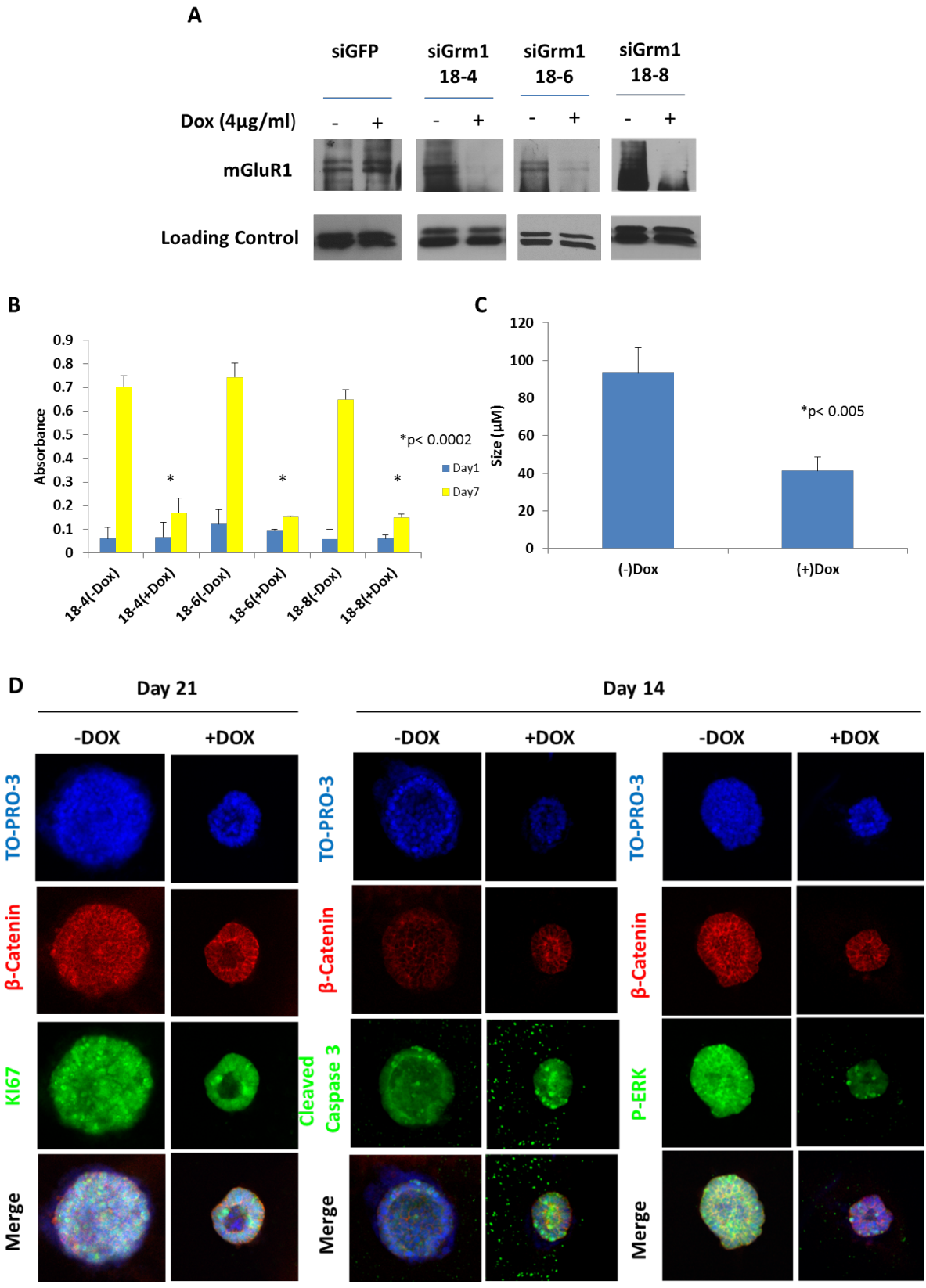
A
siGFP
siGrm1 18-4
siGrm1 18-6
siGrm1 18-8
Dox (4µg/ml)
- + - + - + - +
mGluR1
Loading Control
B
Absorbance
0.9
0.8
0.7
0.6
0.5
0.4
0.3
0.2
0.1
0
*p< 0.0002
Day1
Day7
18-4(-Dox)
18-4(+Dox)
18-6(-Dox)
18-6(+Dox)
18-8(-Dox)
18-8(+Dox)
C
Size (µM)
120
100
80
60
40
20
0
*p< 0.005
(-)Dox
(+)Dox
D
Day 21
Day 14
-DOX
+DOX
TO-PRO-3
β-Catenin
KI67
Merge
Cleaved Caspase 3
P-ERK

Figure 14. Sustained mGluR1 expression is required to maintain transformed phenotypes *in vitro*.

(A) Several independent clones were isolated from introduction of inducible siRNA to GFP (control) or Grm1 in iMMEC-Grm1 cells. In the presence of the inducer, doxycycline, mGluR1 expression was reduced at the protein level as assessed by immunoblots only in siGrm1-iMMEC but not siGFP-iMMEC clones. (B) MTT cell viability/proliferation assays were performed in the same set of cells and a decrease in the number of viable cells was detected only in the presence of doxycycline, *P<0.0002, for dox treatment versus no treatment. (C) The size of siGrm1-iMMEC acini was measured on day 14, following treatment with doxycycline (4 μg/ml) and compared to not-treated acini (P<0.0001). (D) Knock down of mGluR1 expression by siRNA to Grm1 led to phenotypic reversion of iMMEC-Grm1 clones at day 14 or 21 after treatment with doxycycline (4 μg/ml) in 3D cultures. Acini were stained with Ki-67, cleaved-caspase 3, phosphorylated-ERK (green), and β-catenin (red; to visualize epithelial cells) and TO-PRO-3 (blue; to visualize nuclei).

Table 2. Percent of hollow lumen in dox-treated siGrm1-iMMEC and siGFP-iMMEC are shown.

Day 14	(-)Dox	(+)Dox
siGrm1	30%	72%
siGFP	30%	18%

A total of 40 acini were evaluated for lumen formation.

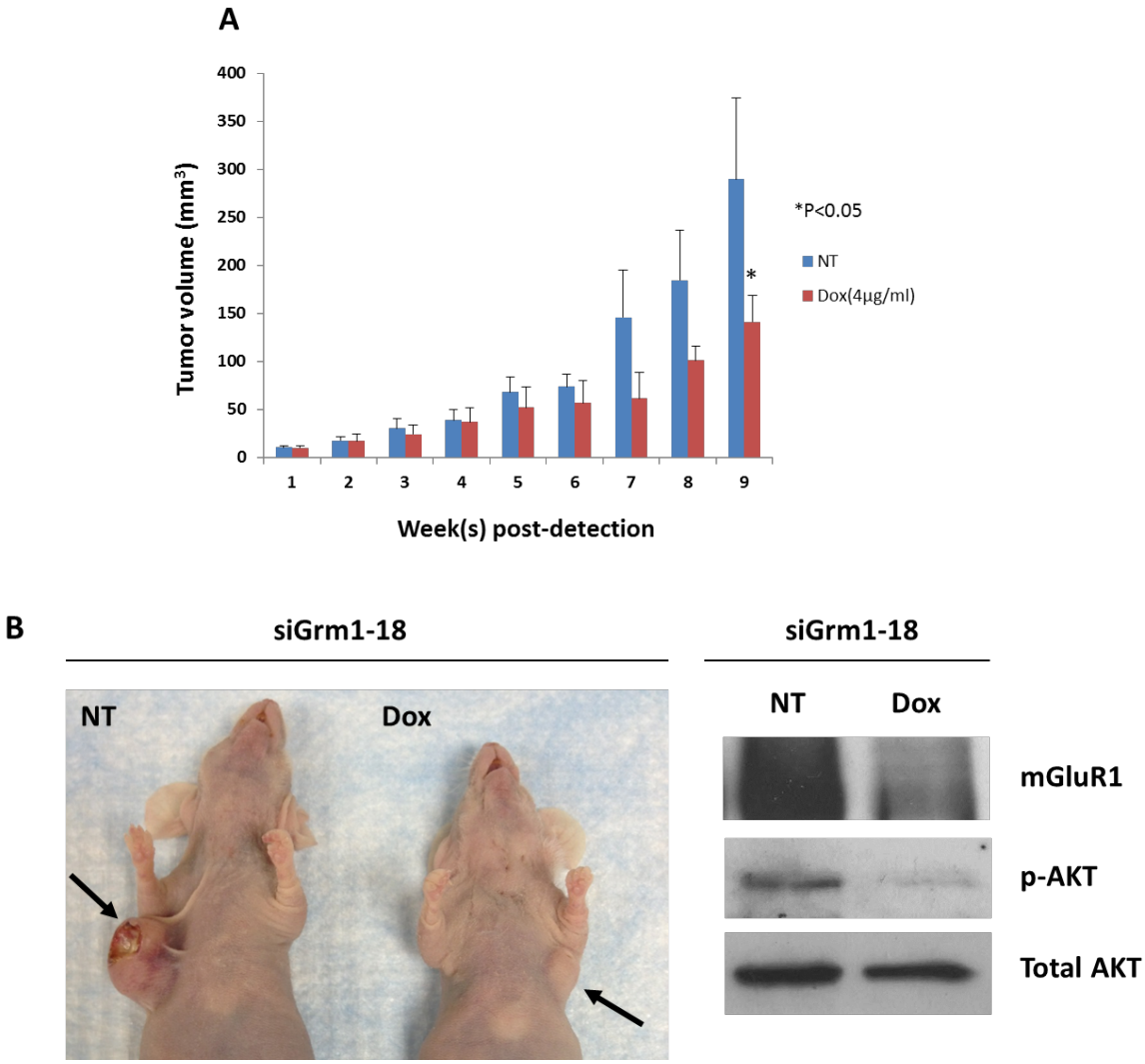

Figure 15. Sustained mGluR1 expression is required to maintain transformed phenotypes *in vivo*.

(A) *In vivo* inhibition of tumor development by siGrm1. Mice bearing mammary tumors generated from siGrm1-iMMEC cells were treated with doxycycline (0.2% w/v in drinking water) to induce siRNA expression to knockdown levels of Grm1. Results indicate that sustained expression of Grm1 is partially necessary to maintain iMMEC-Grm1 tumor progression, ($p<0.05$,t-test,n=5). Not-treated siGrm1-iMMEC allografts progressed with similar growth kinetics as iMMEC-Grm1 cells. (B) Representative tumor photographs

taken at 16 weeks post-doxycycline treatment. Immunoblotting demonstrated decreased levels of mGluR1 and activated AKT in allografts from dox-treated siGrm1-iMMECs.

GRM1 in human breast cancer

3.3.6 mGluR1 is expressed in breast cancer cells and breast cancer tissue biopsies

To investigate the relevance of glutamatergic signaling in human breast cancer, we first extended our studies to breast cancer cell lines. Expression of mGluR1 was detected in several estrogen receptor- and HER2- expressing breast cancer cell lines by Western immunoblot and immunofluorescence staining (Figure 16A). Previously, we showed that expression of exogenous Grm1 in iMMECs resulted in the sustained expression of P-ERK in 3D morphogenesis assays and the signal was diminished when Grm1 was suppressed. The functionality of mGluR1 in breast cancer cells was shown using mGluR1 agonist-induced ERK phosphorylation. L-Quisqualate–induced ERK activation was inhibited when SK-BR-3 cells were pretreated with mGluR1-specific antagonist, Bay-36-7620 for 30 min before induction with L-Quisqualate (Figure 16B). Taken together, these results showed that mGluR1 receptors in breast cancer cells were functional and responded to mGluR1 agonist and antagonist.

To further explore the relevance of mGluR1 in human breast cancer, we compared mGluR1 expression in paired breast tumor-normal adjacent tissue specimens and found that mGluR1 expression in tumors was indeed higher than in normal adjacent tissues, as analyzed by unbiased quantitative assessment of the immunostaining (Figure 16C). In the adjacent tissue samples, we noticed an interesting pattern of mGluR1 expression localized only to the apical surface of the mammary glands.

Possible alterations in the growth properties of these ER-positive breast cancer cells by reducing mGluR1 expression were also examined. Applying similar approaches as we have done in the mouse iMMEC system, we introduced inducible siRNA to GRM1 into mGluR1-expressing MCF7 (siGRM1-MCF7) breast cancer cells (Figure 16D). In the presence of the inducer, doxycycline, levels of mGluR1 were reduced, as shown by Western immunoblots for two independent siGRM1-MCF7 clones (Figure 16D) and this suppression of mGluR1 expression decreased the number of viable MCF7 cells in MTT cell proliferation/viability assays (Figure 16E).

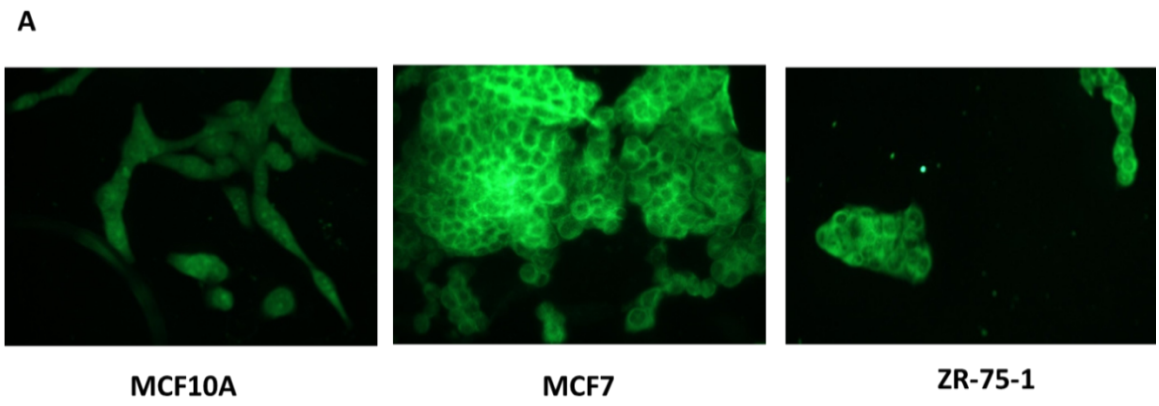
A
MCF10A
MCF7
ZR-75-1

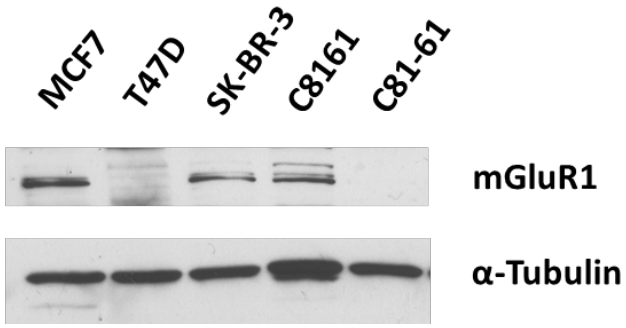
MCF7
T47D
SK-BR-3
C8161
C81-61
mGluR1
α-Tubulin

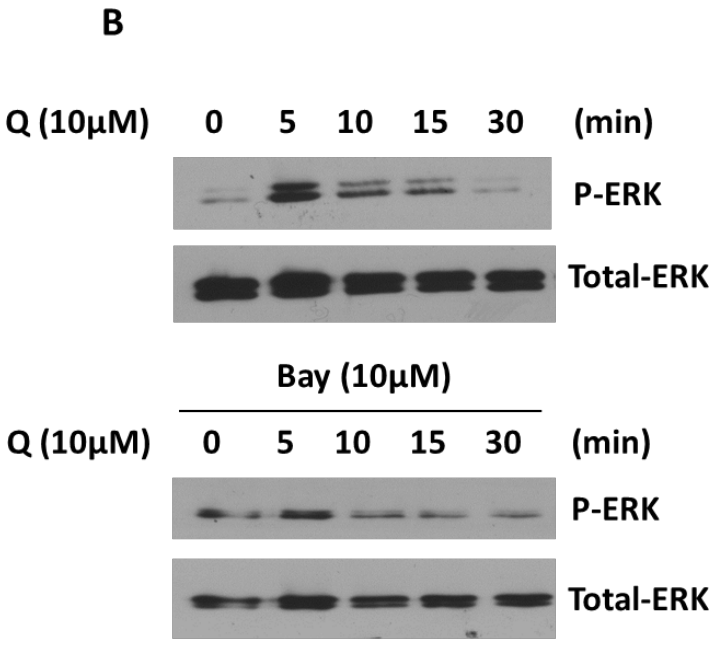
B
Q (10μM) 0 5 10 15 30 (min)
P-ERK
Total-ERK
Bay (10μM)
Q (10μM) 0 5 10 15 30 (min)
P-ERK
Total-ERK

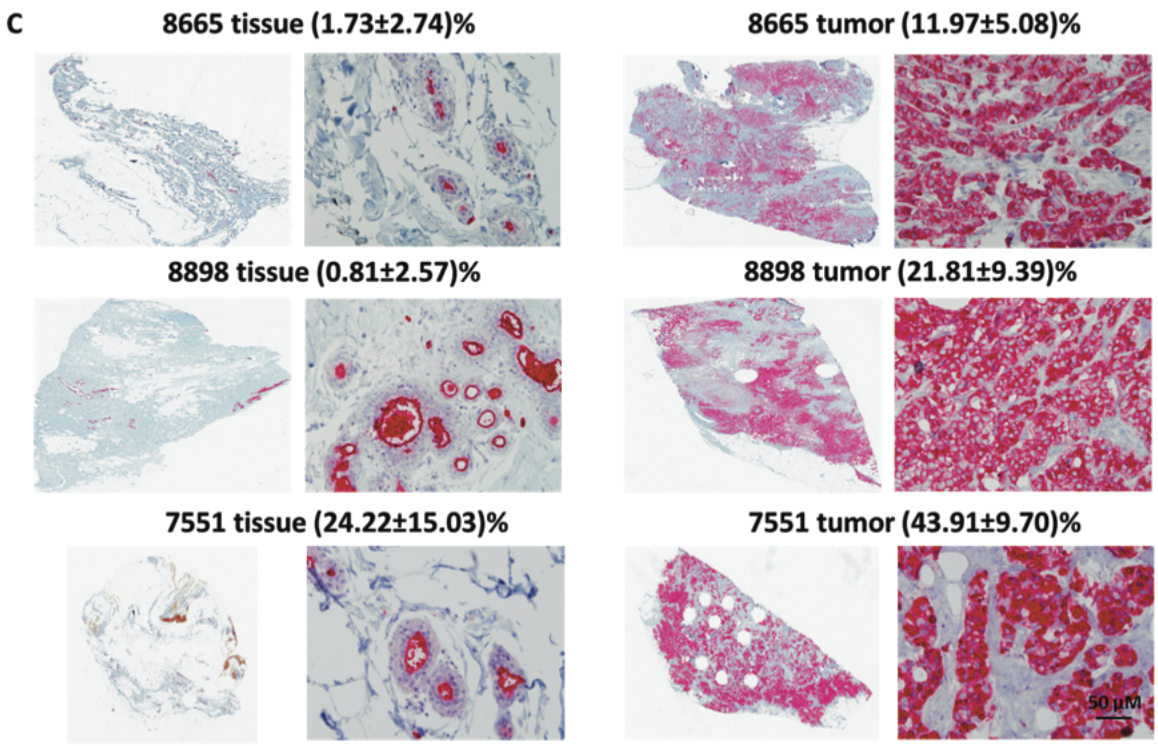
C
8665 tissue (1.73±2.74)%
8665 tumor (11.97±5.08)%
8898 tissue (0.81±2.57)%
8898 tumor (21.81±9.39)%
7551 tissue (24.22±15.03)%
7551 tumor (43.91±9.70)%
50 µM

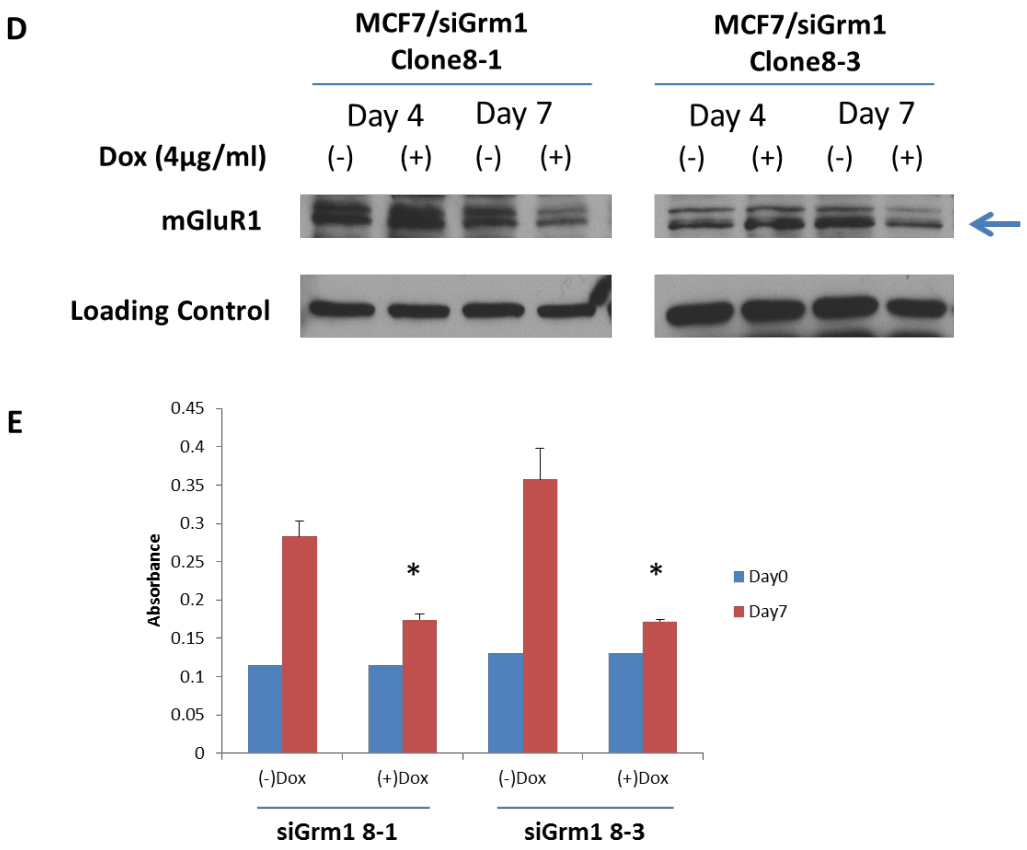

Figure 16. Functional mGluR1 in human breast cancer cells.

(A) mGluR1 expression by immunofluorescence and western blot in breast cancer cells. C8161, C81-61 (positive and negative control respectively); breast cancer cell lines MCF7, T47D, ZR-75-1 [ER+]; SK-BR-3 [HER2+]; MCF10A [non-transformed ER-immortalized human mammary epithelial cells]. (B) Treatments of breast cancer cells with mGluR1 agonist, L-Quisqualate (10 µM) up to 30 min resulted in ERK phosphorylation. Pretreatment of these cells with Bay 36-7620 (10 µM) for 30 min before L-Quisqualate induction resulted in no modulation of phosphorylated ERK (p-ERK; SK-BR-3). The membrane was stripped and reprobed with total ERK. (C) IHC for mGluR1 in paired breast tumor (T) and adjacent normal (N) biopsies. mGluR1-positive cells (% of total cells) scored in each digitized slide by an unbiased quantitative assessment using Aperio ScanScopeGL and ImageScope software. Photomicrographs of IHC,

representative paired tissue sections. P<0.001, comparing tumor and normal biopsies. 10 x and 400 x magnification. (D) Inducible si-GRM1 RNA constructs were introduced into MCF7 breast cancer cells; several independent clones were isolated and characterized. In the presence of doxycycline, endogenous mGluR1 levels were reduced as assessed by immunoblots. (E) Reduction of viable cell numbers when siGRM1-MCF7 cells were treated with doxycycline, *P<0.002 for both clones, comparing dox treatment versus no treatment.

3.3.7. Human breast cancer cells respond to anti-glutamatergic drug Riluzole

Earlier we reported elevated levels of extracellular glutamate only in human melanoma cell lines with mGluR1 expression [80]. We also observed similar trend in iMMEC-Grm1 cells (Figure 1b), therefore we were curious to see if this phenomenon also extended to mGluR1-expressing ER+ human breast cancer cells. Both MCF7 and T47D secreted enhanced levels of extracellular glutamate (Figure 17A), these results are similar to earlier report by Seidlitz and colleagues where they showed elevated levels of extracellular glutamate in triple negative breast cancer cell line, MDA-MB-231 [104]. Previously, we demonstrated altered *in vitro* cell growth and *in vivo* xenograft tumor progression in human melanoma cells treated with an inhibitor of glutamate release, Riluzole [80, 124, 125]. Riluzole is an FDA-approved drug for the treatment of amyotrophic lateral sclerosis, ALS [127]. The exact mechanism on how Riluzole inhibits the release of glutamate is unknown, but functionally, Riluzole acts as an antagonist of mGluR1. In a Phase 0 clinical trial using single agent Riluzole for 14 days in resectable stage III and IV melanoma patients, 34% of them showed significant decrease in phospho-AKT and/or phospho-ERK in post-treatment tumor samples, in association with significant decrease in melanoma metabolic activity by FDG-PET [126]. In a Phase II single agent Riluzole trial, we detected a reduction in both phospho-ERK and phospho-AKT in paired tumors similar to the Phase 0 results. Stable disease was also observed in about 30-40% of stages III/IV non-resectable melanoma patients but the clinical responses were not durable, suggesting that Riluzole has modest anti-tumor activity but additional inhibitors are needed in the treatment of melanoma pathogenesis [175].

First, we showed a dose-dependent growth inhibition by Riluzole in three breast cancer cell lines, about 40% inhibition after treatment for 96 hours at 50 μM (Figure 17B). Next, cell cycle analyses were performed on breast cancer cells treated with

Riluzole at the same concentration for the indicated time periods. MCF7 cells showed alterations resulting in the accumulation at G2/M at 48 hours (Figure 17C). For SK-BR-3, there was a considerable increase in cells accumulated in the sub-G1 phase of the cell cycle after 48 hours indicative of cellular apoptosis. MCF7 human breast cancer cells do not express caspase-3 as a result of a 47 base-pair deletion within exon 3 of the *casp-3* gene [176]. Despite this, MCF7 cells have been shown to undergo morphological apoptosis after treatment with a variety of agents and conditions suggesting caspase-3 independent DNA fragmentation [177-179]. Indeed, we detected proteolytic processing of PARP in MCF7 cells within 24 hours of Riluzole treatment despite lack of accumulation of cells in sub-G1 in cell cycle profiles (Figure 17D).

Moreover, we observed an increase in ɣ-H2AX and 53BP1 levels in MCF7 and T47D cells. H2AX, a member of H2A histone family has been shown to be phosphorylated on serine residue 139 (known as ɣ-H2AX) after the activation of the caspase cascade and as a result of apoptotic DNA fragmentation. However, using transformed mGluR1-expressing immortalized baby mouse kidney epithelial cells (iBMK) that are deficient in apoptosis through the deletion of BAX and BAK (D3-Grm1 cells), we showed that Riluzole treated-D3-Grm1 cells resulted in clear co-localization of nuclear ɣ-H2AX and 53BP1 foci whereas D3-vector cells yielded an overall diffused pattern of ɣ-H2AX and undectable 53BP1 staining [180]. This supports that Riluzole is capable of inducing DNA damage in cells expressing functional mGluR1 in a mechanism that is independent of apoptosis.

As with most human cancers, breast tumors are heterogeneous in nature and usually involve multiple oncogenic events occurring in parallel or as part of the same signaling pathway. Given our earlier published results implicating AKT in Grm1-induced melanomagenesis [76, 126] and the well described role of PI3K/AKT axis in breast cancer pathogenesis and treatment resistance [181], we evaluated the anti-tumor activity

of the AKT inhibitor MK-2206 [182] as single agent and in combination with Riluzole. We found that either Riluzole or MK-2206 alone decreased MCF7 xenograft tumor progression *in vivo*. However, concurrent inhibition of glutamate signaling and AKT at only half the optimal single agent doses resulted in statistically significant suppression of tumor growth (Figure 18A), as calculated by the combination index method [172]. Consistent with our *in vitro* results, we also detected a significant increase in the number of ɣ-H2AX-positive cells in the post-Riluzole treated xenograft tumor (Figure 18B). Taken together, our data presents a novel approach to improving the therapeutic outcome of ER+ patients that are resistant to hormone therapy.

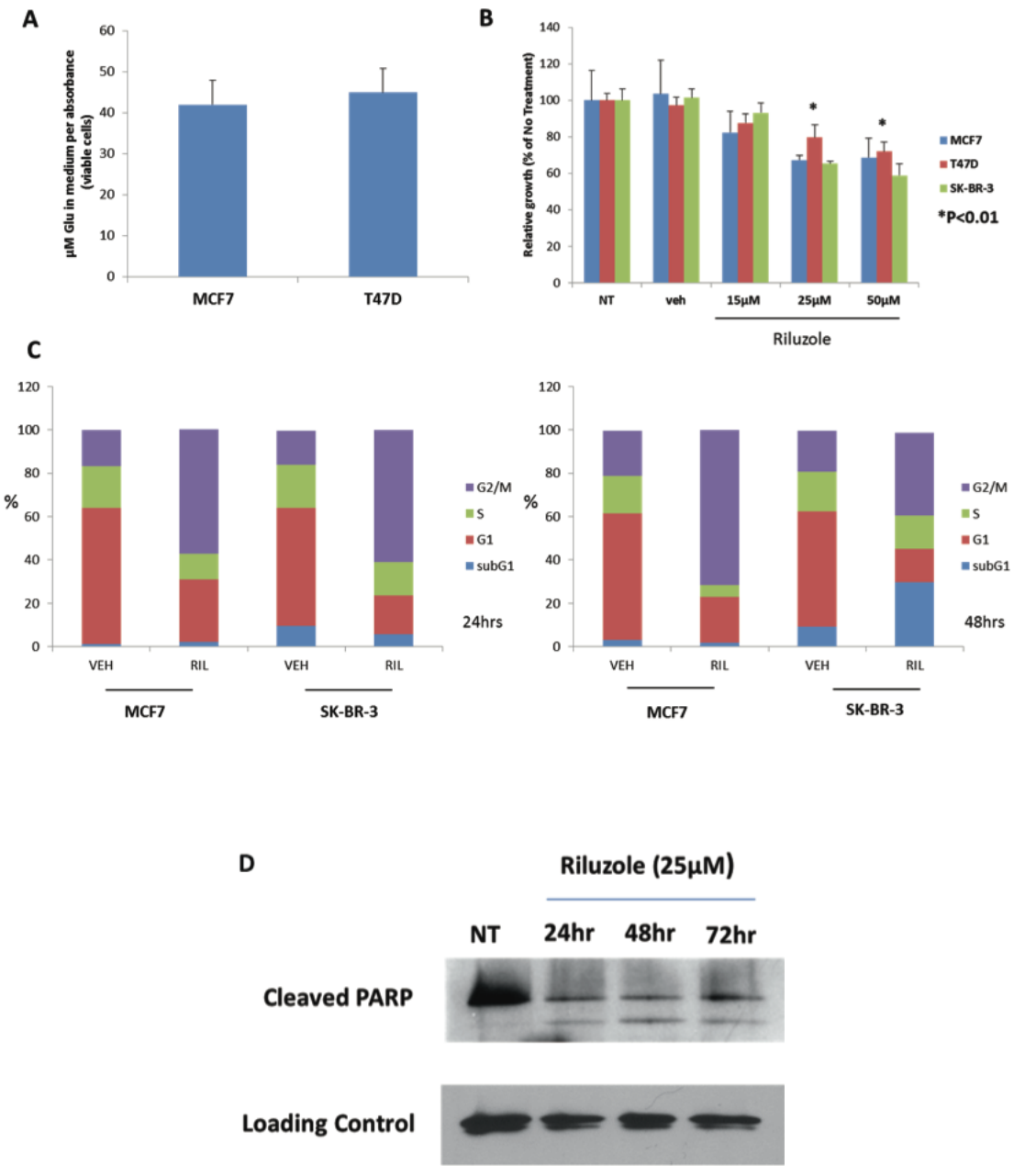
A
µM Glu in medium per absorbance (viable cells)
MCF7
T47D
B
Relative growth (% of No Treatment)
NT
veh
15µM
25µM
50µM
Riluzole
MCF7
T47D
SK-BR-3
*P<0.01
C
%
G2/M
S
G1
subG1
24hrs
48hrs
VEH
RIL
MCF7
SK-BR-3

D
Riluzole (25µM)
NT
24hr
48hr
72hr
Cleaved PARP
Loading Control

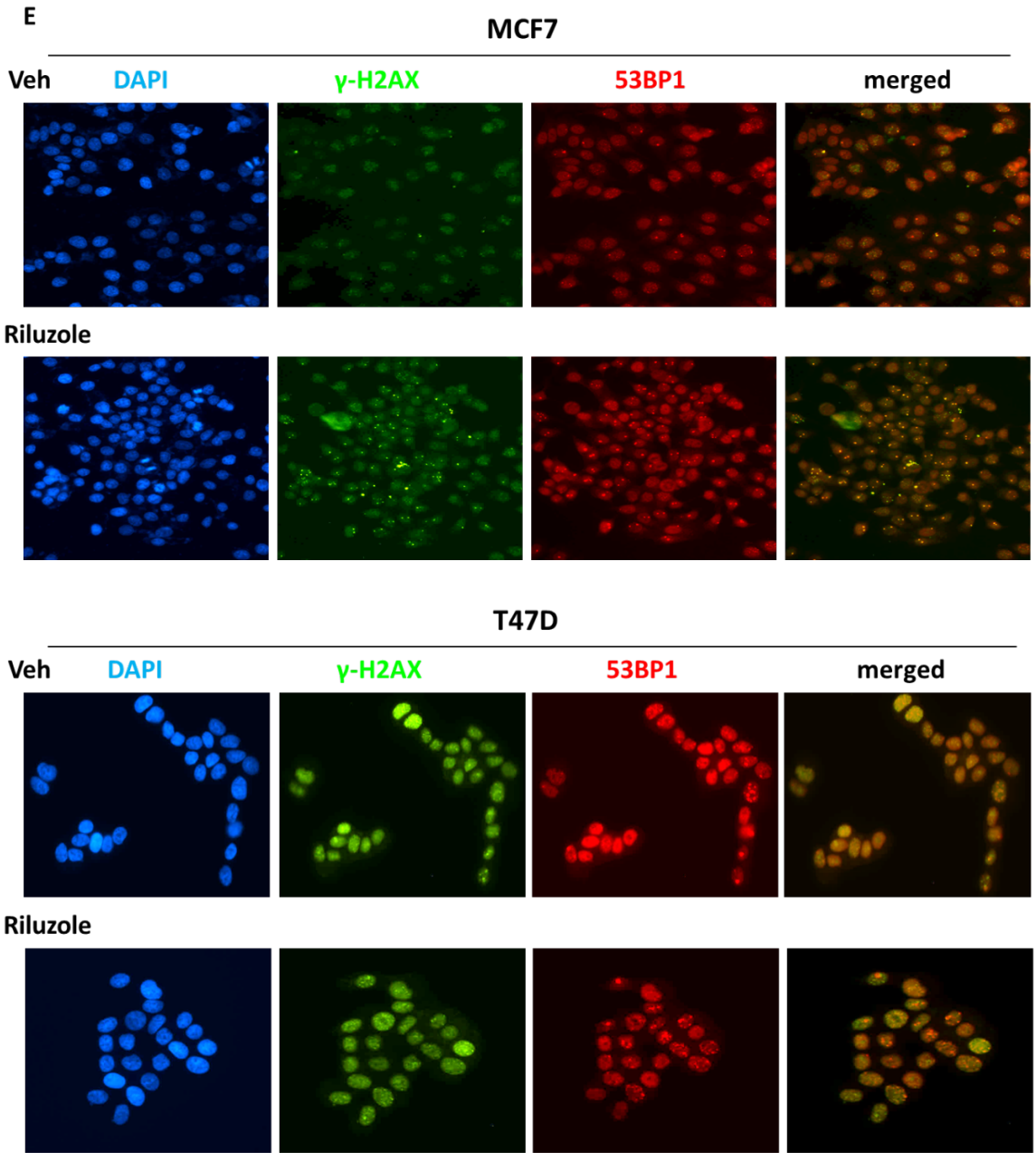
E
MCF7
Veh
DAPI
γ-H2AX
53BP1
merged
Riluzole
T47D
Veh
DAPI
γ-H2AX
53BP1
merged
Riluzole

Figure 17. Anti-glutamatergic drug Riluzole modulates breast cancer cell growth.

(A) Estrogen receptor positive breast cancer cells release glutamate. μM Glu per absorbance measured by MTT assays. (B) MTT cell proliferation-viability assays were performed after treatment of ER-positive breast cancer cells with Riluzole for 96 h. Breast cancer cell lines exhibited reduced cell proliferation in the presence of Riluzole. (C) Breast cancer cell lines examined displayed apparent cytostatic (MCF7) or cytotoxic/apoptotic (SK-BR-3) effects in the presence of Riluzole (50 μM). (D) Elevated levels of PARP cleavage in MCF7 cells treated with Riluzole. (E) Riluzole induces DNA double stranded breaks (DSBs) in mGluR1-expressing breast cancer cells. Immunofluorescence staining was performed using antibodies against 53BP1 [red] and ɣ-H2AX (green) to show co-localization to sites of DNA DSBs. DAPI (blue) is nuclear counterstain.

A

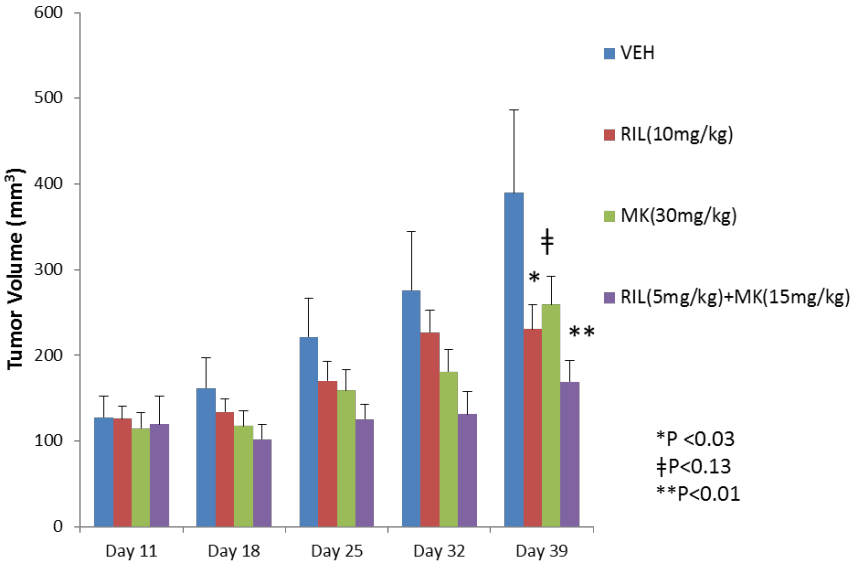

B

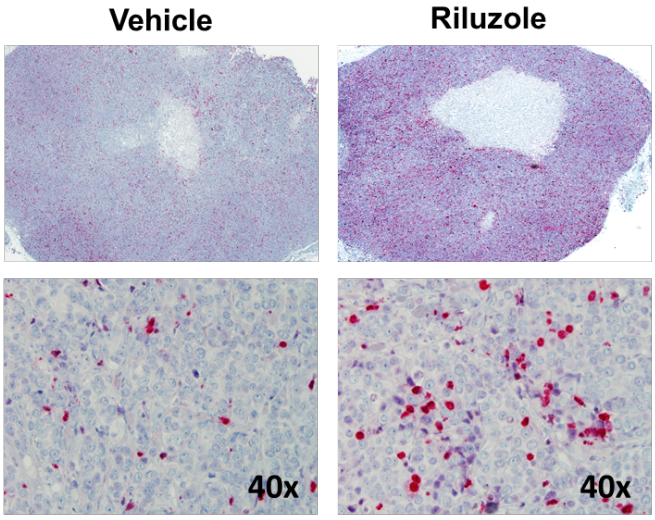

	γH2AX
Vehicle (DMSO)	6.6 ± 0.35%
Riluzole (10μM)	9.7 ± 0.81%

***P < 0.001**

Figure 18. Riluzole suppresses tumor growth of MCF7 xenografts.

(A) *In vivo* reduction of tumor progression by Riluzole combined with allosteric AKT inhibitor, MK-2206. Mice bearing mammary MCF7 xenograft tumors were divided into four treatment groups: vehicle (DMSO), Riluzole (10 mg/kg), MK-2206 (30 mg/kg) or a combination of Riluzole (5 mg/kg) and MK-2206 (15 mg/kg). (B) Marker of DNA damage detected in post-treated human breast cancer xenograft. IHC against ɣ-H2AX in pre- and post-Riluzole treated MCF7 xenograft. Positive staining is indicated by pinkish color in the nucleus. Image magnification at 10 x and 40 x.

3.4 Discussion

There is mounting evidence that glutamatergic signaling plays a role in epithelial tumorigenesis [103, 123, 162]. In this report, we used a mouse mammary epithelial cell model, involving *in vitro* 3D-morphogenesis assays and *in vivo* mammary tumorigenicity studies in nude mice, to examine the tumor-initiating potential of Grm1 in breast cells. Our results demonstrate that ectopic expression of mGluR1 in immortalized mouse mammary epithelial cells (iMMECs) disorganizes 3D-acinar architecture and likely promotes cellular transformation, as mGluR1-expressing mammary cells failed to establish hollow and polarized acini. Furthermore, mGluR1 expression in iMMECs was sufficient to promote poorly differentiated tumor development in a system of very low inherent tumorigenic potential [164]. In support of a driving role for Grm1 in mammary tumorigenesis, Grm1 knockdown by an inducible siRNA system suppressed iMMEC-Grm1 allograft tumor growth and decreased cell growth of mGluR1- and ER-expressing MCF7 human breast cancer cells.

mGluR1 is a member of the seven transmembrane G-protein coupled receptor (GPCR) superfamily, which represents a potent group of highly druggable targets encompassing approximately more than a quarter of all FDA-approved drugs [183]. Found in abundance in post-synaptic locations, mGluR1 is activated by its natural ligand, the major neurotransmitter L-glutamate, and was first thought to be functionally restricted to the central nervous system. However, mGluR1 expression has recently been demonstrated in peripheral tissues. The notion that wild-type GPCRs may harbor oncogenic potential is not entirely surprising. This concept underscores several key characteristics of a tumorigenic GPCR, such as aberrant expression or response to excessive locally circulating ligand produced by the tumor or neighboring cells [184]. Autocrine and/or possibly paracrine loops have been found to be exhibited in mGluR1-

expressing human melanoma cells [80]. It is also well established that glioma cells release excessive glutamate not only to enhance cell motility and invasion, but also to aid in the expansion of tumor cells through its excitatoxicity effects [185]. Interestingly, triple-negative MDA-MB-231 breast cancer cells have been reported to release extracellular glutamate, which may function as a cytokine that promotes bone invasion, thus enhancing metastasis [104]. Here, we demonstrate that ectopic mGluR1 expression in estrogen receptor-positive iMMECs results in amplified release of extracellular glutamate consistent with our previous studies in melanoma [75, 144].

In this thesis aim, we also report that introduction of exogenous Grm1 in a mouse mammary epithelial cell model system leads to altered cell growth characteristics, including increased proliferation and suppression of central mammary cell apoptosis resulting in larger acini and delayed lumen formation in 3D-morphogenesis assays. Using phosphorylated-ERK levels as a marker of glutamatergic signaling, we found that mGluR1 activates MAP Kinase, a pathway that regulates cell proliferation and is often deregulated in cancer. At day 7 post-plating in 3D-culture, both vector- and mGluR1-expressing iMMEC clones exhibited similar levels of activated ERK, presumably due to the early proliferative spheroid organization step in mammary morphogenesis. However, by day 14, phospho-ERK levels were completely diminished in acini generated by vector-, but not mGluR1-expressing iMMECs. Indeed, components of the MAPK pathway have been shown to not only regulate proliferation signals in mammary epithelial cells, but also function in the control of cell survival by regulating the activity of proapoptotic molecules, such as Bim [186, 187]. We have previously shown that mGluR1 supports cell survival through activation of the PI3K/AKT pathway in Grm1-transformed mouse melanocytic clones and that AKT2 knockdown by siRNA in these cells leads to apparent reduction in the levels of the anti-apoptotic protein, BCL2 [76]. Interestingly, in the current study, we also detected stimulation of AKT in excised tumors

generated by mGluR1-expressing iMMECs in nude mice *in vivo*, but not in the same cells under normal culture conditions *in vitro* (Figure 13B). Speyer and colleagues also detected activated AKT only when the cultured cells were stimulated with mGluR1 agonist, L-Quisqualate [103]. Taken together, these results suggest that stimulation of the PI3K/AKT axis may require stimulation of the receptor by its agonist *in vitro* or in an *in vivo* microenvironment.

There are many advantages to employing 3D-culture systems, especially in studies of glandular epithelium such as that of the mammary gland, as compared to traditional 2D-cell cultures. These 3D systems allow the distinction of non-malignant cells from malignant cells by various phenotypic alterations. Non-transformed cells usually form polarized, growth arrested acini-like spheroids in the presence of laminin-rich extracellular matrix, while transformed cells may exhibit perturbed lumen formation, polarity, and acinar structure and size [164, 165, 167]. We now present such findings in mGluR1-expressing iMMECs, which generate larger, non-hollowing and non-polarized acini exhibiting increased cell proliferation and persistent ERK activation. Interestingly, cell proliferation, as measured by MTT cell viability assays, was minimally affected by mGluR1 expression in iMMECs plated in 2D-cultures, thus, suggesting that cell-cell interactions in a more physiologically relevant 3D-context are crucial for Grm1 to exert its transformative effects in mammary epithelial cells (Supplemental Figure 2). Moreover, we were also able to regulate mGluR1 expression in iMMEC-Grm1 clones by an inducible silencing RNA system to Grm1, where a reduction in mGluR1 expression levels correlated with phenotypic reversion in 3D-cultures. Notably, we demonstrated that orthotopic implantation of mGluR1-expressing iMMECs into the mammary fat pads of athymic mice was sufficient and also required to promote robust tumor formation supporting the idea that Grm1 may be an important player in mammary tumorigenesis.

We investigated the consequences of GRM1 modulation in MCF7, a breast cancer cell line belonging to the luminal A subtype. Patients with hormone receptor (ER)-positive luminal A tumors usually have better prognosis, as such malignancies respond to estrogen deprivation; however, about half of the patients with advanced ER-positive disease show resistance to hormonal intervention. In a recently published study [107], 17β-estradiol increased the expression of mGluR1 in MCF7 cells and this increase was inhibited by pre-treatment with a selective estrogen receptor modulator, 4-hydroxytamoxifen suggesting a novel interaction between mGluR1 and hormone signaling. Importantly, a polymorphic variant of GRM1 was shown to be associated with risk for luminal breast cancer and mGluR1 expression at the mRNA level correlated with decreased survival in tamoxifen-treated patients. It is of great interest that, unlike the widely used MCF10A human mammary epithelial cells, iMMECs are estrogen receptor α-expressing cells [167]. Whether Grm1-mediated transformation of iMMECs is dependent on ER is a provocative question and is currently being investigated.

Taken together, our findings provide a novel insight that aberrant glutamate signaling can initiate tumorigenic properties in normal mammary epithelial cells. Based on our results, and in agreement with two recent reports [103, 107], we propose that modulation of glutamatergic signaling alone or in combination with other small molecule inhibitors such as MK-2206, may offer therapeutic benefits to patients with either luminal or basal subtype of the disease.

3.5 Supplemental Figures

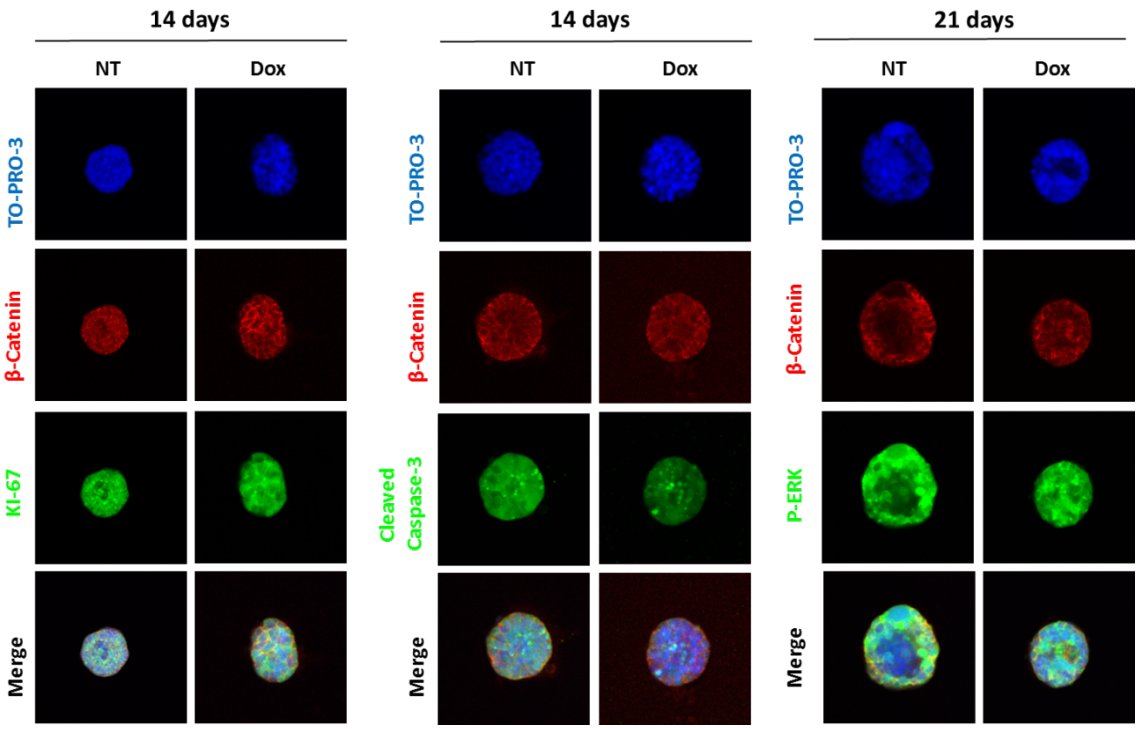

Figure S1. siRNA to GFP in iMMEC-Grm1 did not lead to phenotypic reversion at day 14 or 21 after treatment with doxycycline (4 µg/ml) in 3D-cultures.

Acini were immunostained for Ki-67, cleaved-caspase 3, phosphorylated-ERK (green), β-catenin (red; to visualize epithelial cells) and TO-PRO-3 (blue; to visualize nuclei).

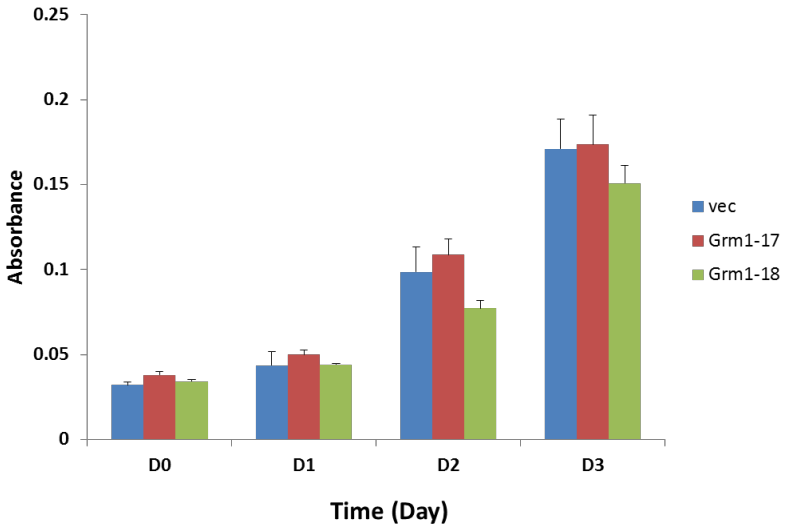

Figure S2. Ectopic expression of mGluR1 did not affect the overall growth rate of iMMECs in *in vitro* MTT assays. Each data point is the average of quadruplicate measurements.

CHAPTER 4

DISSERTATION SUMMARY AND FUTURE DIRECTIONS

4.1 Dissertation Summary

G-protein coupled receptors (GPCR) represent a class of therapeutic targets that have been widely exploited for drug design and development and currently no single class of protein ranks higher than GPCRs in terms of drug discovery potential [183]. This superfamily is subdivided into three families and mGluRs belong to Class C GPCRs [188]. The surprising accumulating evidence suggesting other functional roles of mGluRs in human malignancies in addition to synaptic transmission has presented intriguing possibilities to make mGluRs putative novel targets for human cancers. It is becoming apparent that mGluRs participate in the tumor progression of more cancer types than anticipated (Table 1).

The focus of mGluR1 in this dissertation was divided into two malignancies: 1) melanoma: to understand and explore the key effectors of mGluR1 signaling in transformed Grm1-melanocytic clones and 2) breast cancer: to study the oncogenic role of mGluR1 in mammary epithelial cells and the biological consequences of targeting glutamate signaling in the corresponding tumor type.

In the first aim, we studied the role of IGF-1R in mediating downstream signals from mGluR1 to AKT. We demonstrate for the first time, that agonist stimulation of mGluR1 leads to transactivation of IGF-1R. We then determined the requirement of IGF-1R in maintaining the tumorigenic phenotype of transformed Grm1-melanocytic clones. Our results also indicate that IGF-1R activation may lead to acquired resistance against mGluR1-targeted drugs in melanoma patients. Further, we demonstrated that inhibition of melanoma xenografts was more superior when targeting both mGluR1 and IGF-1R receptors compared with single agents. The involvement of this potential multilayered cooperation in chemoresistance provides a clear basis for targeting IGF-1R in

combination with mGluR1 as a novel therapeutic approach for mGluR1-expressing melanomas.

In the second aim, we demonstrate that mGluR1 triggers events that are important for the transformation of mammary epithelial cells. We found that forced expression of mGluR1 leads to changes in 3D acinar architecture that is consistent with oncogenic transformation. These include decreased central acinar cell death, abrogation of lumen formation and cell polarity alterations. MAP Kinase, a pathway known to transmit and amplify signals involved in cell proliferation was also sustained at late time-points in mammary morphogenesis. Furthermore, mGluR1-expressing iMMECs form tumors when implanted into the fat pads of athymic mice. Persistent mGluR1 expression was required for the maintenance of transformed phenotype both *in vitro* and *in vivo* as demonstrated by an inducible Grm1-silencing RNA. Our results, combined with the finding that mGluR1 is highly expressed in human breast tumors but not normal tissues suggest that mGluR1 may play an important role in the initiation and progression of breast cancer. Moreover, mGluR1 expression in mammary epithelial cells led to elevated levels of extracellular glutamate and we demonstrate that ER-positive MCF7 breast cancer xenograft responds to Riluzole, an inhibitor of glutamate release. Our findings imply a functional role for glutamate signaling in breast cancer cell growth and that the glutamatergic system may be a potential therapeutic target in breast cancer.

4.2 Future Directions

The work presented in this thesis not only identified a potential key member of mGluR1 downstream signaling using transformed Grm1-melanocytic clones as a model but also demonstrated the oncogenic potential of Grm1 in mammary epithelial cells. The next steps taken can be split into more detailed mechanistic investigation of mGluR1 oncogenic activity and further evaluation of mGluR1 as a therapeutic target in breast cancer.

4.2.1 Functional interactions of Grm1 with other oncogenes or signaling pathways in promoting the transformation of mammary epithelial cells

We have shown that AKT, particularly the AKT2 isoform, to be strongly activated in allograft tumors generated by mGluR1-expressing mouse melanocytes and in human melanoma biopsy specimens [76]. siRNA to AKT2 reduces Grm1-mouse-melanocytic allograft tumor volume [76]. To tie in my first aim with my second aim, we will study the mechanism(s) by which mGluR1 activates AKT in mammary and breast cancer cells. My first thesis aim implicates IGF-1R in mGluR1-induced PI3K/AKT pathway activation in melanoma. Furthermore, we noticed high levels of activated AKT in allografts of iMMEC-Grm1 but not in cultured cells (Figure 13B). Given the great interest in the role of IGF-1 signaling in mammary tumorigenesis, we will first investigate whether IGF-1R also mediates signaling from mGluR1 to AKT in iMMEC-Grm1 clones using pharmacologic (PPP, OSI-906) and genetic (DN IGF-1R mutant) IGF-1R inhibition. Subsequently, we will transfect IGF-1RDN into iMMEC-Grm1 clones and observe for full or partial rescue of the transformed phenotype in *in vitro* 3D morphogenesis assays and *in vivo* tumorigenesis assays.

Fibroblasts derived from IGF-1R null mice (R-) cells have been shown to be resistant to transformation by a variety of viral and cellular oncogenes such as SV40T antigen and/or activated Ha-ras oncogene [189]. Interestingly, enhanced IGF-1R signaling in non-transformed breast epithelial cell line, MCF10A has been shown to contribute to hyperproliferative phenotypes in 3D culture and this was reversed by AKT2 downregulation but not AKT1 [139]. In fact, reduction in AKT1 levels in IGF-1R-stimulated cells resulted in epithelial-mesenchymal transition (EMT)–like morphology and AKT1 expression has been reported to suppress metastasis of mammary tumors [190, 191].

So far, we have detected IGF-1R expression in iMMEC-Grm1 clones. We predict that mGluR1 exerts its transformative properties in part through the IGF-1R/AKT2 signaling axis in mammary epithelial cells. Alternatively, a genome-wide expression profiling on inducible siGrm1-MCF7 cells grown in 3D culture will be performed. We will identify significantly altered genes following induction of siGrm1 with doxycycline.

Hirshfield and colleagues have implicated ER as a potential functional partner of mGluR1 signaling in breast cancer. A polymorphic variant of GRM1 resulting in a proline>serine change is associated with increased likelihood of ER-positive or PR-positive disease, later age of diagnosis and decreased recurrence of breast cancer [107]. It has been hypothesized that the proline isoform leads to increased receptor activity thus conferring a more aggressive phenotype. It is certainly worthwhile to evaluate the tumorigenic potential of proline or serine isoforms of GRM1 as well as their contribution to tamoxifen resistance. Our work has indicated that overexpression of mGluR1 has a measurable phenotype thus, morphological changes caused by polymorphic variants of GRM1 can be compared to those described here.

Interestingly, not only does estrogen increase mGluR1 expression but colocalization of mGluR1 and ERα has also been demonstrated [192]. The possible role

of mGluR1 in tamoxifen resistance in ER-positive breast cancers was also suggested whereby mGluR1 expression correlates with a shorter distant metastasis-free survival in tamoxifen-treated patients suggesting a luminal subset with poorer prognosis [107]. Unlike MCF10A cells, iMMECs express ER [164] making them ideal to study mGluR1 in an active estrogen signaling setting. Cells with activated AKT2 have been reported to be estrogen-independent and resistant to the anti-hormonal therapeutic agent Tamoxifen [193]. Constitutively activated AKT2 or AKT2 activated by epidermal growth factor (EGF) or IGF-1 promotes the transcriptional activity of ERα. It is tempting to speculate that aberrant expression of mGluR1 contributes to constitutive activation of the IGF-1R/AKT axis which in turn confers anti-hormonal therapeutic resistance. We hypothesize that breast tumors bearing ER expression evolve to become reliant on mGluR1 making them sensitive to inhibition of glutamate signaling. At a clinical level, it will be exciting to examine whether inhibition of glutamate signaling, either alone or in combination with anti-hormonal therapies may offer a much needed option for therapeutically resistant tumors bearing ER and mGluR1.

4.2.2 mGluR1 is required for oncogenic transformation of breast cancer cells

The second aim presented in this thesis focused primarily on ER-positive breast cancers based on Hirshfield and colleagues' findings [107]. Gorski and colleagues have been actively studying the effectiveness of pharmacological inhibition of mGluR1 in triple negative cell line, MDA-MB-231 [103]. MDA-MB-231 falls under the basal subtype classification, a disease that currently has poor prognosis due to unavailable therapeutic targets [94]. While non-malignant cells typically organize into polarized growth arrested structures in 3D cultures, breast cancer cells exhibit dramatic morphological differences in 3D which is not apparent in monolayer cultures again emphasizing the advantage of 3D models. In 3D, MDA-MB-231 cells exhibit disorganized and invasive morphology with

stellate projections whereas MCF7 cells form spherical colonies lacking lumens similar to those produced by iMMEC-Grm1 [194]. To further demonstrate the requirement of mGluR1 in mammary tumorigenesis, we will use an inducible siRNA to GRM1 in MDA-MB-231 and MCF7 to observe for phenotypic changes in 3D acinar morphogenesis when GRM1 is suppressed. We expect that reduction of mGluR1 expression will lead to dramatic changes in morphology by restoring organized globular shapes in MDA-MB-231 and lumen formation in MCF7 cells grown in 3D culture. We also anticipate that GRM1 knockdown leads to impaired growth of MDA-MB-231 and MCF7 xenografts thus further demonstrating that mGluR1 is necessary for mammary tumorigenesis.

4.2.3 Mechanisms underlying the enhanced antitumor effect of Riluzole in breast cancer

As described earlier in Chapter 1.4, the mode of action of Riluzole in inhibiting tumor growth and progression is not well understood. Riluzole has been demonstrated to decrease growth and motility of mGluR1-expressing melanoma cells [80, 125, 195]. The surprising and previously unknown finding that Riluzole not only results in the suppression of tumor growth but also increased formation of ɣ-H2AX foci in mGluR1-expressing melanoma xenografts [124] similar to the effects of ionizing radiation has prompted us to study the function of Riluzole as a DNA damaging agent [180]. We hypothesize that by disrupting the release of glutamate, Riluzole results in the intracellular build-up of glutamate, which interferes with the homeostasis of glutamate and cystine exchange, thus, modulating glutathione (GSH) synthesis and increases oxidative stress, DNA damage and genome instability [184].

In the second aim, we measured and demonstrated that DNA damage levels are also increased in breast cancer cells treated with Riluzole (Figure 17E and 18B). Riluzole is an indirect antagonist of mGluR1 signaling thus, future studies include

determining whether mGluR1 expression is required for this response by comparing cells that are mGluR1- positive and negative. Additionally, a variety of breast cancer cells with different molecular subtypes will also be compared for DNA damage responses to Riluzole. As AKT has been implicated in modulating DNA damage responses and genome instability [196], we expect that the enhanced efficacy of concurrent inhibition of mGluR1 and AKT is due to greater DNA damage in the cancer cells.

4.2.4 Aberrant expression of mGluR1 in luminal epithelial cells

The mature mammary gland features two major types of cells, the outermost layer of myoepithelial cells and an inner layer of luminal epithelial cells [197]. Our results and those by Hirshfield and colleagues demonstrate that in breast carcinoma, the frequency and the relative level of mGluR1 expression is significantly greater than those found in benign tissues. Interestingly, a significantly higher proportion of ER-positive breast tumors (83%) were found to express mGluR1 as compared to ER-negative tumors (66%) [107]. Surprisingly, when comparing receptor expression in tumors versus adjacent tissues of the same patient we noticed an intriguing pattern of mGluR1 expression localized only to the inner luminal cells of the mammary gland (Figure 16C). Furthermore, all four patients exhibited hormone receptor positive (ER/PR+) tumors which tend to be luminal breast cancers.

A significant body of evidence supports the aberrant expression/overexpression of mGluRs as important contributors to cancer [198]. Somatic mutations in GRMs have been identified in human malignancies [152, 199] and recently, mutations in GRM1 and GRM5 were found in two distinct melanoma cell lines derived from metastatic patients [200]. Moving forward, characterization of identified mutations is warranted to validate

their role as drivers in cancer. Key questions regarding the regulation of mGluR1 in breast tissues and breast cancer cells will be of great interest for future investigations.

CHAPTER 5

REFERENCES

1. Curtis, D.R., J.W. Phillis, and J.C. Watkins, *Chemical excitation of spinal neurones.* Nature, 1959. **183**(4661): p. 611-2.
2. Hayashi, T., *A physiological study of epileptic seizures following cortical stimulation in animals and its application to human clinics.* Jpn J Physiol, 1952. **3**(1): p. 46-64.
3. Raynal, C., P.D. Delmas, and C. Chenu, *Bone sialoprotein stimulates in vitro bone resorption.* Endocrinology, 1996. **137**(6): p. 2347-54.
4. Chenu, C., et al., *Glutamate receptors are expressed by bone cells and are involved in bone resorption.* Bone, 1998. **22**(4): p. 295-9.
5. Patton, A.J., et al., *Expression of an N-methyl-D-aspartate-type receptor by human and rat osteoblasts and osteoclasts suggests a novel glutamate signaling pathway in bone.* Bone, 1998. **22**(6): p. 645-9.
6. Gu, Y. and S.J. Publicover, *Expression of functional metabotropic glutamate receptors in primary cultured rat osteoblasts. Cross-talk with N-methyl-D-aspartate receptors.* J Biol Chem, 2000. **275**(44): p. 34252-9.
7. Takarada-Iemata, M., et al., *Glutamate preferentially suppresses osteoblastogenesis than adipogenesis through the cystine/glutamate antiporter in mesenchymal stem cells.* J Cell Physiol, 2011. **226**(3): p. 652-65.
8. Frati, C., et al., *Expression of functional mGlu5 metabotropic glutamate receptors in human melanocytes.* J Cell Physiol, 2000. **183**(3): p. 364-72.
9. Hoogduijn, M.J., et al., *Glutamate receptors on human melanocytes regulate the expression of MiTF.* Pigment Cell Res, 2006. **19**(1): p. 58-67.
10. Hodgkinson, C.A., et al., *Mutations at the mouse microphthalmia locus are associated with defects in a gene encoding a novel basic-helix-loop-helix-zipper protein.* Cell, 1993. **74**(2): p. 395-404.
11. Hornyak, T.J., et al., *Transcription factors in melanocyte development: distinct roles for Pax-3 and Mitf.* Mech Dev, 2001. **101**(1-2): p. 47-59.
12. Morhenn, V.B., et al., *Evidence for an NMDA receptor subunit in human keratinocytes and rat cardiocytes.* Eur J Pharmacol, 1994. **268**(3): p. 409-14.
13. Genever, P.G., et al., *Evidence for a novel glutamate-mediated signaling pathway in keratinocytes.* J Invest Dermatol, 1999. **112**(3): p. 337-42.
14. Denda, M., S. Fuziwara, and K. Inoue, *Influx of calcium and chloride ions into epidermal keratinocytes regulates exocytosis of epidermal lamellar bodies and skin permeability barrier homeostasis.* J Invest Dermatol, 2003. **121**(2): p. 362-7.
15. Fuziwara, S., K. Inoue, and M. Denda, *NMDA-type glutamate receptor is associated with cutaneous barrier homeostasis.* J Invest Dermatol, 2003. **120**(6): p. 1023-9.
16. Fischer, M., et al., *Keratinocytes: a source of the transmitter L-glutamate in the epidermis.* Exp Dermatol, 2009. **18**(12): p. 1064-6.
17. Brazel, C.Y., et al., *Glutamate enhances survival and proliferation of neural progenitors derived from the subventricular zone.* Neuroscience, 2005. **131**(1): p. 55-65.
18. Krauthammer, M., et al., *Exome sequencing identifies recurrent somatic RAC1 mutations in melanoma.* Nat Genet, 2012. **44**(9): p. 1006-14.
19. Cappuccio, I., et al., *Endogenous activation of mGlu5 metabotropic glutamate receptors supports self-renewal of cultured mouse embryonic stem cells.* Neuropharmacology, 2005. **49 Suppl 1**: p. 196-205.
20. Spinsanti, P., et al., *Endogenously activated mGlu5 metabotropic glutamate receptors sustain the increase in c-Myc expression induced by leukaemia inhibitory factor in cultured mouse embryonic stem cells.* J Neurochem, 2006. **99**(1): p. 299-307.

21. Young, D., et al., *Isolation and characterization of a new cellular oncogene encoding a protein with multiple potential transmembrane domains.* Cell, 1986. **45**(5): p. 711-9.
22. Gutkind, J.S., et al., *Muscarinic acetylcholine receptor subtypes as agonist-dependent oncogenes.* Proc Natl Acad Sci U S A, 1991. **88**(11): p. 4703-7.
23. Julius, D., et al., *Ectopic expression of the serotonin 1c receptor and the triggering of malignant transformation.* Science, 1989. **244**(4908): p. 1057-62.
24. Bhola, N.E. and J.R. Grandis, *Crosstalk between G-protein-coupled receptors and epidermal growth factor receptor in cancer.* Front Biosci, 2008. **13**: p. 1857-65.
25. Peavy, R.D., et al., *Metabotropic glutamate receptor 5-induced phosphorylation of extracellular signal-regulated kinase in astrocytes depends on transactivation of the epidermal growth factor receptor.* J Neurosci, 2001. **21**(24): p. 9619-28.
26. Thandi, S., J.L. Blank, and R.A. Challiss, *Group-I metabotropic glutamate receptors, mGlu1a and mGlu5a, couple to extracellular signal-regulated kinase (ERK) activation via distinct, but overlapping, signalling pathways.* J Neurochem, 2002. **83**(5): p. 1139-53.
27. Minoshima, T. and S. Nakanishi, *Structural organization of the mouse metabotropic glutamate receptor subtype 3 gene and its regulation by growth factors in cultured cortical astrocytes.* J Biochem, 1999. **126**(5): p. 889-96.
28. Alagarsamy, S., et al., *NMDA-induced phosphorylation and regulation of mGluR5.* Pharmacol Biochem Behav, 2002. **73**(2): p. 299-306.
29. Mao, L. and J.Q. Wang, *Interactions between ionotropic and metabotropic glutamate receptors regulate cAMP response element-binding protein phosphorylation in cultured striatal neurons.* Neuroscience, 2002. **115**(2): p. 395-402.
30. Skeberdis, V.A., et al., *mGluR1-mediated potentiation of NMDA receptors involves a rise in intracellular calcium and activation of protein kinase C.* Neuropharmacology, 2001. **40**(7): p. 856-65.
31. Van Raamsdonk, C.D., et al., *Effects of G-protein mutations on skin color.* Nat Genet, 2004. **36**(9): p. 961-8.
32. Van Raamsdonk, C.D., et al., *Frequent somatic mutations of GNAQ in uveal melanoma and blue naevi.* Nature, 2009. **457**(7229): p. 599-602.
33. Van Raamsdonk, C.D., et al., *Mutations in GNA11 in uveal melanoma.* N Engl J Med, 2010. **363**(23): p. 2191-9.
34. Wong, C.W., et al., *BRAF and NRAS mutations are uncommon in melanomas arising in diverse internal organs.* J Clin Pathol, 2005. **58**(6): p. 640-4.
35. Herlyn, M. and K.L. Nathanson, *Taking the guesswork out of uveal melanoma.* N Engl J Med, 2010. **363**(23): p. 2256-7.
36. Kusters-Vandevelde, H.V., et al., *Activating mutations of the GNAQ gene: a frequent event in primary melanocytic neoplasms of the central nervous system.* Acta Neuropathol, 2009.
37. Cardenas-Navia, L.I., et al., *Novel somatic mutations in heterotrimeric G proteins in melanoma.* Cancer Biol Ther, 2010. **10**(1): p. 33-7.
38. Firnhaber, J.M., *Diagnosis and treatment of Basal cell and squamous cell carcinoma.* Am Fam Physician, 2012. **86**(2): p. 161-8.
39. American, C.S., *Cancer Facts & Figures 2013*, in *Atlanta, GA: American Cancer Society*2013.
40. Le Douarin, N.M. and E. Dupin, *Multipotentiality of the neural crest.* Curr Opin Genet Dev, 2003. **13**(5): p. 529-36.

41. D'Orazio, J., et al., *UV Radiation and the Skin.* Int J Mol Sci, 2013. **14**(6): p. 12222-48.
42. Witkin, E.M., *Ultraviolet-induced mutation and DNA repair.* Annu Rev Microbiol, 1969. **23**: p. 487-514.
43. Rass, K. and J. Reichrath, *UV damage and DNA repair in malignant melanoma and nonmelanoma skin cancer.* Adv Exp Med Biol, 2008. **624**: p. 162-78.
44. Winsey, S.L., et al., *A variant within the DNA repair gene XRCC3 is associated with the development of melanoma skin cancer.* Cancer Res, 2000. **60**(20): p. 5612-6.
45. Goode, E.L., C.M. Ulrich, and J.D. Potter, *Polymorphisms in DNA repair genes and associations with cancer risk.* Cancer Epidemiol Biomarkers Prev, 2002. **11**(12): p. 1513-30.
46. Armstrong, B.K., *The epidemiology and prevention of cancer in Australia.* Aust N Z J Surg, 1988. **58**(3): p. 179-87.
47. Bauer, J. and C. Garbe, *Acquired melanocytic nevi as risk factor for melanoma development. A comprehensive review of epidemiological data.* Pigment Cell Res, 2003. **16**(3): p. 297-306.
48. Herlyn, M., *Human melanoma: development and progression.* Cancer Metastasis Rev, 1990. **9**(2): p. 101-12.
49. Sauter, E.R. and M. Herlyn, *Molecular biology of human melanoma development and progression.* Mol Carcinog, 1998. **23**(3): p. 132-43.
50. Kamb, A., et al., *Analysis of the p16 gene (CDKN2) as a candidate for the chromosome 9p melanoma susceptibility locus.* Nat Genet, 1994. **8**(1): p. 23-6.
51. Quelle, D.E., et al., *Alternative reading frames of the INK4a tumor suppressor gene encode two unrelated proteins capable of inducing cell cycle arrest.* Cell, 1995. **83**(6): p. 993-1000.
52. Fountain, J.W., et al., *Homozygous deletions within human chromosome band 9p21 in melanoma.* Proc Natl Acad Sci U S A, 1992. **89**(21): p. 10557-61.
53. Goldstein, A.M., et al., *Association of MC1R variants and risk of melanoma in melanoma-prone families with CDKN2A mutations.* Cancer Epidemiol Biomarkers Prev, 2005. **14**(9): p. 2208-12.
54. van der Velden, P.A., et al., *Melanocortin-1 receptor variant R151C modifies melanoma risk in Dutch families with melanoma.* Am J Hum Genet, 2001. **69**(4): p. 774-9.
55. Mitra, D., et al., *An ultraviolet-radiation-independent pathway to melanoma carcinogenesis in the red hair/fair skin background.* Nature, 2012. **491**(7424): p. 449-53.
56. Davies, H., et al., *Mutations of the BRAF gene in human cancer.* Nature, 2002. **417**(6892): p. 949-54.
57. Yeh, I., A. von Deimling, and B.C. Bastian, *Clonal BRAF Mutations in Melanocytic Nevi and Initiating Role of BRAF in Melanocytic Neoplasia.* J Natl Cancer Inst, 2013. **105**(12): p. 917-9.
58. Bollag, G., et al., *Clinical efficacy of a RAF inhibitor needs broad target blockade in BRAF-mutant melanoma.* Nature, 2010. **467**(7315): p. 596-9.
59. Flaherty, K.T., et al., *Inhibition of mutated, activated BRAF in metastatic melanoma.* N Engl J Med, 2010. **363**(9): p. 809-19.
60. Dankort, D., et al., *Braf(V600E) cooperates with Pten loss to induce metastatic melanoma.* Nat Genet, 2009. **41**(5): p. 544-52.
61. Chin, L., et al., *Cooperative effects of INK4a and ras in melanoma susceptibility in vivo.* Genes Dev, 1997. **11**(21): p. 2822-34.

62. Gschwind, A., O.M. Fischer, and A. Ullrich, *The discovery of receptor tyrosine kinases: targets for cancer therapy.* Nat Rev Cancer, 2004. **4**(5): p. 361-70.
63. Prickett, T.D., et al., *Analysis of the tyrosine kinome in melanoma reveals recurrent mutations in ERBB4.* Nat Genet, 2009. **41**(10): p. 1127-32.
64. Tworkoski, K., et al., *Phosphoproteomic screen identifies potential therapeutic targets in melanoma.* Mol Cancer Res, 2011. **9**(6): p. 801-12.
65. Berger, M.F., et al., *Melanoma genome sequencing reveals frequent PREX2 mutations.* Nature, 2012. **485**(7399): p. 502-6.
66. Garibyan, L. and D.E. Fisher, *How sunlight causes melanoma.* Curr Oncol Rep, 2010. **12**(5): p. 319-26.
67. Hodis, E., et al., *A landscape of driver mutations in melanoma.* Cell, 2012. **150**(2): p. 251-63.
68. Aiba, A., et al., *Deficient cerebellar long-term depression and impaired motor learning in mGluR1 mutant mice.* Cell, 1994. **79**(2): p. 377-88.
69. Gil-Sanz, C., et al., *Involvement of the mGluR1 receptor in hippocampal synaptic plasticity and associative learning in behaving mice.* Cereb Cortex, 2008. **18**(7): p. 1653-63.
70. Chen, S., et al., *Commitment of mouse fibroblasts to adipocyte differentiation by DNA transfection.* Science, 1989. **244**(4904): p. 582-5.
71. Chen, S., et al., *Spontaneous melanocytosis in transgenic mice.* J Invest Dermatol, 1996. **106**(5): p. 1145-51.
72. Pollock, P.M., et al., *Melanoma mouse model implicates metabotropic glutamate signaling in melanocytic neoplasia.* Nat Genet, 2003. **34**(1): p. 108-12.
73. Ohtani, Y., et al., *Metabotropic glutamate receptor subtype-1 is essential for in vivo growth of melanoma.* Oncogene, 2008. **27**(57): p. 7162-70.
74. Marin, Y.E., et al., *Grm5 expression is not required for the oncogenic role of Grm1 in melanocytes.* Neuropharmacology, 2005. **49 Suppl 1**: p. 70-9.
75. Shin, S.S., et al., *Oncogenic activities of metabotropic glutamate receptor 1 (Grm1) in melanocyte transformation.* Pigment Cell Melanoma Res, 2008. **21**(3): p. 368-78.
76. Shin, S.S., et al., *AKT2 is a downstream target of metabotropic glutamate receptor 1 (Grm1).* Pigment Cell Melanoma Res, 2010. **23**(1): p. 103-11.
77. Maehama, T. and J.E. Dixon, *The tumor suppressor, PTEN/MMAC1, dephosphorylates the lipid second messenger, phosphatidylinositol 3,4,5-trisphosphate.* J Biol Chem, 1998. **273**(22): p. 13375-8.
78. Nogueira, C., et al., *Cooperative interactions of PTEN deficiency and RAS activation in melanoma metastasis.* Oncogene, 2010. **29**(47): p. 6222-32.
79. Cheung, M., et al., *Akt3 and mutant V600E B-Raf cooperate to promote early melanoma development.* Cancer Res, 2008. **68**(9): p. 3429-39.
80. Namkoong, J., et al., *Metabotropic glutamate receptor 1 and glutamate signaling in human melanoma.* Cancer Res, 2007. **67**(5): p. 2298-305.
81. Wangari-Talbot, J., et al., *Functional effects of GRM1 suppression in human melanoma cells.* Mol Cancer Res, 2012. **10**(11): p. 1440-50.
82. Choi, K.Y., et al., *Expression of the metabotropic glutamate receptor 5 (mGluR5) induces melanoma in transgenic mice.* Proc Natl Acad Sci U S A, 2011. **108**(37): p. 15219-24.
83. Graham, T.E., et al., *Glutamate ingestion: the plasma and muscle free amino acid pools of resting humans.* Am J Physiol Endocrinol Metab, 2000. **278**(1): p. E83-9.
84. Wei, X., et al., *Exome sequencing identifies GRIN2A as frequently mutated in melanoma.* Nat Genet, 2011. **43**(5): p. 442-6.

85. Prickett, T.D., et al., *Exon capture analysis of G protein-coupled receptors identifies activating mutations in GRM3 in melanoma.* Nat Genet, 2011.
86. Chapman, P.B., et al., *Improved survival with vemurafenib in melanoma with BRAF V600E mutation.* N Engl J Med, 2011. **364**(26): p. 2507-16.
87. Johannessen, C.M., et al., *COT drives resistance to RAF inhibition through MAP kinase pathway reactivation.* Nature, 2010. **468**(7326): p. 968-72.
88. Nazarian, R., et al., *Melanomas acquire resistance to B-RAF(V600E) inhibition by RTK or N-RAS upregulation.* Nature, 2010. **468**(7326): p. 973-7.
89. Poulikakos, P.I., et al., *RAF inhibitor resistance is mediated by dimerization of aberrantly spliced BRAF(V600E).* Nature, 2011.
90. Villanueva, J., et al., *Acquired resistance to BRAF inhibitors mediated by a RAF kinase switch in melanoma can be overcome by cotargeting MEK and IGF-1R/PI3K.* Cancer Cell, 2010. **18**(6): p. 683-95.
91. Solit, D.B., et al., *BRAF mutation predicts sensitivity to MEK inhibition.* Nature, 2006. **439**(7074): p. 358-62.
92. Prickett, T.D., et al., *Exon capture analysis of G protein-coupled receptors identifies activating mutations in GRM3 in melanoma.* Nat Genet, 2011. **43**(11): p. 1119-26.
93. Okayama, H., et al., *Identification of Genes Upregulated in ALK-Positive and EGFR/KRAS/ALK-Negative Lung Adenocarcinomas.* Cancer Res, 2012. **72**(1): p. 100-111.
94. Sorlie, T., et al., *Gene expression patterns of breast carcinomas distinguish tumor subclasses with clinical implications.* Proc Natl Acad Sci U S A, 2001. **98**(19): p. 10869-74.
95. Sorlie, T., et al., *Repeated observation of breast tumor subtypes in independent gene expression data sets.* Proc Natl Acad Sci U S A, 2003. **100**(14): p. 8418-23.
96. Sorlie, T., *Molecular portraits of breast cancer: tumour subtypes as distinct disease entities.* Eur J Cancer, 2004. **40**(18): p. 2667-75.
97. *Comprehensive molecular portraits of human breast tumours.* Nature, 2012. **490**(7418): p. 61-70.
98. Curtis, C., et al., *The genomic and transcriptomic architecture of 2,000 breast tumours reveals novel subgroups.* Nature, 2012. **486**(7403): p. 346-52.
99. Goggins, W., W. Gao, and H. Tsao, *Association between female breast cancer and cutaneous melanoma.* Int J Cancer, 2004. **111**(5): p. 792-4.
100. Borg, A., et al., *High frequency of multiple melanomas and breast and pancreas carcinomas in CDKN2A mutation-positive melanoma families.* J Natl Cancer Inst, 2000. **92**(15): p. 1260-6.
101. *Cancer risks in BRCA2 mutation carriers. The Breast Cancer Linkage Consortium.* J Natl Cancer Inst, 1999. **91**(15): p. 1310-6.
102. Spanogle, J.P., et al., *Risk of second primary malignancies following cutaneous melanoma diagnosis: a population-based study.* J Am Acad Dermatol, 2010. **62**(5): p. 757-67.
103. Speyer, C.L., et al., *Metabotropic glutamate receptor-1: a potential therapeutic target for the treatment of breast cancer.* Breast Cancer Res Treat, 2011. **132**(2): p. 565-73.
104. Seidlitz, E.P., et al., *Cancer cell lines release glutamate into the extracellular environment.* Clin Exp Metastasis, 2009. **26**(7): p. 781-7.
105. Chen, Y.C., D.M. Sosnoski, and A.M. Mastro, *Breast cancer metastasis to the bone: mechanisms of bone loss.* Breast Cancer Res, 2010. **12**(6): p. 215.

106. Seidlitz, E.P., M.K. Sharma, and G. Singh, *Extracellular glutamate alters mature osteoclast and osteoblast functions.* Can J Physiol Pharmacol, 2010. **88**(9): p. 929-36.
107. Mehta M.S., D.S.C., Bronfenbrener R., Bilal E., Chen C., Moore D., Rahim H., Aisner S., Kersellius, Teh J., Chen S., Toppmeyer D.L., Ganesan S., Vazquez A. and Hirshfield K.M. , *Metabotropic glutamate receptor 1 expression and its polymorphic variants associate with breast cancer phenotypes.* PLOS ONE, 2013. **8**(7): p. e69851.
108. Sontheimer, H., *A role for glutamate in growth and invasion of primary brain tumors.* J Neurochem, 2008. **105**(2): p. 287-95.
109. Arcella, A., et al., *Pharmacological blockade of group II metabotropic glutamate receptors reduces the growth of glioma cells in vivo.* Neuro Oncol, 2005. **7**(3): p. 236-45.
110. D'Onofrio, M., et al., *Pharmacological blockade of mGlu2/3 metabotropic glutamate receptors reduces cell proliferation in cultured human glioma cells.* J Neurochem, 2003. **84**(6): p. 1288-95.
111. Ciceroni, C., et al., *Type-3 metabotropic glutamate receptors negatively modulate bone morphogenetic protein receptor signaling and support the tumourigenic potential of glioma-initiating cells.* Neuropharmacology, 2008. **55**(4): p. 568-76.
112. Huse, J.T. and E.C. Holland, *Targeting brain cancer: advances in the molecular pathology of malignant glioma and medulloblastoma.* Nat Rev Cancer, 2010. **10**(5): p. 319-31.
113. Melchiorri, D., et al., *Metabotropic glutamate receptors in stem/progenitor cells.* Neuropharmacology, 2007. **53**(4): p. 473-80.
114. Canudas, A.M., et al., *PHCCC, a specific enhancer of type 4 metabotropic glutamate receptors, reduces proliferation and promotes differentiation of cerebellar granule cell neuroprecursors.* J Neurosci, 2004. **24**(46): p. 10343-52.
115. Iacovelli, L., et al., *Pharmacological activation of mGlu4 metabotropic glutamate receptors inhibits the growth of medulloblastomas.* J Neurosci, 2006. **26**(32): p. 8388-97.
116. Ye, P., et al., *In vivo actions of insulin-like growth factor-I (IGF-I) on cerebellum development in transgenic mice: evidence that IGF-I increases proliferation of granule cell progenitors.* Brain Res Dev Brain Res, 1996. **95**(1): p. 44-54.
117. Dahmane, N. and A. Ruiz i Altaba, *Sonic hedgehog regulates the growth and patterning of the cerebellum.* Development, 1999. **126**(14): p. 3089-100.
118. Yokota, N., et al., *Role of Wnt pathway in medulloblastoma oncogenesis.* Int J Cancer, 2002. **101**(2): p. 198-201.
119. Gilbertson, R.J., *Medulloblastoma: signalling a change in treatment.* Lancet Oncol, 2004. **5**(4): p. 209-18.
120. Pazzaglia, S., et al., *High incidence of medulloblastoma following X-ray-irradiation of newborn Ptc1 heterozygous mice.* Oncogene, 2002. **21**(49): p. 7580-4.
121. Yoo, B.C., et al., *Metabotropic glutamate receptor 4-mediated 5-Fluorouracil resistance in a human colon cancer cell line.* Clin Cancer Res, 2004. **10**(12 Pt 1): p. 4176-84.
122. Chang, H.J., et al., *Metabotropic glutamate receptor 4 expression in colorectal carcinoma and its prognostic significance.* Clin Cancer Res, 2005. **11**(9): p. 3288-95.
123. Koochekpour, S., et al., *Serum glutamate levels correlate with Gleason score and glutamate blockade decreases proliferation, migration, and invasion and*

induces apoptosis in prostate cancer cells. Clin Cancer Res, 2012. **18**(21): p. 5888-901.
124. Khan, A.J., et al., *Riluzole enhances ionizing radiation-induced cytotoxicity in human melanoma cells that ectopically express metabotropic glutamate receptor 1 in vitro and in vivo.* Clin Cancer Res, 2011. **17**(7): p. 1807-14.
125. Lee, H.J., et al., *Glutamatergic pathway targeting in melanoma: single-agent and combinatorial therapies.* Clin Cancer Res, 2011. **17**(22): p. 7080-92.
126. Yip, D., et al., *A phase 0 trial of riluzole in patients with resectable stage III and IV melanoma.* Clin Cancer Res, 2009. **15**(11): p. 3896-902.
127. Doble, A., *The pharmacology and mechanism of action of riluzole.* Neurology, 1996. **47**(6 Suppl 4): p. S233-41.
128. Frizzo, M.E., et al., *Riluzole enhances glutamate uptake in rat astrocyte cultures.* Cell Mol Neurobiol, 2004. **24**(1): p. 123-8.
129. Kaelin, W.G., Jr. and C.B. Thompson, *Q&A: Cancer: clues from cell metabolism.* Nature, 2010. **465**(7298): p. 562-4.
130. Wise, D.R. and C.B. Thompson, *Glutamine addiction: a new therapeutic target in cancer.* Trends Biochem Sci, 2010. **35**(8): p. 427-33.
131. Wang, J.B., et al., *Targeting mitochondrial glutaminase activity inhibits oncogenic transformation.* Cancer Cell, 2010. **18**(3): p. 207-19.
132. Busciglio, J. and B.A. Yankner, *Apoptosis and increased generation of reactive oxygen species in Down's syndrome neurons in vitro.* Nature, 1995. **378**(6559): p. 776-9.
133. Kato, S., et al., *A mechanism for glutamate toxicity in the C6 glioma cells involving inhibition of cystine uptake leading to glutathione depletion.* Neuroscience, 1992. **48**(4): p. 903-14.
134. Pereira, C.M. and C.R. Oliveira, *Glutamate toxicity on a PC12 cell line involves glutathione (GSH) depletion and oxidative stress.* Free Radic Biol Med, 1997. **23**(4): p. 637-47.
135. Guo, W., et al., *Disruption of xCT inhibits cell growth via the ROS/autophagy pathway in hepatocellular carcinoma.* Cancer Lett, 2011. **312**(1): p. 55-61.
136. Ogunrinu, T.A. and H. Sontheimer, *Hypoxia increases the dependence of glioma cells on glutathione.* J Biol Chem, 2010. **285**(48): p. 37716-24.
137. Gonzalez, E. and T.E. McGraw, *The Akt kinases: isoform specificity in metabolism and cancer.* Cell Cycle, 2009. **8**(16): p. 2502-8.
138. Gonzalez, E. and T.E. McGraw, *Insulin-modulated Akt subcellular localization determines Akt isoform-specific signaling.* Proc Natl Acad Sci U S A, 2009. **106**(17): p. 7004-9.
139. Irie, H.Y., et al., *Distinct roles of Akt1 and Akt2 in regulating cell migration and epithelial-mesenchymal transition.* J Cell Biol, 2005. **171**(6): p. 1023-34.
140. Stambolic, V. and J.R. Woodgett, *Functional distinctions of protein kinase B/Akt isoforms defined by their influence on cell migration.* Trends Cell Biol, 2006. **16**(9): p. 461-6.
141. Stahl, J.M., et al., *Deregulated Akt3 activity promotes development of malignant melanoma.* Cancer Res, 2004. **64**(19): p. 7002-10.
142. Cohen-Solal, K.A., et al., *Progressive appearance of pigmentation in amelanotic melanoma lesions.* Pigment Cell Res, 2002. **15**(4): p. 282-9.
143. Kim, W.Y., et al., *Epidermal growth factor receptor and K-Ras mutations and resistance of lung cancer to insulin-like growth factor 1 receptor tyrosine kinase inhibitors.* Cancer, 2012. **118**(16): p. 3993-4003.
144. Lee, H.J., et al., *Glutamatergic Pathway Targeting in Melanoma; Single Agent and Combinatorial Therapies.* Clin Cancer Res, 2011.

145. Almendro, V., S. Garcia-Recio, and P. Gascon, *Tyrosine kinase receptor transactivation associated to G protein-coupled receptors.* Curr Drug Targets, 2010. **11**(9): p. 1169-80.
146. Luttrell, D.K. and L.M. Luttrell, *Not so strange bedfellows: G-protein-coupled receptors and Src family kinases.* Oncogene, 2004. **23**(48): p. 7969-78.
147. Sachdev, D., et al., *A dominant negative type I insulin-like growth factor receptor inhibits metastasis of human cancer cells.* J Biol Chem, 2004. **279**(6): p. 5017-24.
148. Gorden, A., et al., *Analysis of BRAF and N-RAS mutations in metastatic melanoma tissues.* Cancer Res, 2003. **63**(14): p. 3955-7.
149. Fassnacht, M., et al., *Adrenocortical carcinoma: a clinician's update.* Nat Rev Endocrinol, 2011. **7**(6): p. 323-35.
150. Mulvihill, M.J., et al., *Discovery of OSI-906: a selective and orally efficacious dual inhibitor of the IGF-1 receptor and insulin receptor.* Future Med Chem, 2009. **1**(6): p. 1153-71.
151. Zhao, H., et al., *Epithelial-mesenchymal transition predicts sensitivity to the dual IGF-1R/IR inhibitor OSI-906 in hepatocellular carcinoma cell lines.* Mol Cancer Ther, 2012. **11**(2): p. 503-13.
152. Esseltine, J.L., et al., *Somatic Mutations in GRM1 in Cancer Alter Metabotropic Glutamate Receptor 1 Intracellular Localization and Signaling.* Mol Pharmacol, 2013.
153. Natarajan, K. and B.C. Berk, *Crosstalk coregulation mechanisms of G protein-coupled receptors and receptor tyrosine kinases.* Methods Mol Biol, 2006. **332**: p. 51-77.
154. Delcourt, N., J. Bockaert, and P. Marin, *GPCR-jacking: from a new route in RTK signalling to a new concept in GPCR activation.* Trends Pharmacol Sci, 2007. **28**(12): p. 602-7.
155. Tu, H., et al., *GABAB receptor activation protects neurons from apoptosis via IGF-1 receptor transactivation.* J Neurosci, 2010. **30**(2): p. 749-59.
156. Zahradka, P., et al., *Transactivation of the insulin-like growth factor-I receptor by angiotensin II mediates downstream signaling from the angiotensin II type 1 receptor to phosphatidylinositol 3-kinase.* Endocrinology, 2004. **145**(6): p. 2978-87.
157. Sitcheran, R., et al., *Essential role for epidermal growth factor receptor in glutamate receptor signaling to NF-kappaB.* Mol Cell Biol, 2008. **28**(16): p. 5061-70.
158. Kanter-Lewensohn, L., et al., *Expression of insulin-like growth factor-1 receptor (IGF-1R) and p27Kip1 in melanocytic tumors: a potential regulatory role of IGF-1 pathway in distribution of p27Kip1 between different cyclins.* Growth Factors, 2000. **17**(3): p. 193-202.
159. Satyamoorthy, K., et al., *Insulin-like growth factor-1 induces survival and growth of biologically early melanoma cells through both the mitogen-activated protein kinase and beta-catenin pathways.* Cancer Res, 2001. **61**(19): p. 7318-24.
160. Molhoek, K.R., et al., *Comprehensive analysis of receptor tyrosine kinase activation in human melanomas reveals autocrine signaling through IGF-1R.* Melanoma Res, 2011. **21**(4): p. 274-84.
161. Straussman, R., et al., *Tumour micro-environment elicits innate resistance to RAF inhibitors through HGF secretion.* Nature, 2012. **487**(7408): p. 500-4.
162. Martino, J.J., et al., *Metabotropic glutamate receptor 1 (Grm1) is an oncogene in epithelial cells.* Oncogene, 2012.
163. Siegel, R., D. Naishadham, and A. Jemal, *Cancer statistics, 2013.* CA Cancer J Clin, 2013. **63**(1): p. 11-30.

164. Karantza-Wadsworth, V. and E. White, *A mouse mammary epithelial cell model to identify molecular mechanisms regulating breast cancer progression.* Methods Enzymol, 2008. **446**: p. 61-76.
165. Debnath, J., S.K. Muthuswamy, and J.S. Brugge, *Morphogenesis and oncogenesis of MCF-10A mammary epithelial acini grown in three-dimensional basement membrane cultures.* Methods, 2003. **30**(3): p. 256-68.
166. Liu, Y., et al., *The protein kinase Pak4 disrupts mammary acinar architecture and promotes mammary tumorigenesis.* Oncogene, 2010. **29**(44): p. 5883-94.
167. Karantza-Wadsworth, V., et al., *Autophagy mitigates metabolic stress and genome damage in mammary tumorigenesis.* Genes Dev, 2007. **21**(13): p. 1621-35.
168. Degenhardt, K. and E. White, *A mouse model system to genetically dissect the molecular mechanisms regulating tumorigenesis.* Clin Cancer Res, 2006. **12**(18): p. 5298-304.
169. Zhu, H., K. Ryan, and S. Chen, *Cloning of novel splice variants of mouse mGluR1.* Brain Res Mol Brain Res, 1999. **73**(1-2): p. 93-103.
170. Stepulak, A., et al., *NMDA antagonist inhibits the extracellular signal-regulated kinase pathway and suppresses cancer growth.* Proc Natl Acad Sci U S A, 2005. **102**(43): p. 15605-10.
171. Wu, T.Y., et al., *In vivo pharmacodynamics of indole-3-carbinol in the inhibition of prostate cancer in transgenic adenocarcinoma of mouse prostate (TRAMP) mice: involvement of Nrf2 and cell cycle/apoptosis signaling pathways.* Mol Carcinog, 2012. **51**(10): p. 761-70.
172. Zhang, Y., et al., *Nontoxic doses of suramin enhance activity of doxorubicin in prostate tumors.* J Pharmacol Exp Ther, 2001. **299**(2): p. 426-33.
173. Dhillon, A.S., et al., *MAP kinase signalling pathways in cancer.* Oncogene, 2007. **26**(22): p. 3279-90.
174. Debnath, J., et al., *The role of apoptosis in creating and maintaining luminal space within normal and oncogene-expressing mammary acini.* Cell, 2002. **111**(1): p. 29-40.
175. Mehnert JM, W., Y., Lee, J.H., Jeong, B.S., Li, J., Dudek, Pruski-Clark, L. L, Kane, M.M., Lin, H., Shih, W., Chen, S., Goydos, J. S., *A phase II trial of riluzole, an antagonist of metabotropic glutamate receptor 1 (GRM1) signaling, in patients with advanced melanoma. .* Submitted, 2013.
176. Janicke, R.U., et al., *Caspase-3 is required for DNA fragmentation and morphological changes associated with apoptosis.* J Biol Chem, 1998. **273**(16): p. 9357-60.
177. Mc Gee, M.M., et al., *Caspase-3 is not essential for DNA fragmentation in MCF-7 cells during apoptosis induced by the pyrrolo-1,5-benzoxazepine, PBOX-6.* FEBS Lett, 2002. **515**(1-3): p. 66-70.
178. Mooney, L.M., et al., *Apoptotic mechanisms in T47D and MCF-7 human breast cancer cells.* Br J Cancer, 2002. **87**(8): p. 909-17.
179. Eck-Enriquez, K., et al., *Pathways through which a regimen of melatonin and retinoic acid induces apoptosis in MCF-7 human breast cancer cells.* Breast Cancer Res Treat, 2000. **61**(3): p. 229-39.
180. Wall, B.A., Shin S.S., Wangari-Talbot J., Yu L.J., Sierra, J., Haffty, B.G., Goydos, J.S., and Chen, S. , *Perturbation of GRM1-mediated signalling with riluzole results in DNA damage in melanoma cells. .* Annual Retreat on Cancer Research NJ, 2012. **Abstract**.
181. Tokunaga, E., et al., *Activation of PI3K/Akt signaling and hormone resistance in breast cancer.* Breast Cancer, 2006. **13**(2): p. 137-44.

182. Hirai, H., et al., *MK-2206, an allosteric Akt inhibitor, enhances antitumor efficacy by standard chemotherapeutic agents or molecular targeted drugs in vitro and in vivo.* Mol Cancer Ther, 2010. **9**(7): p. 1956-67.
183. Overington, J.P., B. Al-Lazikani, and A.L. Hopkins, *How many drug targets are there?* Nat Rev Drug Discov, 2006. **5**(12): p. 993-6.
184. Dorsam, R.T. and J.S. Gutkind, *G-protein-coupled receptors and cancer.* Nat Rev Cancer, 2007. **7**(2): p. 79-94.
185. de Groot, J. and H. Sontheimer, *Glutamate and the biology of gliomas.* Glia, 2011. **59**(8): p. 1181-9.
186. Marani, M., et al., *Role of Bim in the survival pathway induced by Raf in epithelial cells.* Oncogene, 2004. **23**(14): p. 2431-41.
187. Reginato, M.J., et al., *Bim regulation of lumen formation in cultured mammary epithelial acini is targeted by oncogenes.* Mol Cell Biol, 2005. **25**(11): p. 4591-601.
188. Menzaghi, F., D.P. Behan, and D.T. Chalmers, *Constitutively activated G protein-coupled receptors: a novel approach to CNS drug discovery.* Curr Drug Targets CNS Neurol Disord, 2002. **1**(1): p. 105-21.
189. Valentinis, B. and R. Baserga, *IGF-I receptor signalling in transformation and differentiation.* Mol Pathol, 2001. **54**(3): p. 133-7.
190. Hutchinson, J.N., et al., *Activation of Akt-1 (PKB-alpha) can accelerate ErbB-2-mediated mammary tumorigenesis but suppresses tumor invasion.* Cancer Res, 2004. **64**(9): p. 3171-8.
191. Maroulakou, I.G., et al., *Akt1 ablation inhibits, whereas Akt2 ablation accelerates, the development of mammary adenocarcinomas in mouse mammary tumor virus (MMTV)-ErbB2/neu and MMTV-polyoma middle T transgenic mice.* Cancer Res, 2007. **67**(1): p. 167-77.
192. Dolfi, S.C., Mehta, M.S., Kornblum D., Bilal E., Medina D., Ganesan S. and Hirshfield K.M. , *Role of GRM1 In Breast Cancer Pathogenesis.* Annual Retreat on Cancer Research NJ, 2013. **Abstract**.
193. Sun, M., et al., *Phosphatidylinositol-3-OH Kinase (PI3K)/AKT2, activated in breast cancer, regulates and is induced by estrogen receptor alpha (ERalpha) via interaction between ERalpha and PI3K.* Cancer Res, 2001. **61**(16): p. 5985-91.
194. Kenny, P.A., et al., *The morphologies of breast cancer cell lines in three-dimensional assays correlate with their profiles of gene expression.* Mol Oncol, 2007. **1**(1): p. 84-96.
195. Le, M.N., et al., *The glutamate release inhibitor Riluzole decreases migration, invasion, and proliferation of melanoma cells.* J Invest Dermatol, 2010. **130**(9): p. 2240-9.
196. Shtivelman, E., J. Sussman, and D. Stokoe, *A role for PI 3-kinase and PKB activity in the G2/M phase of the cell cycle.* Curr Biol, 2002. **12**(11): p. 919-24.
197. Weigelt, B. and M.J. Bissell, *Unraveling the microenvironmental influences on the normal mammary gland and breast cancer.* Semin Cancer Biol, 2008. **18**(5): p. 311-21.
198. O'Hayre, M., et al., *The emerging mutational landscape of G proteins and G-protein-coupled receptors in cancer.* Nat Rev Cancer, 2013. **13**(6): p. 412-24.
199. Kan, Z., et al., *Diverse somatic mutation patterns and pathway alterations in human cancers.* Nature, 2010. **466**(7308): p. 869-73.
200. Cifola, I., et al., *Comprehensive genomic characterization of cutaneous malignant melanoma cell lines derived from metastatic lesions by whole-exome sequencing and SNP array profiling.* PLoS One, 2013. **8**(5): p. e63597.

CURRICULUM VITAE

JESSICA LI FONG TEH

EDUCATION

RUTGERS UNIVERSITY, PISCATAWAY, NJ October 2013

- PhD in Cell and Developmental Biology

THE PENNSYLVANIA STATE UNIVERSITY, UNIVERSITY PARK, PA August 2007

- Bachelor of science in Biotechnology
- Minor in Microbiology

PUBLICATIONS

J.L. Teh and S. Chen (2012). Glutamatergic Signaling in Cellular Transformation. *Pigment Cell and Melanoma Res.* 25(3):331-42

J Teh and S. Chen (2012). Metabotropic Glutamate Receptors and Cancerous Growth. *WIREs Membr Transp and Signal.* 1: 211-220. doi: 10.1002/wmts.21

J.L. Teh, S.S. Shin, Y. Wen, J.M. Mehnert, J. Goydos and S. Chen. Metabotropic glutamate receptor 1 (mGluR1) mediates melanocyte transformation via transactivation of IGF-1 Receptor. *(Addressing reviewer comments for submission to Pigment Cell & Melanoma Res.)*

J.L. Teh, N. Chen, R. Shah, S.L. Cava, S.C. Dolfi, M.S. Mehta, S. Kongara, S. Price, S. Ganesan, K.R. Reuhl, K.M. Hirshfield, V. Karantza*, S. Chen*. Metabotropic Glutamate Receptor 1 Disrupts Mammary Acinar Architecture and Initiates Malignant Transformation of Mammary Epithelial Cells. *(In preparation for submission)*

M.S. Mehta, S.C. Dolfi, R. Bronfenbrener, E. Bilal, C. Chen, D. Moore, H. Rahim, S. Aisner, R. Kersellius, **J. Teh**, S. Chen, D.L. Toppmeyer, S. Ganesan, A. Vazquez and K.M. Hirshfield. GRM1 Expression and its Polymorphic Variants Associate with Breast Cancer Phenotypes. *PLoS ONE* 8(7): e69851. doi:10.1371/journal.pone.0069851

J. Wangari-Talbot, B. Wall, J. Sierra, **J. Teh**, J.S. Goydos and S. Chen. Glutamate signaling in cancer–new target for therapy. *(Submitted to Anti-Cancer Agents in Medicinal Chemistry)*